University of Crete

Department of Materials Science and Technology

SINGLE - ELECTRON QUANTUM STATES IN GOLD NANOSTRUCTURES

Antonios G. Raptakis

Thesis Committee:

Ioannis N. Remediakis (supervisor)

Georgios Kopidakis

Dimitrios Papazoglou

November 2016

Στους γονείς μου,

που με θωράκισαν με περγαμηνές

για το υπόλοιπο της ζωής μου . . . .

Contents

Abbreviation

Density Functional Theory	**DFT**
Generalized-Gradient Approximation	**GGA**
Exchange Correlation potential	**XC**
Local Density Approximation	**LDA**
Local - Spin Density Approximation	**LSDA**
Grid-based Projector Augmented Wave method	**GPAW**
Atomic Simulation Enviroment	**ASE**
Visual Molecular Dynamics	**VMD**
Periodic Boundary Conditions	**PBC**
Brillouin - Zone points	**kpts**
Grid points	**gpts**
Density of States	**DOS**
Surface State	**SS**

Abstrtact

In this master thesis, we studied surface-localized electronic states of metals. In particular, we determine characteristic properties of Schockley surface states[11,12,13,14,15] for Au and Cu slabs. We did the calculation using Density Functional Theory (DFT)[9,10].

We construct slabs with different number of atomic layers. These layers are parallel to the (100) and (111) plane of FCC structure. We solved the N-electron Schrödinger equation[8] as implemented in the open-source package Grid-based Projector Augmented Wave method (GPAW) [9,10,18].

We locate surface states by observing Bloch States, ($n\bar{k}$), where the probability of finding electrons at surface atoms is much higher than the probability of finding them in bulk atoms. We modify slab thickness (number of layers) and observe when the probability starts to converge. We confirm the surface states by applying three methods. In the first method, we find the diagram of the probability density per atom. The next method was a graphical way to prove the surface state, in which we examine wavefunction plots. For this method, we used VMD and ASE[17]. In the last method, we plot the probability density in real space. All three methods are used to confirm that a particular Bloch state is indeed a surface state.

Subsequently, we repeated the same process for relaxed surfaces, in which the first and the last atom of slabs are allowed to relax.

The next step of the thesis concerns the computational calculation of the workfunction for different thicknesses of slabs. We fitted the square of the absolute value of wavefunction and applying Schockley's Surface State theory, we found values for the metal's workfunction in very good agreement to direct simulation.

Finally, we repeated the same process for Cu slabs.

So far, Schockley's theory was applied and explained results in semiconductors. In this thesis,it is confirmed that this theory could be applied also to metalic surfaces, because it derived from nearly free electrons model.

Περίληψη

Σε αυτή τη μεταπτυχιακή διατριβή μελετήσαμε εντοπισμένες επιφανειακές καταστάσεις σε μέταλλα. Συγκεκριμένα, προσδιορίσαμε χαρακτηριστικές ιδιότητες της θεωρίας του Schockley[11,12,13,14,15] για δομή Χρυσού (Au) και Χαλκού (Cu). Οι υπολογισμοί πραγματοποιήθηκαν χρησιμοποιώντας την Density Functional Theory (DFT).

Ξεκινήσαμε φτιάχνοντας δομές με διαφορετικό αριθμό ατομικών στρωμάτων από τις επίπεδα (100) και (111) της δομής FCC. Λύσαμε την εξίσωση του Schrödinger[8] για N αριθμό ηλεκτρονίων, όπως εφαρμόζεται στο ελεύθερο πακέτο του GPAW[9,10,18].

Εντοπίσαμε επιφανειακές καταστάσεις παρατηρώντας της κατάστασης του Bloch, ($n\bar{k}$), όπου η πιθανότητα να βρούμε ένα ηλεκτρόνιο σε επιφανειακό άτομο είναι πολύ μεγαλύτερη απ' ότι στα εσωτερικά άτομα, τα οποία έχουν την ίδια γεωμετρία με την τρισδιάστατη δομή. Μεταβάλλοντας τον αριθμό των ατομικών στρωμάτων παρατηρούμε μετά από ποιο πάχος η πιθανότητα ξεκινάει να συγκλίνει. Επιβεβαιώσαμε τις επιφανειακές καταστάσεις με 3 διαφορετικές μεθόδους. Στην πρώτη μέθοδο, φτιάξαμε το διάγραμμα της πιθανότητας ανά άτομο. Η επόμενη μέθοδος ήταν μια γραφική απόδειξη επιφανειακής κατάστασης, όπου επεξεργαστήκαμε τις κυματοσυναρτήσεις του συστήματος χρησιμοποιώντας το VMD και το ASE[17]. Στην τελευταία μέθοδο, κάναμε τη γραφική παράσταση της πυκνότητας πιθανότητας στον πραγματικό χώρο. Και οι τρεις μέθοδοι χρησιμοποιήθηκαν για την επιβεβαίωση ότι όντως μια συγκεκριμένη κατάσταση Bloch είναι επιφανειακή κατάσταση.

Στη συνέχεια, επαναλάβαμε την ίδια διαδικασία για relaxed surfaces, στις οποίες το πρώτο και το τελευταίο άτομο της δομής ήταν ελεύθερο να μετακινηθεί και να τοποθετηθεί με τέτοιο τρόπου ώστε να ελαχιστοποιεί την ενέργεια του συστήματος.

Το επόμενο βήμα της εργασίας αφορούσε τον υπολογισμό του έργου εξόδου για τα διαφορετικά πάχη των δομών. Φτιάχνοντας το διάγραμμα της πυκνότητα πιθανότητας και εφαρμόζοντας της θεωρία του Schockley, βρήκαμε τις τιμές για το έργο εξόδου των μεταλλικών επιφανειών που μελετήσαμε και βρισκόταν σε πολύ καλή συμφωνία με την υπολογιστική μέθοδο.

Επαναλάβαμε τις ίδιες διαδικασίες για τις ίδιες μεταλλικές επιφάνειες σε δομές Χαλκού (Cu).

Μέχρι τώρα, η θεωρία του Schockley έχει εφαρμοστεί και εξηγήσει αποτελέσματα για ημιαγωγούς. Σ' αυτή τη μεταπτυχιακή εργασία επιβεβαιώθηκε η χρήση της θεωρίας και για μεταλλικές επιφάνειες, γιατί προέρχεται από το μοντέλο των ελεύθερων ηλεκτρονίων.

1. THEORY and BASIC PRINCIPLES

1.1 Crystal Surfaces and Structures

Crystal structure is the periodic and ordered arrangment of atoms, ions or molecules in a material. It appears in nature to minimize the energy of the system that is formed. The structure is repeated along the principal directions of the three dimensional space.

The most common crystal structure are the cubic one (SC, BCC, FCC). There are also tetragonal, rhombohedral, orthorhombic, monoclinic, triclinic structures.In this thesis we focus on cubic structures because the metals we study have all FCC structure.

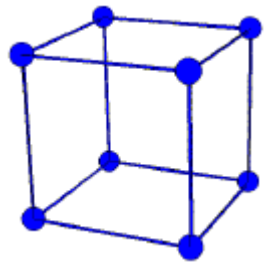

Figure 1.1.1:Simple Cubic (SC) [1]

In ***Simple Cubic (SC)*** structure, there is an atom on the vertices of the unit cell. A unit cell contains $N_i = 8 \cdot \frac{1}{8} = 1$ atom and the nearest neighbor are at distance a, where a is the one side length of the square that two atoms are located. This parameter depends on the material. The filling factor, which is the fraction of volume in a crystal structure that is occupied by constituent particles [3], is :

$$APF_{SC} = N_i \frac{\frac{4\pi}{3} R^3}{a^3} = 1 \cdot \frac{\frac{4\pi}{3} \left(\frac{a}{2}\right)^3}{a^3} = \frac{4\pi}{3} \cdot \frac{1}{8} = \frac{\pi}{6} \approx 52{,}4\,\%$$

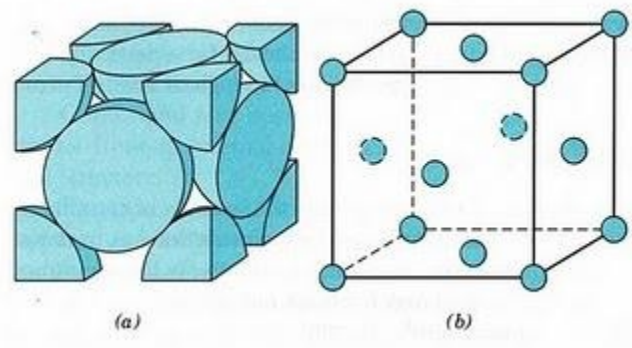

Figure 1.1.2 : Face - Centered – Cubic (FCC) [2]

In ***Face – Centered – Cubic (FCC)*** structure there are atoms on the vertices of the cell and also an atom at the center of every face of the unit cell. A unit cell contains $N_i = 8 \cdot \frac{1}{8} + 6 \cdot \frac{1}{2} = 1 + 3 = 4$ atoms. The nearest neighbor distance is $\frac{a\sqrt{2}}{2}$, where α is a parameter that depends on the material. The filling factor is

$$APF_{FCC}=N_i\frac{\frac{4\pi}{3}R^3}{a^3}=4\frac{\frac{4\pi}{3}\left(\frac{a\sqrt{2}}{4}\right)^3}{a^3}=\frac{\pi\sqrt{2}}{6}=74\%\quad .$$

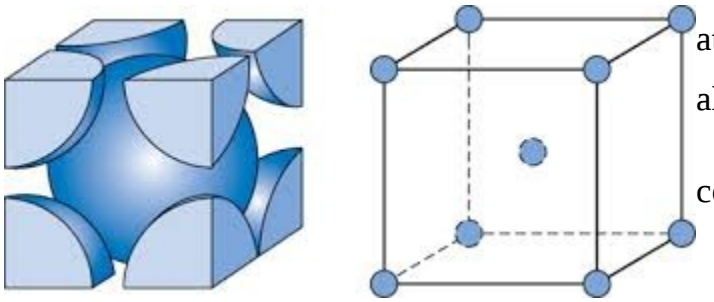

Figure 1.1.3: Body - Centered - Structure (BCC) [2]

In Body – Centered – Cubic (BCC) structure, an atom is located on the vertices of the unit cells, and also an atom at the center of the cube. A unit cell contains $N_i=8\cdot\frac{1}{8}+1=1+1=2$ sites. The nearest neighbor distance is $\frac{a\sqrt{3}}{2}$ correspondingly.

The filling factor is $APF_{FCC}=N_i\frac{\frac{4\pi}{3}R^3}{a^3}=2\frac{\frac{4\pi}{3}\left(\frac{a\sqrt{3}}{4}\right)^3}{a^3}=\frac{\pi\sqrt{3}}{8}=68\%$.

A periodic function $V(\vec{r})$ is a function that obeys $V(\vec{r}+\vec{R}_n)=V(\vec{r})$, where $\vec{R}_n=n_1\vec{a}_1+n_2\vec{a}_2+n_3\vec{a}_3$, with $\vec{a}_1,\vec{a}_2,\vec{a}_3$ are basis vectors and n_1,n_2,n_3 can be any integer number.

Bravais lattice is a set of points in space. These points are defined by the ends of the vectors $\vec{R}_n$. The volume of the unit cell is given by the formula: $V_{BC}=\left|(\vec{a}_1\times\vec{a}_2)\cdot\vec{a}_3\right|$.

The reciprocal Bravais lattice is also a Bravais [5][6][7] lattice and the vectors have the form $\vec{G}_m=m_1\vec{b}_1+m_2\vec{b}_2+m_3\vec{b}_3$ and obey $\vec{R}_n\cdot\vec{G}_m=2\pi\delta_{nm}$. Using this condition, we can define the basis vectors of the reciprocal lattice $\vec{b}_1,\vec{b}_2,\vec{b}_3$:

$$b_1=2\pi\frac{\vec{a}_2\times\vec{a}_3}{(a_1\times a_2)\cdot a_3}\quad,\quad b_2=2\pi\frac{\vec{a}_3\times\vec{a}_1}{(a_1\times a_2)\cdot a_3}\quad,\quad b_3=2\pi\frac{\vec{a}_1\times\vec{a}_2}{(a_1\times a_2)\cdot a_3}$$

Using the formulas above, we can conclude to the table below about the FCC and BCC strustures [6]:

	Basis Vectors	
Structure	*Bravais lattice*	*Reciprocal lattice*
BCC	$\vec{a}_1 = a\,\hat{x}_0$ $\vec{a}_2 = a\,\hat{y}_0$ $\vec{a}_3 = \frac{a}{2}(\hat{x}_0 + \hat{y}_0 + \hat{z}_0)$	$\vec{b}_1 = \frac{2\pi}{a}(-\hat{z}_0 + \hat{x}_0)$ $\vec{b}_2 = \frac{2\pi}{a}(-\hat{z}_0 + \hat{y}_0)$ $\vec{b}_3 = \frac{4\pi}{a}\hat{z}_0$
FCC	$\vec{a}_1 = \frac{a}{2}(\hat{y}_0 + \hat{z}_0)$ $\vec{a}_2 = \frac{a}{2}(\hat{x}_0 + \hat{z}_0)$ $\vec{a}_3 = \frac{a}{2}(\hat{x}_0 + \hat{y}_0)$	$\vec{b}_1 = \frac{2\pi}{a}(-\hat{x}_0 + \hat{y}_0 + \hat{z}_0)$ $\vec{b}_2 = \frac{2\pi}{a}(\hat{x}_0 - \hat{y}_0 + \hat{z}_0)$ $\vec{b}_3 = \frac{2\pi}{a}(\hat{x}_0 + \hat{y}_0 - \hat{z}_0)$

For the reciprocal lattice, the volume of the unit cell is given by the formula: $V_{RL} = |(\vec{b}_1 \times \vec{b}_2) \cdot \vec{b}_3|$, and is related to V_{BC} as $V_{BC} \cdot V_{RL} = (2\pi)^3$.

In a specific three dimensional Bravais lattice, we can define lattice planes by choosing three noncolinear lattice points. A family of lattice planes is the set of all parallel and equidistant lattice planes. Using the reciprocal lattice, all the possible families of the lattice planes can be categorized.

The crystalographic planes are defined by three indices, known as Miller indices. All the planes that are parallel to each other have the same Miller indices.

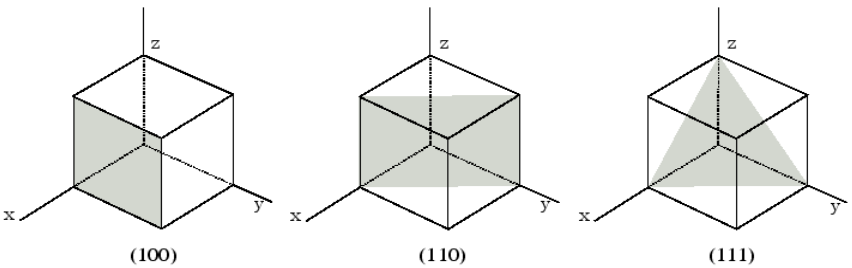

Figure 1.1.4 : lattice planes [4]

Figure 1.1.4 show three lattice planes: the plane (100), (110) and (111).

The (100) plane contains :

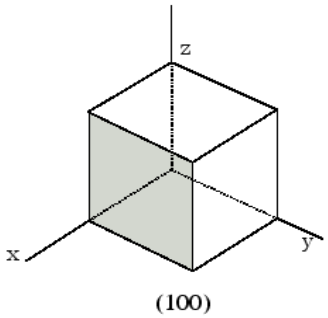

Figure 1.1.5: (100) plane [4]

- $4 \cdot \frac{1}{4} = 1$ atom per unit cell, for the SC structure
- $4 \cdot \frac{1}{4} = 1$ atom per unit cell, for the BCC structure
- $4 \cdot \frac{1}{4} + 1 = 2$ atoms per unit cell, for the FCC structure

The (110) plane contains :

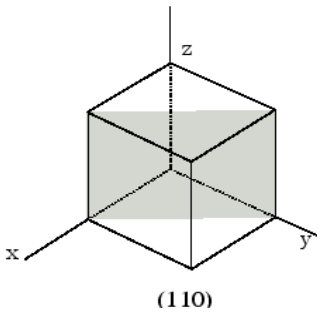

Figure 1.1.6 : (110) plane [4]

- $4 \cdot \frac{1}{4} = 1$ atom per unit cell, for the SC structure
- $4 \cdot \frac{1}{4} + 1 = 2$ atoms per unit cell, for the BCC structure
- $4 \cdot \frac{1}{4} = 1$ atom per unit cell, for the FCC structure

The (111) plane contains :

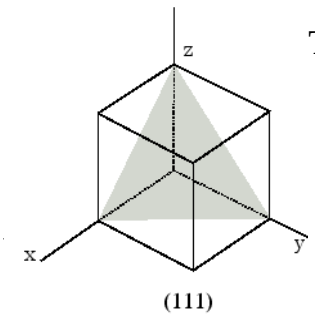

Picure 1.1.7 : (111) plane [4]

- $3 \cdot \frac{1}{6} = \frac{1}{2}$ atom per unit cell, for the SC structure
- $3 \cdot \frac{1}{6} + 1 = \frac{3}{2}$ atoms per unit cell, for the BCC structure
- $3 \cdot \frac{1}{6} + 3 \cdot \frac{1}{2} = 2$ atoms per unit cell, for the FCC structure

In this thesis we focus on the planes (100) and (111).

1.2 N-Electron Schrödinger equation

When we have to calculate properties and quantities in solid-state materials, it is important to find the Hamiltonian operator which describes the system. In this case, we start with the many – body Schrödinger equation. The Hamiltonian contains the kinetic energy of all the particles within the solid and their interaction energies. [8] Not all the electrons contribute to the same extent to the total energy. Electrons can be divided into two categories, the valence electrons and core electrons. Core electrons are strongly bound to the nucleous and therefore do not participate to the chemical bonding, as the valence electrons do. So, the Hamiltonian of the system would include two constituents, which are distinguished in the valence electrons and the lattice ions, and can be described by the following formula :

$$H = H_{el} + H_{ion} + H_{el-ion} = -\frac{\hbar^2}{2m_e}\sum_i \nabla_i^2 - \sum_{i,I}\frac{Z_I e^2}{4\pi\varepsilon_0|r_i - R_I|} + \frac{1}{2}\sum_{i\neq j}\frac{e^2}{4\pi\varepsilon_0|r_i - r_j|} - \sum_I \frac{\hbar^2}{2M_I}\nabla_I^2 + \frac{1}{2}\sum_{I\neq j}\frac{Z_I Z_j e^2}{4\pi\varepsilon_0|R_I - R_j|}$$

The Hamiltonian would be distinguished in three terms:

- *The electrons part:*

$$H_{el} = \sum_i \frac{p_i^2}{2m_e} + \frac{1}{2}\sum_{i\neq j}\frac{e^2}{4\pi\varepsilon_0|r_i - r_j|} = -\frac{\hbar^2}{2m_e}\sum_i \nabla_i^2 - \frac{1}{2}\sum_{i\neq j}\frac{e^2}{4\pi\varepsilon_0|r_i - r_j|}$$

Using the atomic units ($\frac{e^2}{4\pi\varepsilon_0} = \hbar = m_e = 1$) the above equation could be formed:

$$H_{el} = \sum_i \frac{p_i^2}{2} + \frac{1}{2}\sum_{i\neq j}\frac{1}{|r_i - r_j|}$$

It includes the kinetic energy of all the electrons. Their potential energy is described by a Coulomb term. The sums run over all the electrons indices excluding self- interaction for $i \neq j$.

- *The nuclei part:*

$$H_{ion}=\sum_I \frac{P_I^2}{2M_I}+\frac{1}{2}\sum_{I\neq J}\frac{Z_I Z_J e^2}{4\pi\varepsilon_0|R_I-R_J|}=-\sum_i \frac{\hbar^2}{2M_I}\nabla_I^2-\frac{1}{2}\sum_{I\neq J}\frac{Z_I Z_J e^2}{4\pi\varepsilon_0|R_I-R_J|}$$

The formula includes the total kinetic energy of the nuclei and the potential term which consist of the Coulomb interactions. The Z_I and Z_J are representing the atomic numbers. The sums run over all the ion indices again excluding self-interaction for $I\neq J$.

- *The electron - nuclei interaction part:*

$$H_{el-ion}=\frac{1}{2}\sum_{I\neq j}\frac{Z_I Z_j e^2}{4\pi\varepsilon_0|R_I-R_j|}$$

It is constructed corresponding to the electron-nuclei interaction as a sum of two-particle interacttions between electrons and ions depending on their distance to each other and the atomic numbers.

Those equations are the basis for the quantum mechanical analysis of most solid state properties. Now we make the transition from the Hamilton function to the Hamilton operator. If we use the coordinate representation we get a Hamilton operator depending on all the electron and ion coordinates and correspondingly a wavefunction as a function of all the coordinates and spin.

In order to solve a very difficult problem with so many factors, we have to make some approximations. Using the Born – Oppenheimer approximation we assume that the nuclear motion is slow and thus in comparison to the electrons, the nuclei is fixed. The solution of the energy eigenvalues equation could be formed:

$$\hat{H}\psi=E\psi\Rightarrow(H_{el}+H_{el-ion})\psi=E\psi$$

The ions positions are fixed, so the many - electron wavefunction $\psi(r_1\sigma_1,r_2\sigma_2,\ldots,r_n\sigma_n;R_1,R_2,\ldots,R_k)$ is a function of all electron positions and spin and the ion positions are only parameters.

1.3 Density Functional Theory

Denstiy Functional Theory (DFT) is a computational quantum mechanical method to reseach the electronic structure of a many-particle system. It is a method which is used for problems which can not be solved analytically.

The theoretical basis of the DFT was given by the two Hohenberg – Kohn theorems (H – K) [9], [10]. The first theorem exhibits that the ground state properties of a many-electron system are uniquely determined by an electron density that depends on only 3 spatial coordinates. The second indicates that the electron density which minimizes the energy of the overall functional is the true electron density corresponding to the full ground state solution of the Schrödinger equation.

As I mentioned at the previous chapter, the solution of a quantum mechanical problem starts from the Schrödinger's equation $H\Psi = E\Psi$, where in this problem it is a formula described by the following formula:

$$H = H_{el} + H_{el-ion} + H_{ion} = -\frac{\hbar^2}{2m_e}\sum_i \nabla_i^2 - \sum_{i,I}\frac{Z_I e^2}{4\pi\varepsilon_0|r_i - R_I|} + \frac{1}{2}\sum_{i\neq j}\frac{e^2}{4\pi\varepsilon_0|r_i - r_j|} - \sum_I \frac{\hbar^2}{2M_I}\nabla_I^2 + \frac{1}{2}\sum_{I\neq j}\frac{Z_I Z_j e^2}{4\pi\varepsilon_0|R_I - R_j|}$$

In this case, every operator which is included in the Hamiltonian is described by the electron density as $\hat{H} = H(n(r))$.

The electron density is n(r) obeys the normalization relation:

$$N = \int n(r)dr$$

One starts the solution using the one electron Schrödinger equation:

$$\left(-\frac{1}{2}\nabla^2 + u(r) + u([n];r) + u_{xc}^{\sigma}([n_\uparrow, n_\downarrow];r)\right)\Psi_{\alpha\sigma}(r) = E_{\alpha\sigma}\Psi_{\alpha\sigma}(r)$$

$$n_\sigma(r)=\sum_a \Theta(\mu-E_{a\sigma})\left|\Psi_{a\sigma}(r)\right|^2, n(r)=n_\uparrow(r), n_\downarrow(r)$$

σ is the z-component of the spin, α includes the rest of the electron quantum numbers. The above formula contains the step function theta, in which want to emphasize to orbitals with one electron while the other are empty. μ is the chemical potential.

The equation contains the external potential u(r) and also the effective potential using the classical Hartree potential $u([n];r)=\int d^3r' \frac{n(r')}{|r-r'|}$.

The total electron energy will be given by :

$$E=T_s[n_\uparrow, n_\downarrow]+\int d^2r\, n(r)u(r)+U[n]+E_{xc}([n_\uparrow, n_\downarrow])$$

where $\begin{cases} T_s[n_\uparrow, n_\downarrow]=\sum_{a\sigma}\Theta(\mu-E_{a\sigma})\langle\Psi_{a\sigma}|-\frac{1}{2}\nabla^2|\Psi_{a\sigma}\rangle \\ U[n]=\frac{1}{2}\int d^3r\, d^3r' \frac{n(r)n(r')}{|r-r'|} \end{cases}$

As last term we have the exchange-correlation energy E_{XC} , whose derivative $\frac{\delta E_{xc}}{\delta n_\sigma(r)}$ gives exchange - correlation potential.

LDA

The Local Density Approximation is used to determine the exchange - correlation functionals.

$$E_{xc}^{LDA}[n(r)]=\int d^3r\, n(r)E_{xc}^{unif}(n(r))$$

$E_{xc}^{unif}=E_x^{unif}+E_c^{unif}$ is the exchange and correlation energy per particle in an uniform electron density n, which can be distinguished in exchange and correlation contribution respectively.

LSDA

It is the Local Spin Density Approximation. The difference with the previous approximation is that this formula includes the electron spin $E_{xc}^{LSDA}[n_{\uparrow}, n_{\downarrow}] = \int d^3 r\, n(r)\, E_{xc}(n_{\uparrow}, n_{\downarrow})$.

GGA

LDA considers that the density is piecewise constant and overestimate the exchange-correlation energy. This overestimation of the energy is corrected using the gradient of the density. These corrections are referred to as generalized gradient approximations (GGA) and is given by the below formula:

$$E_{xc}^{GGA}[n(r)] = \int d^3 r\, n(r) f(n(r), \nabla n(r))$$

1.4 Electronic Surface States

A surface is the termination of a bulk crystal. A fraction of the chemical bonds which constitute the bulk crystal structure are broken at the surface. These bonds have to be broken to create the surface and thus the formation of a surface costs energy. In comparison with the bulk properties, the electronic structure near to the surface is notably different. Even an ideal surface with its atoms at bulk-like positions displays new electronic levels and modified many-body effects due to the change in the chemical bonding. Many macroscopic effects and phenomena on surfaces are related to this change in electronic structure. On the theoretical side, the general approach is similar to that for the bulk-crystal, but now we solve the Schrödinger's equation for an electron near the surface. [11],[12],[13]

In comparison with the bulk problem, two major difficulties arise for the surface, the symmetry and the surface-structure. For the first difficulty, even in the ideal case, symmetry only exists in directions within the plane of the surface. Perpendicular to the surface, the periodicity breaks down and the mathematical solution becomes much more complicated. The second difficulty is more severe, because of changes in atom's positions. A complete calculation of the electronic structure requires a knowledge of the atomic positions (coordinates). This is complicated, becuase of the changed chemical bonding near the surface. This change frequently results in surface relaxation and reconstruction. This means that the atoms are displaced from the ideal positions which they would occupy if the bulk crystal were simply truncated.

Consequently, surface states are electronic states found at the surface of materials. They are formed due to the sharp transition from solid material that ends with a surface and are found only at the atom layers closest to the surface. The termination of a material with a surface leads to a change of the electronic band structure from the bulk material to the vacuum. In the weakened potential at the surface, new electronic states can be formed, so called surface states.

1.5 Shockley Surface States

Shockley States are named after the American physicist William Shockley. Shockley states are the states that result when solving the Schrödinger equation in the framework of the nearly free electron approximation for clean and ideal surfaces. Shockley states are thus states that arise due to the change in the electron potential associated solely with the crystal termination. [11]

When we investigate the electronic surface states of an ideal crystal, we assume perfect two dimensional periodicity within the surface. [13],[14] However, we have broken symmetry perpendicular to the surface. The most general one-electron wavefunction Φ_{ss} for states near an ideal surface has plane-wave (Bloch) character for coordinates parallel to the surface $r_{\|} = (x,y)$:

$$\Phi_{ss}(r_{\|}, z) = u_{k_{\|}}(r_{\|}, z)\exp(i k_{\|} r_{\|}) \quad \text{(eq. 1.5.1)}$$

where $k_{\|} = (k_x,k_y)$ is a wavevector parallel to the surface. The simplest model to derive most of the important properties of surface states is the one-dimensional semi-infinite chain of periodically arranged atoms. The surface is then represented by the end of the chain. The results gained from the 1D surface can then be generalized for the 2D crystal surface. We assume, similar to the nearly free electron model, a cosine-like potential along the chain.

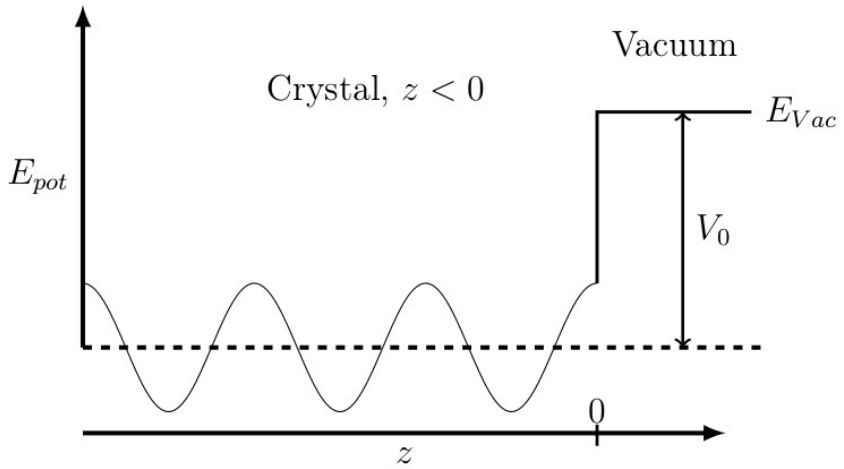

Figure 1.5.1: Nearly – free – electron model for a cosine potential along a linear chain [11]

$$V(z)=\begin{cases} V_0, for\ z>0 \\ \hat{V}\left(e^{\frac{2\pi iz}{a}}+e^{\frac{-2\pi iz}{a}}\right)=2\hat{V}\cos\left(\frac{2\pi z}{a}\right), for\ z<0 \end{cases} \quad (1)$$

Now, we have to solve Schrödinger's equation:

$$\hat{H}\psi=E\psi\Rightarrow\left[-\frac{\hbar^2}{2m}\frac{d^2}{dz^2}+V(z)\right]\Psi(z)=E\Psi(z) \quad ,$$

using the potential (1) for V(z).

For the solution, we start deep inside the crystal, z<<0, far away from the surface z = 0. In this case, we consider that the potential can be assumed to be periodic, V(z) = V(z+na). For this problem, we get the well-known bulk solutions:

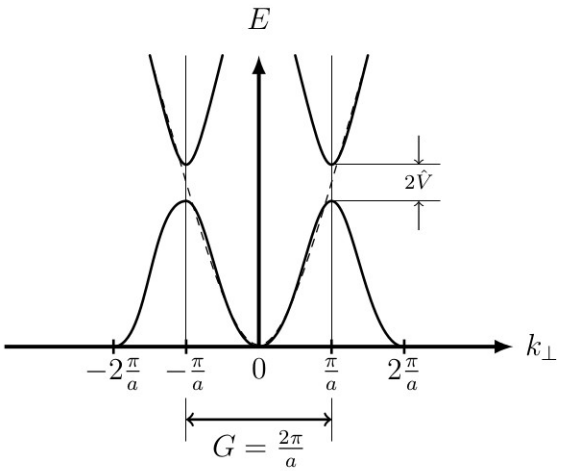

Figure 1.5.2: Energy Bands for one - electron bulk states [11]

Away from the Brillouin zone boundaries $k_\perp=\pm\frac{\pi}{a}$, the eigenstates of the Hamiltonian are plane waves and their energies are those of the free electron parabola. Near the boundaries we get the characteristic band splitting. This happens due to the fact that in lowest-order approximation of the electron wave function is a superposition of two plane waves:

$$\psi(z)=A\,e^{ik_\perp z}+B\,e^{\left(i\left(k_\perp-\frac{2\pi}{a}\right)z\right)} \quad \text{(eq. 1.5.2)}$$

Substituting into the Schrödinger's equation we get the matrix:

$$\begin{bmatrix} \frac{\hbar^2}{2m}k_\perp^2 - E(k_\perp) & \hat{V} \\ \hat{V} & \frac{\hbar^2}{2m}(k_\perp - \frac{2\pi}{a})^2 - E(k_\perp) \end{bmatrix} \cdot \begin{bmatrix} A \\ B \end{bmatrix} = 0 \quad \text{(eq. 1.5.3)}$$

Around the Brillouin zone boundary, near to $k_\perp = \pm\frac{G}{2} = \pm\frac{\pi}{a}$, with $k_\perp = \kappa + \pi/\alpha$, where small values of κ correspond to the $k_\perp$. Two elements of the above matrix will be changed:

$$\begin{bmatrix} \frac{\hbar^2}{2m}(\kappa + \frac{\pi}{a})^2 - E(\kappa) & \hat{V} \\ \hat{V} & \frac{\hbar^2}{2m}(\kappa - \frac{\pi}{a})^2 - E(\kappa) \end{bmatrix} \cdot \begin{bmatrix} A \\ B \end{bmatrix} = 0$$

And also the approximation of the electron wavefunction will be written:

$$\psi(z) = A e^{i(\kappa + \frac{\pi}{a})z} + B e^{i(\kappa - \frac{\pi}{a})z} = e^{ikz}(A e^{i\frac{\pi}{a}z} + B e^{-i\frac{\pi}{a}z})$$

$$\Rightarrow \psi(z) = e^{ikz}(A\exp(i\frac{\pi}{a}z) + B\exp(-i\frac{\pi}{a}z)) \quad \text{(eq. 2.5.4)}$$

Now, it is interesting to solve the above system to get the energy eigenvalues :

$$\begin{cases} (\frac{\hbar^2}{2m}(\kappa + \frac{\pi}{a})^2 - E)A + V B = 0 \\ Va + [\frac{\hbar^2}{2m}(\kappa - \frac{\pi}{a})^2 - E]b = 0 \end{cases} \Rightarrow \begin{cases} B = \dfrac{E - \frac{\hbar^2}{2m}(\kappa + \frac{\pi}{a})^2}{V} A \\ A = \dfrac{E - \frac{\hbar^2}{2m}(\kappa - \frac{\pi}{a})^2}{V} B \end{cases}$$

Substituting B The wavefunction will be formed:

$$\psi(z) = A e^{ikz}[\exp(i\frac{\pi}{a}z) + \frac{E - \frac{\hbar^2}{2m}(\kappa + \frac{\pi}{a})^2}{V}\exp(-i\frac{\pi}{a}z)] \quad \text{(eq. 1.5.5)}$$

where A is a normalization factor. The energy eigenvalues must be clarified.

$$(\frac{\hbar^2}{2m}(\kappa-\frac{\pi}{a})^2-E)\frac{(E-\frac{\hbar^2}{2m}(\kappa-\frac{\pi}{a})^2)}{V}B+VB=0$$

$$\Rightarrow -V^2=-(E-\frac{\hbar^2}{2m}(\kappa-\frac{\pi}{a})^2)(E-\frac{\hbar^2}{2m}(\kappa-\frac{\pi}{a})^2)$$

$$\Rightarrow E^2-\frac{\hbar^2}{2m}[(\kappa-\frac{\pi}{a})^2+(\kappa+\frac{\pi}{a})^2]E+(\frac{\hbar^2}{2m}(\kappa^2-(\frac{\pi}{a})^2))^2-V^2=0$$

$$\Rightarrow E^2-\frac{\hbar^2}{2m}(2\kappa^2+2(\frac{\pi}{a})^2)E+(\frac{\hbar^2}{2m}(\kappa^2-(\frac{\pi}{a})^2))^2-V^2=0$$

$$\Rightarrow E^2-\frac{\hbar^2}{m}(\kappa^2+(\frac{\pi}{a})^2)E+(\frac{\hbar^2}{2m}(\kappa^2-(\frac{\pi}{a})^2))^2-V^2=0$$

The target is to find the energy eigenvalues. The polyonymal's discriminant is:

$$\Delta=(\frac{\hbar^2}{m}(\kappa^2+(\frac{\pi}{a})^2))^2-4[(\frac{\hbar^2}{2m}(\kappa^2-(\frac{\pi}{a})^2))^2-V^2]=(\frac{\hbar^2}{m}(\kappa^2+(\frac{\pi}{a})^2))^2-4(\frac{\hbar^2}{2m}(\kappa^2-(\frac{\pi}{a})^2))^2+4V^2$$

$$\Rightarrow \Delta=(\frac{\hbar^2}{m}(\kappa^2+(\frac{\pi}{a})^2))^2-(\frac{\hbar^2}{m}(\kappa^2-(\frac{\pi}{a})^2))^2+4V^2=\frac{\hbar^2}{m}[(\kappa^2+(\frac{\pi}{a})^2)^2-(\kappa^2-(\frac{\pi}{a})^2)^2]+4V^2$$

$$\Rightarrow \Delta=(\frac{\hbar^2}{m})^2[4\kappa^2(\frac{\pi}{a})^2]+4V^2=4[(\frac{\hbar^2\kappa\pi}{ma})^2+V^2]$$

So, the solutions can be determinated:

$$E_{\pm}=\frac{1}{2}[\frac{\hbar^2}{m}(\kappa^2+(\frac{\pi}{a})^2)\pm 2\sqrt{(\frac{\hbar^2\kappa\pi}{ma})^2+V^2}]=\frac{\hbar^2}{2m}(\kappa^2+(\frac{\pi}{a})^2)\pm\sqrt{V^2((\frac{\hbar^2\kappa\pi}{maV})^2+1)}$$

$$\Rightarrow E_{\pm}=\frac{\hbar^2}{2m}(\kappa^2+(\frac{\pi}{a})^2)\pm|V|\sqrt{(\frac{\hbar^2\kappa\pi}{maV})^2+1}=\frac{\hbar^2}{2m}((\kappa+\frac{\pi}{a})^2-2\kappa\frac{\pi}{a})\pm|V|\sqrt{(\frac{\hbar^2\kappa\pi}{maV})^2+1}$$

$$\Rightarrow E_{\pm}=\frac{\hbar^2}{2m}(\kappa+\frac{\pi}{a})^2-\frac{\hbar^2\kappa\pi}{m\alpha}\pm|V|\sqrt{(\frac{\hbar^2\kappa\pi}{maV})^2+1}=\frac{\hbar^2}{2m}(\frac{\pi}{a}+\kappa)^2\pm|\hat{V}|[-\frac{\hbar^2\pi\kappa}{ma|\hat{V}|}\pm\sqrt{(\frac{\hbar^2\pi\kappa}{ma|\hat{V}|})^2+1}]$$

$$E_{\pm}=\frac{\hbar^2}{2m}(\frac{\pi}{a}+\kappa)^2\pm|\hat{V}|[-\frac{\hbar^2\pi\kappa}{ma|\hat{V}|}\pm\sqrt{(\frac{\hbar^2\pi\kappa}{ma|\hat{V}|})^2+1}] \quad \text{(eq. 1.5.6)}$$

- *Deep inside the crystal*

The solution of the wavefunction have to be separated into three regions, deep inside the crystal, near to the surface and after the vacuum.

For regions deep inside the crystal (z << 0, subscript i) the electron wave functions ψ_i are obtained by using the above energy eigenvalues and substituting appropriate leads to:

$$\begin{cases}\psi(z)=A\,e^{ikz}[\exp(i\frac{\pi}{a}z)+\dfrac{E-\frac{\hbar^2}{2m}(\kappa+\frac{\pi}{a})^2}{V}\exp(-i\frac{\pi}{a}z)] \\ E_{\pm}=\frac{\hbar^2}{2m}(\frac{\pi}{a}+\kappa)^2\pm|\hat{V}|[-\frac{\hbar^2\pi\kappa}{ma|\hat{V}|}\pm\sqrt{\frac{\hbar^2\pi\kappa}{ma|\hat{V}|}+1}]\end{cases}$$

$$\Rightarrow \Psi_{deep\,inside}=\Psi_i=A\,e^{i\kappa z}[e^{i\pi z/a}+\frac{|\hat{V}|}{\hat{V}}[-\frac{\hbar^2\pi\kappa}{ma|\hat{V}|}\pm\sqrt{\frac{\hbar^2\pi\kappa}{ma|\hat{V}|}+1}]e^{-i\pi z/a}]$$

where A is a normalization factor. Deep inside the crystal, we get the familiar electronic bands $E(k_\perp)$,which are periodic in reciprocal $k_\perp$ - space. Near the zone boundaries we have splitting into allowed and forbidden energy bands where the forbidden energy region has a width of $2|\hat{V}|$ as you can see from the energy formula for κ =0:

$$E_{\pm}(\kappa=0)=\frac{\hbar^2}{2m}(\frac{\pi}{a})^2\pm|\hat{V}| \quad \text{(eq. 1.5.7)}$$

$$\begin{cases} for\ E_{+(\kappa=0)}: \psi_i(z) = A e^{ikz}[\exp(i\frac{\pi}{a}z) + \frac{E_+ - \frac{\hbar^2}{2m}(\frac{\pi}{a})^2}{V}\exp(-i\frac{\pi}{a}z)] = A e^{ikz}[e^{i\frac{\pi}{a}z} + \frac{|\hat{V}|}{V}e^{-i\frac{\pi}{a}z}] \\ for\ E_{-(\kappa=0)}: \psi_i(z) = A e^{ikz}[\exp(i\frac{\pi}{a}z) + \frac{E_- - \frac{\hbar^2}{2m}(\frac{\pi}{a})^2}{V}\exp(-i\frac{\pi}{a}z)] = A e^{ikz}[e^{i\frac{\pi}{a}z} - \frac{|\hat{V}|}{V}e^{-i\frac{\pi}{a}z}] \end{cases}$$

if V>0 then:

$$\begin{cases} for\ E_{+(\kappa=0)}: \psi_i(z) = A e^{ikz}[e^{i\frac{\pi}{a}z} + e^{-i\frac{\pi}{a}z}] \sim e^{ikz}\cos(\frac{\pi}{a}z) \\ for\ E_{-(\kappa=0)}: \psi_i(z) = A e^{ikz}[e^{i\frac{\pi}{a}z} - e^{-i\frac{\pi}{a}z}] \sim e^{ikz}\sin(\frac{\pi}{a}z) \end{cases}$$

Otherwise (V<0):

$$\begin{cases} for\ E_{+(\kappa=0)}: \psi_i(z) = A e^{ikz}[e^{i\frac{\pi}{a}z} - e^{-i\frac{\pi}{a}z}] \sim e^{ikz}\sin(\frac{\pi}{a}z) \\ for\ E_{-(\kappa=0)}: \psi_i(z) = A e^{ikz}[e^{i\frac{\pi}{a}z} + e^{-i\frac{\pi}{a}z}] \sim e^{ikz}\cos(\frac{\pi}{a}z) \end{cases}$$

This results are absolutely related with the splitting near to the zone boundaries [15].

Summarized in a table they can be written:

	Energy	***Wavefunction***	
		V>0	***V<0***
Top of the gap	$\frac{\hbar^2}{2m}(\frac{\pi}{a})^2 + \lvert\hat{V}\rvert$	$\sim\cos(\frac{\pi}{a}z)$	$\sim\sin(\frac{\pi}{a}z)$
Bottom of the gap	$\frac{\hbar^2}{2m}(\frac{\pi}{a})^2 - \lvert\hat{V}\rvert$	$\sim\sin(\frac{\pi}{a}z)$	$\sim\cos(\frac{\pi}{a}z)$

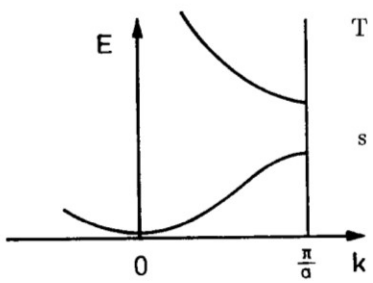

Figure 1.5.3 : Energy gap [15]

We now proceed the solution of the Schrödinger's equation near a solid surface and also near the end of the chain.

- *In the vacuum region:*

The wavefunction solution in the constant potetnial V_0 has to be exponentially decaying:

$$\Psi_0 = D e^{-\sqrt{\frac{2m}{\hbar^2}(V_0 - E)}z}, E < V_0 \quad \text{(eq. 2.5.8)}$$

We are interested to find the solution near a solid surface.

- *Near the Surface :*

There are two ways to determine the surface solutions.

Since Ψ_0 has no complex contribution $e^{i\kappa z}$ it can only be matched with the solutions inside the crystal ψ_i if you have a superposition of an incoming and a reflected wave (standing wave):

$$\Psi_0(z=0) = a\Psi_i(z=0,\kappa) + \beta\Psi_i(z=0,-\kappa) \quad \text{(eq. 1.5.9)}$$

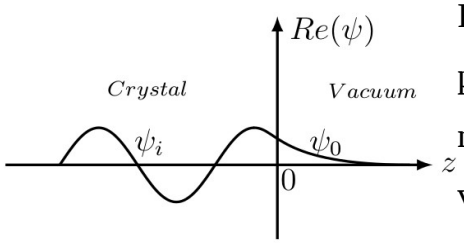

Figure 1.5.4 : Real part of wavefunction for a standing Bloch wave

From the Figure, we can understand that a surface state is possible to be described by a standing Bloch wave and matched with an exponentially decaying tail Ψ_0 in the vacuum.

The other way for the surface solutions could become possible if we allow complex wave vectors. Letting κ to be imaginary (κ = -iq) (1.5.10) and defining $\gamma = i\sin(2\delta) = -i\frac{\hbar^2 \pi q}{ma|\hat{V}|}$ (2.5.11) , the energy formula would be formed :

$$E = E_{\pm} = \frac{\hbar^2}{2m}\left(\frac{\pi}{a} + \kappa\right)^2 + |\hat{V}|\left[-\frac{\hbar^2 \pi \kappa}{ma|\hat{V}|} \pm \sqrt{\left(\frac{\hbar^2 \pi \kappa}{ma|\hat{V}|}\right)^2 + 1}\right]$$

$$\Rightarrow E = \frac{\hbar^2}{2m}\left(\frac{\pi}{a} - iq\right)^2 + |\hat{V}|\left[i\frac{\hbar^2 \pi q}{ma|\hat{V}|} \pm \sqrt{\left(-i\frac{\hbar^2 \pi q}{ma|\hat{V}|}\right)^2 + 1}\right]$$

$$\Rightarrow E = \frac{\hbar^2}{2m}\left(\left(\frac{\pi}{a}\right)^2 - q^2 - 2iq\frac{\pi}{a}\right) + i\frac{\hbar^2 \pi q}{ma} \pm |\hat{V}|\sqrt{1 - \left(\frac{\hbar^2 \pi q}{ma|\hat{V}|}\right)^2}$$

$$\Rightarrow E = \frac{\hbar^2}{2m}\left(\left(\frac{\pi}{a}\right)^2 - q^2\right) \pm |\hat{V}|\sqrt{1 - \left(\frac{\hbar^2 \pi q}{ma|\hat{V}|}\right)^2} \quad (2.5.12)$$

Corresponding, for the wavefunction :

$$\Psi'_i = A e^{i\kappa z}\left[e^{i\pi z/a} \pm \frac{|\hat{V}|}{\hat{V}}\left[-\frac{\hbar^2 \pi \kappa}{ma|\hat{V}|} \pm \sqrt{\left(\frac{\hbar^2 \pi \kappa}{ma|\hat{V}|}\right)^2 + 1}\right]e^{-i\pi z/a}\right], \kappa = -iq$$

$$\Rightarrow \Psi'_i = A e^{qz}\left[e^{i\pi z/a} \pm \frac{|\hat{V}|}{\hat{V}}\left[i\frac{\hbar^2 \pi q}{ma|\hat{V}|} \pm \sqrt{\left(-i\frac{\hbar^2 \pi q}{ma|\hat{V}|}\right)^2 + 1}\right]e^{-i\pi z/a}\right]$$

$$\Rightarrow \Psi'_i = A e^{qz}\left[e^{i\pi z/a} \pm \frac{|\hat{V}|}{\hat{V}}\left[i\frac{\hbar^2 \pi q}{ma|\hat{V}|} \pm \sqrt{1 + \left(-i\frac{\hbar^2 \pi q}{ma|\hat{V}|}\right)^2}\right]e^{-i\pi z/a}\right], \gamma = i\sin(2\delta) = -i\frac{\hbar^2 \pi q}{ma|\hat{V}|}$$

$$\Rightarrow \Psi'_i = A e^{qz}\left[e^{i\pi z/a} \pm \frac{|\hat{V}|}{\hat{V}}\left[i \cdot \sin(2\delta) \pm \sqrt{1 + (i \cdot \sin(2\delta))^2}\right]e^{-i\pi z/a}\right]$$

$$\Rightarrow \Psi'_i = A\,e^{qz}\left[e^{i\pi z/a} \pm \frac{|\widehat{V}|}{\widehat{V}}\left[i\cdot\sin(2\delta) \pm \sqrt{1-\sin^2(2\delta)}\right]e^{-i\pi z/a}\right], \sin^2(2\delta)+\cos^2(2\delta)=1$$

$$\Rightarrow \Psi'_i = A\,e^{qz}\left[e^{i\pi z/a} \pm \frac{|\widehat{V}|}{\widehat{V}}\left[i\cdot\sin(2\delta) \pm \sqrt{1-\sin^2(2\delta)}\right]e^{-i\pi z/a}\right], \sin^2(2\delta)+\cos^2(2\delta)=1$$

$$\Rightarrow \Psi'_i = A\,e^{qz}\left[e^{i\pi z/a} \pm \frac{|\widehat{V}|}{\widehat{V}}\left[i\cdot\sin(2\delta) \pm |\cos|(2\delta)\right]e^{-i\pi z/a}\right]$$

Although, $\pm\frac{|\widehat{V}|}{\widehat{V}} = \begin{cases} +1\,, if\ V>0 \\ -1\,, if\ V<0 \end{cases}$, the above wavefunction would be formed:

$$\Rightarrow \Psi'_i = A\,e^{qz}\left[e^{i\pi z/a} \pm \left[\cos(2\delta) \pm i\cdot\sin(2\delta)\right]e^{-i\pi z/a}\right], e^{\pm 2i\delta} = \cos(2\delta) \pm i\cdot\sin(2\delta)$$

$$\Rightarrow \Psi'_i = A\,e^{qz}\left[e^{i\pi z/a} \pm e^{\pm 2i\delta}\,e^{-i\pi z/a}\right]$$

$$\Rightarrow \Psi'_i = A\,e^{qz\pm i\delta}\left[e^{i\frac{\pi}{a}z\pm i\delta} \pm e^{-i\frac{\pi}{a}z\pm i\delta}\right]$$

$$\Rightarrow \begin{cases} \Psi'_i(z\le 0) = 2Ae^{q+i\delta}\cos\left(\frac{\pi}{\alpha}z \pm \delta\right) \sim e^{q+i\delta}\cos\left(\frac{\pi}{\alpha}z \pm \delta\right) \\ \Psi'_i(z\le 0) = 2iAe^{q-i\delta}\sin\left(\frac{\pi}{\alpha}z \pm \delta\right) \sim e^{q-i\delta}\sin\left(\frac{\pi}{\alpha}z \pm \delta\right) \end{cases}$$, q = -iκ (eq. 1.5.13)

where A is a normalization factor.

The probability density is: $\Rightarrow \begin{cases} |\Psi'_i(z\le 0)|^2 \sim e^{2qz}\cos^2\left(\frac{\pi}{\alpha}z \pm \delta\right) \\ |\Psi'_i(z\le 0)|^2 \sim e^{2qz}\sin^2\left(\frac{\pi}{\alpha}z \pm \delta\right) \end{cases}$

So, concisely, the wavefunction fro z<0 and z>0 , could be described:

$$\Rightarrow \begin{cases} \Psi'_i = A\,e^{qz\pm i\delta}\left[e^{i\frac{\pi}{a}z\pm i\delta} \pm e^{-i\frac{\pi}{a}z\pm i\delta}\right] \\ \Psi_0 = De^{-\sqrt{\frac{2m}{\hbar^2}(V_0-E)}z}\,, E<V_0 \end{cases}$$

At the surface should apply:

$$\begin{cases} \Psi_0(z=0) = \Psi'_i(z=0) \\ \dfrac{d\Psi_0}{dz}_{(z=0)} = \dfrac{d\Psi'_i}{dz}_{(z=0)} \end{cases}$$

Using these conditions, we can find the parameters A and D.

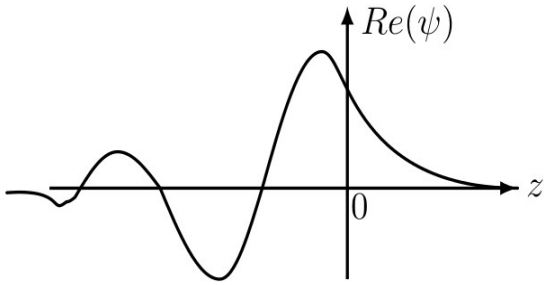

Figure 1.5.5 : Real part of one electron wavefunction for a surface state localized at the surface [11]

From the Figure 1.5.5, we can understand that a surface state wavefunction is localized at the surface. It is qualitatively Figure. As we expected, the amplitude vanishes for values far away from the surface and the electrons are localized within a couple of Ås of the surface plane.

As, it was shown , the energies eigenvalues are obtained as:

$$E(q) = \frac{\hbar^2}{2m}\left[\left(\frac{\pi}{a}\right)^2 - q^2\right] \pm |\hat{V}| \sqrt{1 - \left(\frac{\hbar^2 \pi q}{ma|\hat{V}|}\right)} \quad \text{(eq. 1.5.14)}$$

The values of E remain real and ψ doesn't diverge for z<<0 if $0 < q < q_{max} = ma|\hat{V}|\hbar^2\pi$. For these specific values of q and as we can observe from the formula of the Energy E(q) (eq. 1.5.14), all energies fall into the forbidden gap of the bulk electronic-band structure.

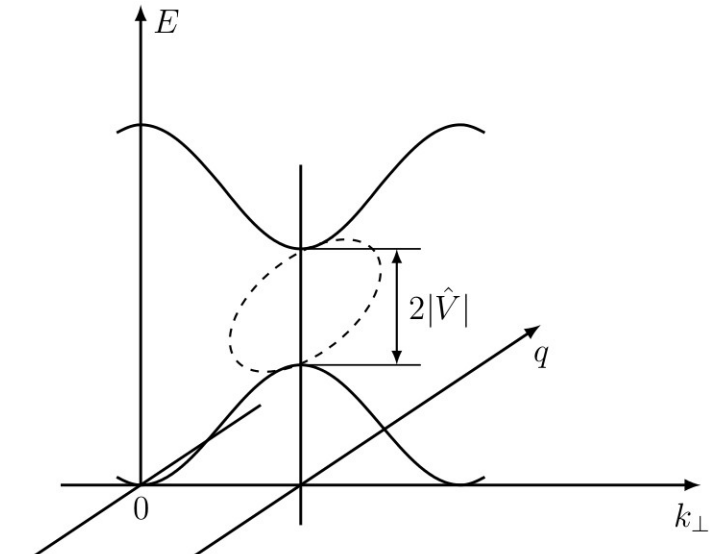

Figure 1.5.6 : Electronic band structure for a semi-infinite chain of atoms [11]

Another important consequence the matching conditions are restricting the allowed values for the energy eigenvalues. Within the continuous range of energy levels in the forbidden bulk band gap only one energy level is fixed by our matching conditions. So, this calculation of the semi-infinite chain yields as solution a single electron surface state located in the gap of the bulk states.

Now we can generalize this result of the one dimensional semi-infinite chain to the surface of a three dimensional crystal. The two dimensional translation symmetry parallel to the surface leads to a general Bloch-type wavefunction $\Phi_{ss}(r_\parallel, z)$ for the surface state. The model changes in $r_\parallel$ and are contributed by $e^{ik_\parallel r_\parallel}$ and the energy increases by the term $\hbar^2 k_\parallel^2 / 2m$.

$$\Phi_{ss}(r_\parallel, z) = u_{k_\parallel}(r_\parallel, z) \exp(i k_\parallel r_\parallel)$$

$$\Rightarrow \Phi_{ss}(r_\parallel, z) = \Psi(z) u_{k_\parallel}(r_\parallel) \exp(i k_\parallel r_\parallel)$$

Energy eigenvalues are then functions of $k_\perp = \pi/a - iq$ and $k_\parallel$. As a consequence the matching conditions which have to be fulfilled for every single $k_\parallel$ separately yield a (in general different) energy level for every $k_\parallel$ for the surface state. From that we get a two dimensional

band structure for the electronic surface states $E_{ss}(k_{\parallel})$.

$$E_{surface} = E_{k_\perp} + E_{ss}(k_{\parallel})$$

$$\Rightarrow E_{surface} = \frac{\hbar^2 k_\perp^2}{2m^*} + \frac{\hbar^2 k_{\parallel}^2}{2m^*}$$

where m^* is the effective mass of the electron.

It has to be mentioned that also the bulk electronic states live on the surface with only small modifications. One has to take them into account when mapping the true surface states.

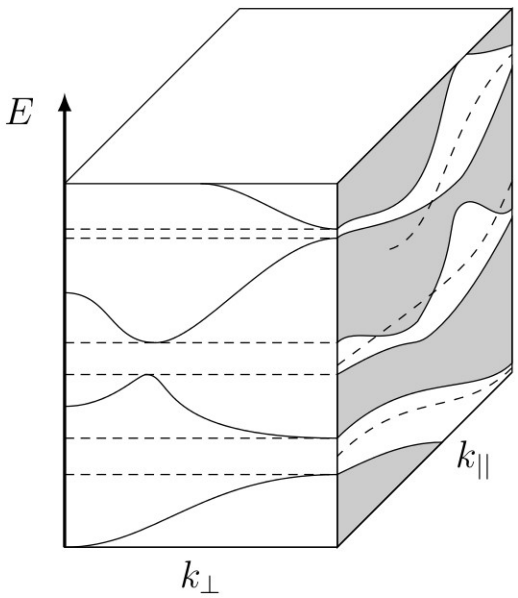

Figure 1.5.7 : Hypothetical electronic band structure of a crystal [11]

A surface state is described by the energy and its wave vector $k_{\parallel}$ parallel to the surface. Bulk state is characterized by both $k_{\parallel}$ and $k_\perp$ wave numbers. In the two-dimensional Brillouin zone of the surface, for each value of $k_{\parallel}$ therefore a rod of $k_\perp$ (where the symmetry is broken)is extending into the three-dimensional Brillouin zone of the Bulk. Bulk energy bands that are being cut by these rods allow states that penetrate deep into the crystal. One therefore generally distinguishes between true surface states and surface resonances. True surface states are characterized by energy bands that are not degenerate with bulk energy bands. These states are existing in the forbidden gap only and are therefore localized at the surface.

1.6 Tamm Surface States

Tamm States are named after the Russian physicist Igor Tamm respectively. Tamm States are called the surface states that are calculated by using the tight-binding model. In the tight binding approach, the electronic wavefunctions are usually expressed as linear combination of atomic orbitals (LCAO). [7] In contrast to the nearly free electron model used to describe the Shockley states, the Tamm states are suitable to describe also transition metals and wide gap semiconductors.

The lattice potential is constructed from a superposition of N free atom potentials at the position R_l, $V(\vec{r})=\sum_l U(\vec{r}-\vec{R}_l)$.

The non-self-consistent Schrödinger equation for the bands is

$$\hat{H}\psi = E\Psi \Rightarrow [-\frac{1}{2}\nabla^2 + V(\vec{r})]\Psi = E\Psi$$

$$\Rightarrow [-\frac{1}{2}\nabla^2 + U(\vec{r}) + (V(\vec{r}) - U(\vec{r}))]\Psi = E\Psi \quad (2.6.1)$$

The simplest trial function ansatz is a superposition of s-like Wannier orbitals:

$$\Psi_k(\vec{r}) = \sum_l a_{l,k}\Phi(\vec{r}-\vec{R}_l) \quad (1.6.2)$$

$$\text{and} \quad [-\frac{1}{2}\nabla^2 + U(\vec{r})]\Psi = E_0\Psi \quad (1.6.3)$$

When (1.6.2) is substituted into (1.6.1), a large number of Hamiltonian matrix elements are generated between orbitals centred on different sites.

$$\int d^3x \Phi^*(\vec{r}-\vec{R}_l)(V(\vec{r}) - U(\vec{r}-\vec{R}_l))\Phi(\vec{r}-\vec{R}_{l'}) = \begin{cases} -a, if\ l = l' \neq N, 1 \\ -\gamma, if\ l = l' \pm 1 \\ -a', if\ l = l' = N = 1 \\ 0, otherwise \end{cases}$$

$$\begin{bmatrix} H_{11} & \cdots & H_{1N} \\ H_{12} & \cdots & H_{2N} \\ \vdots & \ddots & \vdots \\ H_{N1} & \cdots & H_{NN} \end{bmatrix} \cdot \begin{bmatrix} c_1 \\ c_2 \\ \vdots \\ c_N \end{bmatrix} = E \cdot \begin{bmatrix} c_1 \\ c_2 \\ \vdots \\ c_N \end{bmatrix}$$

$$\Rightarrow \begin{bmatrix} E_0 - a' & -\gamma & 0 & \cdots & 0 \\ -\gamma & E_0 - \alpha & -\gamma & \cdots & 0 \\ 0 & -\gamma & E_0 - \alpha & \cdots & 0 \\ \vdots & \vdots & \vdots & \ddots & \vdots \\ 0 & \cdots & \cdots & -\gamma & E_0 - a' \end{bmatrix} \cdot \begin{bmatrix} c_1 \\ c_2 \\ c_3 \\ \vdots \\ c_N \end{bmatrix} = E \cdot \begin{bmatrix} c_1 \\ c_2 \\ c_3 \\ \vdots \\ c_N \end{bmatrix}$$

The result is a recursion relation for the expansion coefficients:

$$\begin{cases} \gamma c_{l-1} + (E - E_0 + a) c_l + \gamma c_{l+1} = 0 \\ (E - E_0 + a') c_1 + \gamma c_2 = 0 \\ \gamma c_{N-1} + (E - E_0 + \alpha') c_N = 0 \end{cases}$$

If $c_{l,k} = Ae^{ilkd} + Be^{-ilkd}$, and substituting l' =1,l $\pm$ 1 , then the $c_{l,k}$ would be written:

$$\begin{cases} c_{l-1} = Ae^{i(l-1)kd} + B^{-i(l-1)kd} \\ c_1 = Ae^{ikd} + B^{-ikd} \\ c_{l+1} = Ae^{i(l+1)kd} + Be^{-i(l+1)kd} \end{cases}$$

Thus, the dispersion of the energy spectrum will be formed:

$$E = E_k = E_0 - a - 2\gamma \cos(kd) \quad (1.6.4)$$

The solution will be completed if we found an expression for k. Using appropriately the equations, the parameter k would be written: $k = \frac{2\pi}{Nd} n$ and $a_{l,k} = \frac{1}{\sqrt{N}} e^{ikdl}$ with N different solutions, $-N/2 \leqslant n \leqslant N/2$.

As I mentioned above , the simplest trial function ansatz is a superposition of s-like Wannier orbitals: $\Psi_k(\vec{r})=\sum_l a_{l,k}\Phi(\vec{r}-\vec{R_l}) \qquad \Rightarrow \Psi_k(\vec{r})=\sum_l \frac{1}{\sqrt{N}} e^{ikdl}\Phi(\vec{r}-\vec{R_l})$

All these solutions have equal probability $|a_{l,k}|^2=\frac{1}{N}$ on each atom of the chain. This is not true for solutions on openended and semi-infinite chains, because all the atoms of the chain has the same probability.

This deadlock lead us to the concept of the local densities of states (LDOS) [16]. The density of states shows us how many states are in a given energy intervall at E.

$$\rho(E)\,dE=\sum_k \delta(E'-E_k)\,dE\,,\; E\leqslant E'\leqslant E+dE$$

As I mentioned above, we are interested in the local density of states :

$$\rho(E,r)=\sum_k |\Psi_k(r)|^2\,\delta(E'-E_k)=\sum_k |\langle \Psi_k(r)|\Psi_k(r)\rangle|^2\,\delta(E'-E_k)$$

or the density of states on atom - l : $\rho(E,l)=\sum_k \int_{cell\,of\,atom\,l} |\Psi_k(r)|^2\,\delta(E'-E_k)\,d^3r$

Using this way, we can define a surface state as a state with a large local density of states at the surface atom. On long chains or in crystals this is possible, when the amplitude of the wavefunction decays strongly towards the bulk. If this decay is exponential as for complex k, we speak of proper surface states. On the other hand, in cases where the amplitude near boundaries is much larger than on the bulk atoms. Although, these amplitudes persist throughout the crystal, we speak of surface resonances.

Specifically, if $|a'-a|>|\gamma|$ two of the roots are complex. For each, the corresponding eigenfunction has appreciable amplitude only on a surface atom and the energy of these states split off either above or below the bulk continuum ($E=E_k=E_0-a-2\gamma cos(kd)$).

Tamm surface states occur only if there is a strong enough disturbance ($a'\neq a$) of the potential right at the surface - exactly what one might expect at a semiconductor surface with broken bonds. [16]

2. Calculations and Results

2.1 DFT calculations and surfaces

In this project I study surface states. The basic target was to simulate a structure which would be infinite in the xy plane and finite along the z-axis. The periodicity will extend only on the xy-plane.

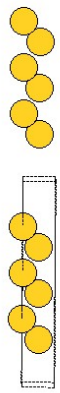

Figure 2.1.1: slab model of (100) plane, xz-plane with 6 atom laywers

The planes (100) and (111) are studied in this project.

We study both Au and Cu system.

To find the surface states, I followed three different methods that are based on wavefunctions and the probabilities:

1) Localization Probability

2) The Probability plot

3) The Probability Density along z-axis

We consider unrelaxed (ideal) surfaces as well as relaxed ones, where first and last layer of each slab are allowed to move in order to obtain the structure that minimizes the total energy.

2.2 Computational method

I studied two different planes, the (100) and the (111) plane. The plane (100) is orthogonal, as opposed to the plane (111), which is rhombohedral. Both planes contain one atom per cell.

Slab models were constructed using the relevant tool from Atomic Simulation Enviroment (ASE). For all cases, we use a unit cell where a slab of metal lies in the middle of the unit cell, separated by a thick vacuum region along z-axis (see Fig. 2.1.1). An essential part of the code is the vacuum that there is between the cells. The bigger is the vacuum, the better the results, because we avoid interactions between slabs.

To calculate the total energy, we used Grid-Projector Augmented Wave method (GPAW). It is an open source python code based on PAW method [17]. This method uses pseudo-wavefunctions according to the Born-Oppenheimer approximation, and make it possible to reconstruct the wavefunction more smooth near to the core, where there are a lot of correlations.

GPAW uses real-space grid for the calculations. This method has significant computational cost, especially in term of CPU time and memory space that occupies. However, it is very accurate and can be very easily parallelized and take advantage of modern multi-core computers.

In gpaw, the parameters that we have to consider are number of grid points and the k-points. The number of k-points is relative to the Brillouin zone. The number of the grid points is inversally proportional to the grid width, which is defined:

$h = \frac{a}{gpts + 1}$, where a is the length of the simulation box.

The accuracy of the results is depending to the number of the grid points. A big number of grid points leads the programm to a very time consuming calculations, so we have to find an appropriate number of grid points in order to have accurate results and not so much time to calculate.

In most materials, the grid width should be around 0,2 Å, in order to have good energy converge.

The k-points is also an important parameter. It is related with the Brillouin zone and the reciprocal lattice of the system, and also with the periodicity of the wavefunction. According to the Bloch's theorem, in a periodic system the energy eigenvalues can be described by a periodic function u(r), as: $\psi(r)=e^{i\vec{k}\cdot\vec{r}}u(r)$.

As was the case for grid points, the more $\vec{k}$ vectors are used, the more accurate the calculations are. At the same time, the computation time increases with increasing number of k-points. So we have to find again the smallest possible number of k-points that provides the desired accuracy of the results.

For the calculations below, the number of k-points was kpts=(9,9,1) (total of 81 $\vec{k}$, vectors), which provide periodicity to the xy plane only.

Below are some Figures with slabs builded by the (100) and (111) planes. Figures 2.2.1 and 2.2.2 describe FCC structure. Figure 2.2.3 is a simulation of a 5-atomic layers slab of Au(100), with 10 Å vacuum either the sides of slab. Figure 2.2.4 is exactly the same simulation as Figure 2.2.3, but for Au(111).

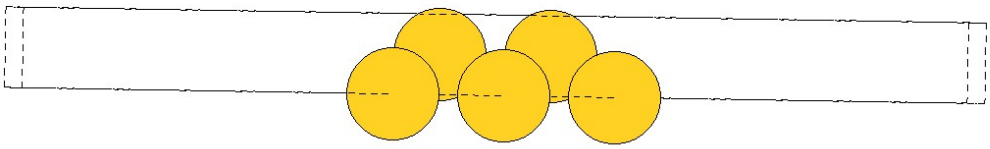

Figure 2.1.3: Simulation cell picturing a (100) slab with 5 atomic layers

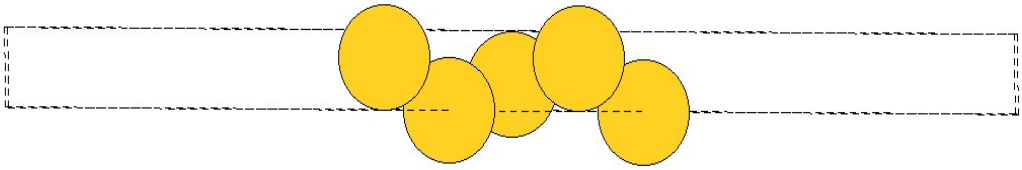

Figure 2.1.4:Simulation cell picturing a (111) slab with 5 atomic layers

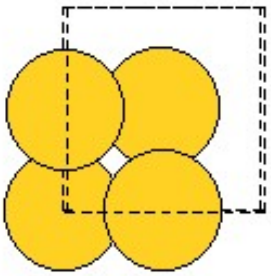

Figure 2.2.1: unit cell of the FCC structure ((100) plane)

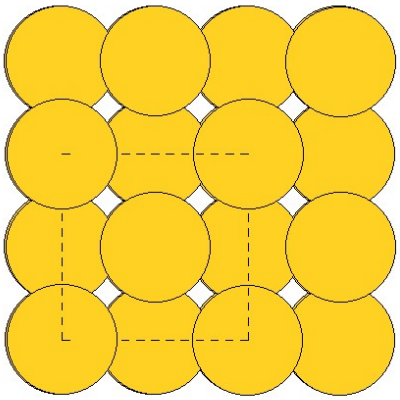

Figure 2.2.2: unit cell repeated along all axis((100) - plane)

2.3 Methods for locating surface states

This chapter includes the main results of this thesis. I follow specific methods to the results. At below subchapters we present three methods that confirm the results and the case of surface state.

- *Localization Probability:*

This method gives Probability per atom. A wavefunction that describes a Bloch state can be projected on atomic orbital. Using Dirac formalism the probability density could be described as:

$$|\psi_{n\vec{k}}(\vec{r})> = \sum c_{a,l,m} R(|\vec{r}-\vec{r}_a|)|Y_{l,m}(\theta_a,\varphi_a)>$$

$$\Rightarrow P_a = \sum_{l,m} |c_{a,l,m}|^2 \text{ and } \sum_a P_a = 1$$

a = number of atom

R(r) = sphericaly symmetric radial part of the wavefunction

The indices a correspond to the atoms that an slab contains. The indices l,m are coming from the spherical harmonics. We focused on τ = 0. In case τ = 0 is not included in the calculation, we use τ with the smallest magnitude. This way we examine the Bloch state with the highest symmetry. The probability per atom is calculated finding the lowest k-point of the system, and then we calculate the square of the absolute value of the product of pseudo wavefunction with the spherical harmonics for every band and all the atoms per band. The sum of the probabilities per band for the atoms must be equal to 1 ($\sum_a P_a = 1$). The next step was to find the maximum value of the probability, which is calculated for all the atoms per band, for the surface atoms of the slab. After a certain thickness, the probability for a surface state is getting to converge. If we measure a probability of 80-90 percentage for the first atom (or the first two atoms) of slab, it would give us strong evidence for the existence of a surface state.

- *Probability Plots*

This method is a graphical way to view a surface state. It is also a validation of the previous method. We save the numbers of bands that presented the highest probability for the edge atoms of slabs. Using the Atomic Simulation Enviroment (ASE) we create files (in .cube format) with the wavefunctions per atom for the specific states one for each. The next step is to plot these files using VMD (Visual Molecular Dynamics) and see the figure with the shell. The plot veryfies that these wavefunctions are indeed localized on edge atoms. [19]

- *Probability Density related with the distance on z-axis*

This time we calculate the square of the pseudo wavefunction for the specific number of band ($P(z)=|\Psi(z)|^2$) . The x- and y- components are averaged out:

$$P(z)=\int\int |\psi(x,y,z)|^2 dx\,dy$$

We normalize P(z) so that $\int P(z)\,dz=1$ within the simulation cell.

2.3.1 Localization Probability

This method is based on the probability density of the electrons. In a surface state, the electron is localized near the surfaces of the material. In other words, the electrons have to be localized on the first or the last atom of the simulation cell.

For each electronic state, we calculate the propability that the electron is localized at each atom. We then chose those bands that yield high probabilities at the edge atoms.

Some results of the plane (100) for various slab thickness.Each layer contains contains one atom per cell as it is shown in the structures of the Figures 2.3.1.1 and 2.3.1.2.

- *For the first atom*

Layers	***Band no.***	***Energy (eV)***	***E_{fermi} (eV)***	***E - E_{fermi} (eV)***	***Probability on surface atom***
10	52	-6,7475	-4,8850	-1,8625	~ 55 %
11	58	-6,7905	-4,9488	-1,8417	~ 73,5 %
12	63	-6,7776	-4,9137	-1,8639	~ 61 %
13	70	-6,7798	-4,9259	-1,8541	~ 72 %
14	76	-6,7815	-4,9261	-1,8554	~ 74 %
15	80	-6,7800	-4,9084	-1,8716	~ 74 %

Table 2.3.1.1: Electronic states localized at the first atom of each (100) slab. For each slab, we present the energy at the localized state, its difference from the Fermi level and the probability that this electron will be found at

Observing the Table 2.3.1, it is clear that after the fourteen atom-layers, the probability of a surface state is starting to converge. The surface state for each case is being observed five to eight bands above (on average six bands). As the atoms are increasing, the total number of the bands is increasing correspondingly. So, the Surface State is being observed at "similar" number of band as the number of atoms increases. A proof of this, is that the difference between the enegy of the band that a surface state is being observed and the Fermi level, is approximately constant as the number of atoms increase and the difference starts from the second decimal point.

Observing the Figure 2.3.1.1, the first atom has ~ 55% probability (the atom with the number 0) and the second has ~ 16%. So the first two atoms (near to the surface)present ~ 71% probability. The Figure 2.3.1.2 shows that The first atom has ~ 74% probability and the second has ~ 21%. So the first two atoms (near to the surface)present ~ 95% probability. It is a clear surface state!!

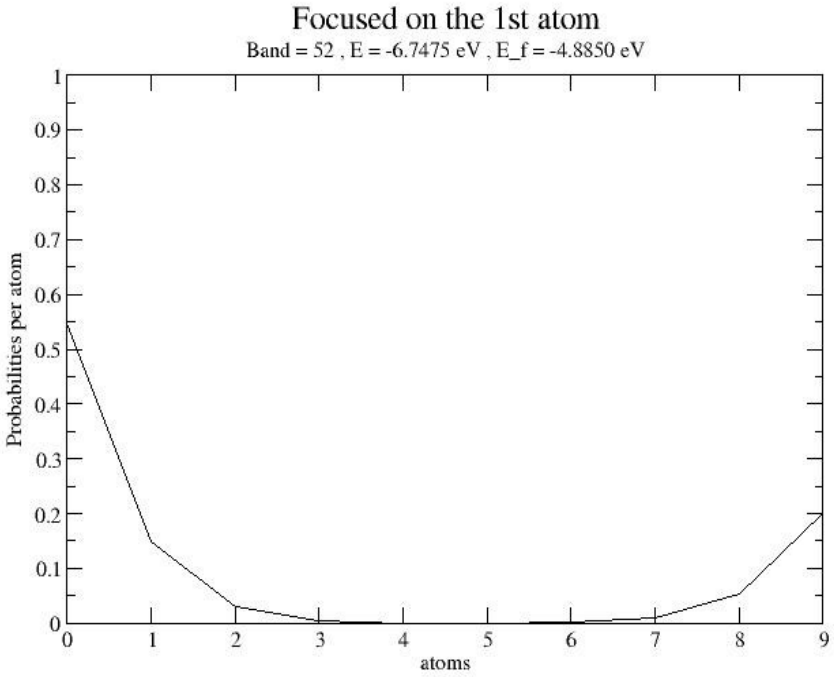

Figure 2.3.1.1: Probability of localization for a Au (100) slab with 10 layers.

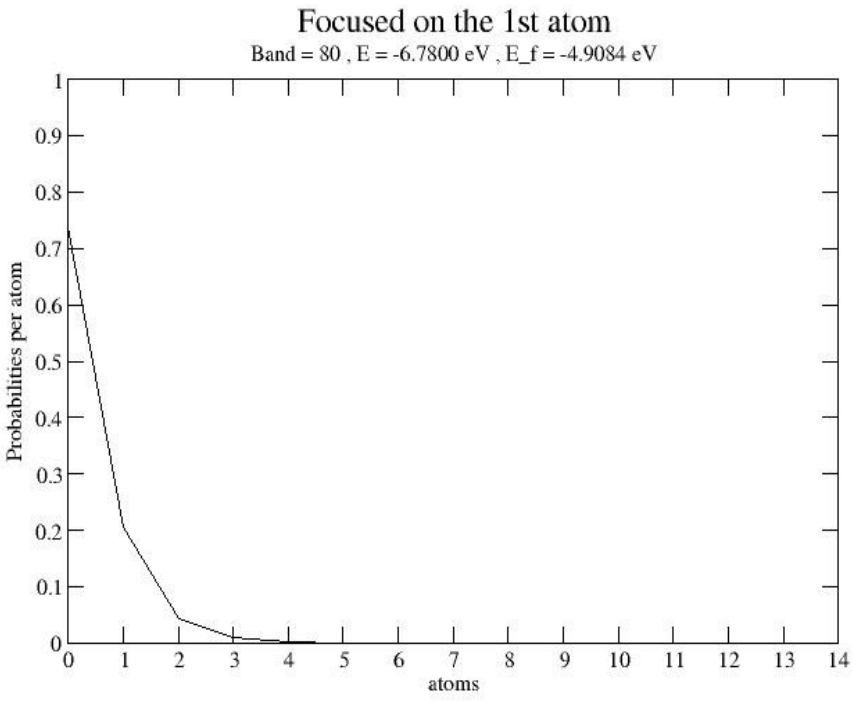

Figure 2.3.1.2: Same as Fig 2.3.1.1 for Au (100)slab with 15 layers.

We repeat the process and locate bands that are localized at the last layer of our simulation cell.

Layers	***Band***	***Energy (eV)***	***E_{fermi} (eV)***	***E - E_{fermi} (eV)***	***Probability on surface atom***
10	53	-6,7467	-4,8850	-1,8617	~ 55 %
11	57	-6,7994	-4,9488	-1,8506	~ 73,5 %
12	64	-6,7774	-4,9137	-1,8637	~ 61 %
13	69	-6,7800	-4,9259	-1,8538	~ 72 %
14	75	-6,7822	-4,9261	-1,8561	~ 74 %
15	81	-6,7795	-4,9084	-1,8711	~ 74 %

Table 2.3.1.2: Same as the Table 2.3.1.1 for the last atom of the Au (100) slab.

Continuing the process for the last atom on the (100) plane, we got the results quoting on the Table 2.3.2. Observing the table, it is clear that what was refered above is applied and in this case: *'Surface State is being observed at "similar" number of band as the number of atoms increases.'* The proof is exactly the same and related with the difference between the band energy and the Fermi energy.

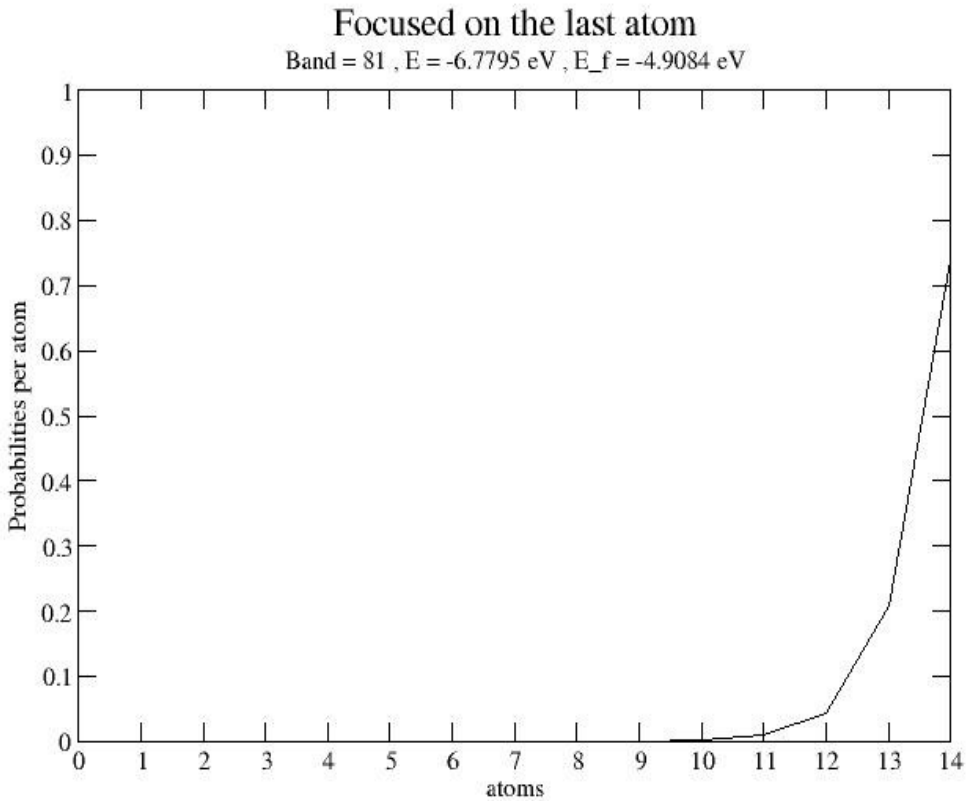

Figure 2.3.1.3: Same as Fig 2.3.1.2 for a band localized at the last atom.

Comparing the two Tables, someone could observe that the surface states for either the first or the last atom, occur at nearby (or 'neighboring') bands.

At the Figure 2.3.1.3, the last layer has ~ 74% probability (the atom with the number 14). It is a clear surface state at the other side of the slab.

Observing the Tables and the Figures of this subchapter, we can see that in small thickness slabs, the probability is shared at the edge layers (Fig 2.3.1.1). Increasing the thickness of slabs, it is defined localization on the one edge layer or the other of slab.

2.3.2 Probability Plots

In this subchapter is described the second way of the surface state appearance. This way is graphic. This way is a graphical verification of the previous process, which is refered before.

Figure 2.3.2.1 describes a 10-atomic layer slab with the peobability density almost shared on edge atoms, the first atom has around 55% probability, the second has ~ 14% and the last 20%. This situation occurs on band 52. Figure 2.3.2.2 describes the same situation as Fig. 2.3.2.1 but for 15 layer slab and different number of band. In this figure there is a clear surface state, because the first atom has ~ 86,4 % and the second ~ 21% probability density. The sum of the is around 97,4%. Clear Surface state!

Figures 2.3.2.3 and 2.3.2.4 describes the same situation as the Fig. 2.3.2.2 with periodicity on specific axis.

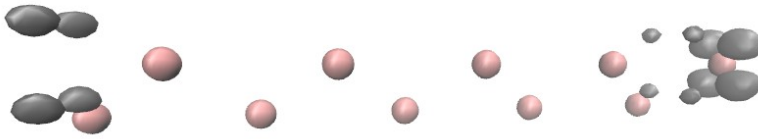

Figure 2.3.2.1: Contour plot of $|\psi|^2$ for band 52 in Au(100) slab with 10 layers. Compare to Fig. 2.3.1.1 .

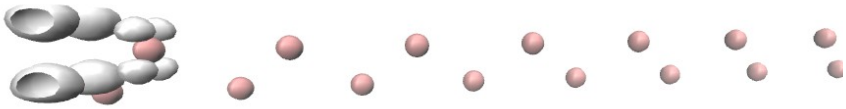

Figure 2.3.2.2: Same as Fig 2.3.2.1 for band 80 in Au(100) with 15 layers.

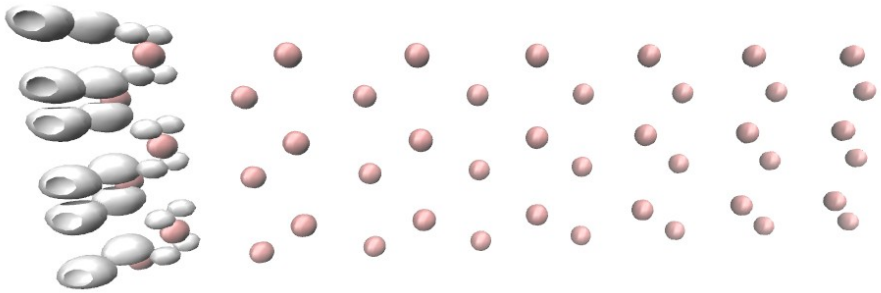

Figure 2.3.2.3: Same as Fig. 2.3.2.2, periodic on y-axis.

Figure 2.3.2.4: Same as Fig 2.3.2.2, periodic on z-axis

2.3.3 Probability Density along z-axis

In this subchapter we presented results from the third method. In the following table (Table 2.3.3.1) we present the positions of the Au slab with 10 atom – layer chain and Fig. 2.3.3.1 describes the probability density functional with the distance of the atoms on z – axis.

atom	*X – axis*	*Y – axis*	*Z - axis*
0	1.4425	1.4425	10.0000
1	0.0000	0.0000	12.0400
2	1.4425	1.4425	14.0800
3	0.0000	0.0000	16.1200
4	1.4425	1.4425	18.1600
5	0.0000	0.0000	20.2000
6	1.4425	1.4425	22.2400
7	0.0000	0.0000	24.2800
8	1.4425	1.4425	26.3200
9	0.0000	0.0000	28.3600

Table 2.3.3.1: Cartesian coordinates (in Å) of atoms in a ten-layer Au(100) slab.

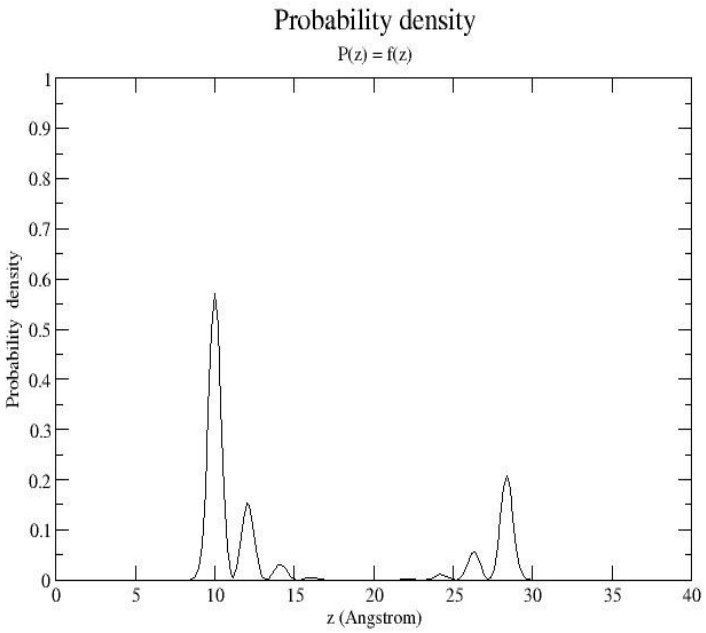

Figure 2.3.3.1: Probability density for Au(100) with 10– layers slab and for band 52.

Figure 2.3.3.1 presents exactly the same situation as the Figures 2.3.1.1 and 2.3.2.1, this time uses z-dependent probability density. Observing the Table 2.3.3.1, there is periodicity on the xy plane, in contrast to the z-axis where the slab is bounded between z = 10 and z = 28,36 Å.

Doing the same work for an Au chain with 15 atom – layer chain:

atom	*X – axis*	*Y – axis*	*Z - axis*
0	0.0000	0.0000	10.0000
1	1.4425	1.4425	12.0400
2	0.0000	0.0000	14.0800
3	1.4425	1.4425	16.1200
4	0.0000	0.0000	18.1600
5	1.4425	1.4425	20.2000
6	0.0000	0.0000	22.2400
7	1.4425	1.4425	24.2800
8	0.0000	0.0000	26.3200
9	1.4425	1.4425	28.3600
10	0.0000	0.0000	30.4000
11	1.4425	1.4425	32.4400
12	0.0000	0.0000	34.4800
13	1.4425	1.4425	36.5200
14	0.0000	0.0000	38.5600

Table 2.3.3.2: Cartesian coordinates (in Å) of atoms in a 15-layer Au(100) slab.

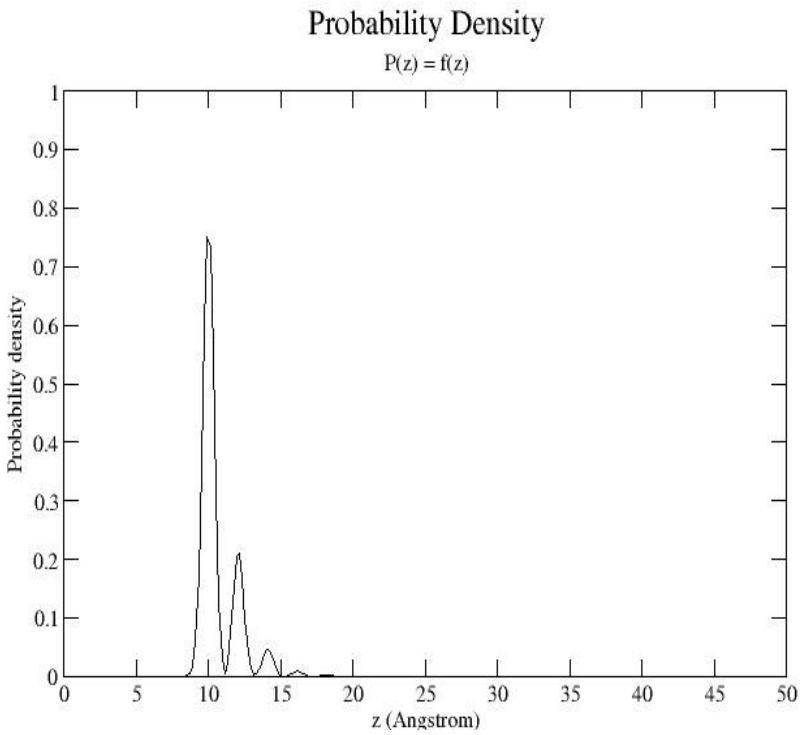

Figure 2.3.3.2: Probability density for Au(100) with 15– layers slab and for band 80.

Fig. 2.3.3.2 and 2.3.3.3 describe a clear surface state on the first and the last atom respectively, using the third method (Probability Density as a function of z). Table 2.3.3.2 shows the atom-positions. The first atom is at ten Å of the z-axis, where the surface state is located. Similarly, last atom, is at about 38,5 Å of the slab.

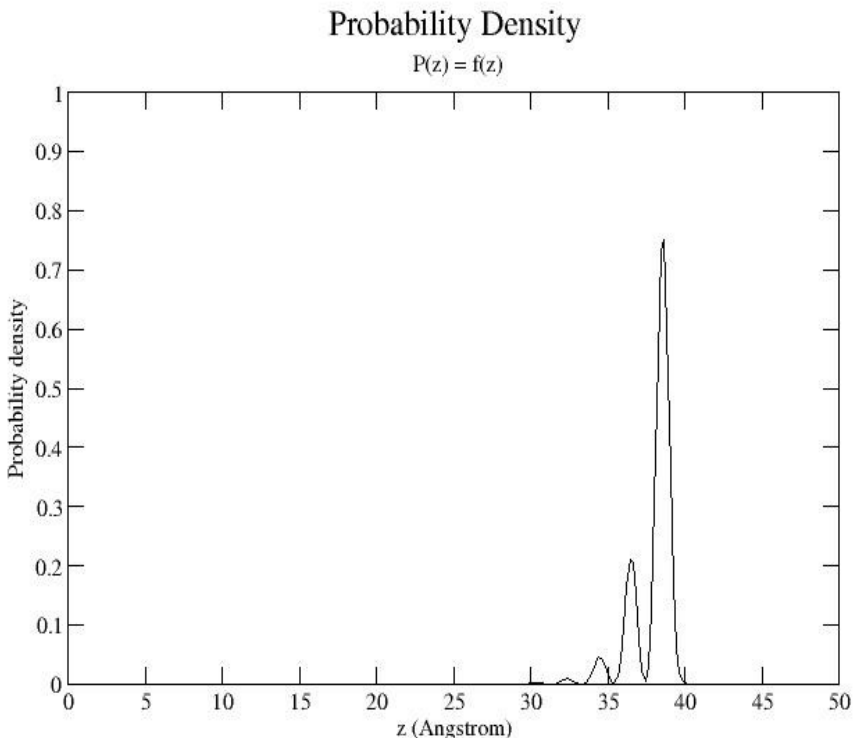

Figure 2.3.3.3: Probability density for the last atom of Au(100) with 10– layers slab and for band 81.

2.3.4 Au(111)

In this subchapter we present exactly the same work, but for Au (111). Continuing the process, surface states are confirmed by the same methods. Each layer contains one atom per cell as it is shown in the structures in Figures 2.3.4.1.

- *First atom*

Layers	Band no.	Energy (eV)	E_{fermi} (eV)	$E - E_{fermi}$ (eV)	Probability on surface atom	Similarly Bands
10	32	-9,0378	-4,9778	-4,0600	~ 44 %	33 , 34 , 35
11	38	-9,0385	-5,0091	-4,0294	~ 87 %	39
12	39	-9,0620	-4,9881	-4,0739	~ 87 %	40
13	45	-9,0731	-5,0381	-4,0350	~ 87 %	46
14	49	-9,0695	-5,0187	-4,0508	~ 87 %	50
15	52	-9,0470	-5,0061	-4,0409	~ 88 %	53

Table 2.3.4.1: Electronic States localized at the first atom of each (111) slab. For each slab, we present the energy at the localized state, its difference from the Fermi Level and the probability that this electron will be found at the first atom

- *Last atom*

Layers	Band no.	Energy (eV)	E_{fermi} (eV)	$E - E_{fermi}$ (eV)	Probability on surface atom	Similarly Bands
10	32	-9,0378	-4,9778	-4,0600	~ 44 %	33 , 34 , 35
11	38	-9,0481	-5,0091	-4,0390	~ 87 %	37
12	41	-9,0566	-4,9881	-4,0685	~ 87 %	42
13	43	-9,0745	-5,0381	-4,0364	~ 87 %	44
14	47	-9,0797	-5,0187	-4,0610	~ 87 %	48
15	50	-9,0554	-5,0061	-4,0493	~ 88 %	51

Table 2.3.4.2: Same as Table 2.3.4.1 for the last atom of the Au(111) slab..

Starting with the case of the 10 atom – layers slab, is proved that the three methods which were showed above confirms the same result.

Band no	***Energy (eV)***	***E_{fermi} (eV)***	***E - E_{fermi} (eV)***	***Probability on surface atom***	***Similarly Bands***
First atom					
32	-9,0378	-4,9778	-4,0600	~ 44 %	33 , 34 , 35
Last atom					
32	-9,0378	-4,9778	-4,0600	~ 44 %	33 , 34 , 35

Table 2.3.4.3: Electronic States localized at the first and the last atom simultaneously with the same probability at the same number of Band. In small thickness slabs, the probability is shared at the edge layers, as Au(100) occurs.

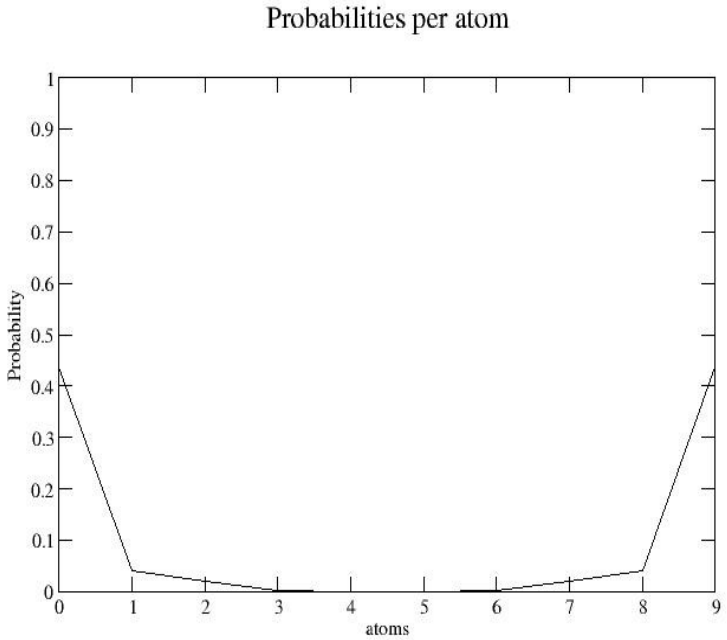

Figure 2.3.4.1: Probability of localization for a Au(111) slab with 10 layers.

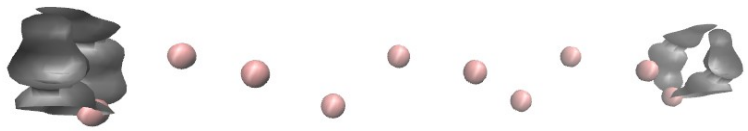

Figure 2.3.4.2: Contour plot of $|\psi|^2$ for band 52 in Au(100) slab with 10 layers. Compare to Fig. 2.3.4.1 .

atom	***X – axis***	***Y – axis***	***Z - axis***
0	0.0000	0.0000	10.0000
1	1.4425	0.8328	12.3556
2	0.0000	1.6657	14.7112
3	0.0000	0.0000	17.0668
4	1.4425	0.8328	19.4224
5	0.0000	1.6657	21.7779
6	0.0000	0.0000	24.1335
7	1.4425	0.8328	26.4891
8	0.0000	1.6657	28.8447
9	0.0000	0.0000	31.2003

Table 2.3.4.4: Cartesian coordinates (in Å) of a ten-layer slab.

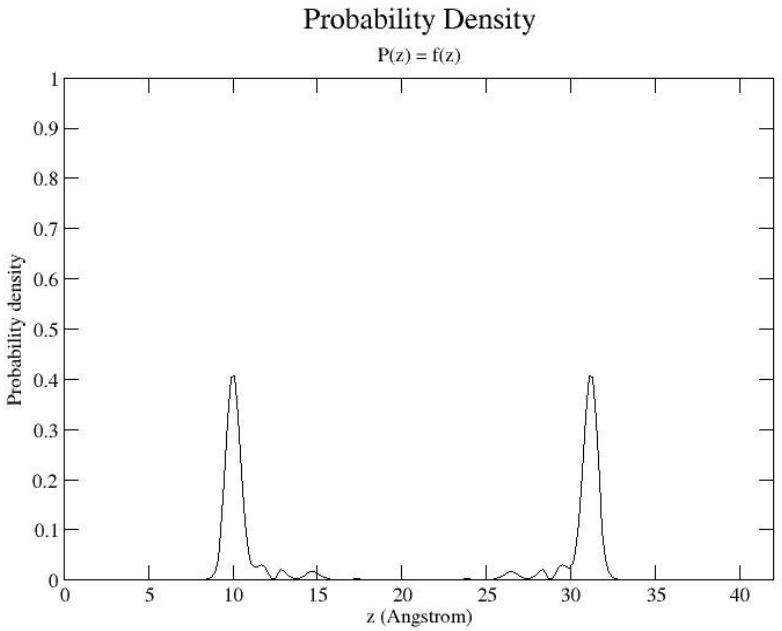

Figure 2.3.4.3: Probability density for Au (111)slab with 10 layers and for band 32.

Bands	***Energy (eV)***	***E – E Surf. St. (eV)***
31	-9,3127	-0,275
32	-9.0377	0
33	-9.0373	0,0004
34	-9.0370	0,0007
35	-9.0366	0,0011
36	-8.7815	-0,2562

Table 2.3.4.5: Near Band Energies of the electronic state that localized at the first and the last atom for a Au(111) slab with 10 layers and the Energy difference with the SS.

In this case, there is the same situation on the first and the last atom and it is confirmed by the three ways. Although, the remarkable point in this case is that the same probabilities appear at the bands 33, 34 and 35. It is explained by the energy. These bands are almost degenerated because differ from the second decimal place and later.

At the table below are the values of the Energy depending on the band and the differentiation between the Energy of the SS and the Energy bands of the table. The little difference between the Energy of the band that there is a surface state and the near bands is explained later. For now, the explaination coming from the symmetries.

Continuing with the case of the 15 atom – layers chain.

Band	***Energy (eV)***	***E_{fermi} (eV)***	***E - E_{fermi} (eV)***	***Probability on surface atom***	***Similarly Bands***
First atom					
52	-9,0470	-5,0061	-4,0409	~ 88 %	53
Last atom					
50	-9,0554	-5,0061	-4,0493	~ 88 %	51

Table 2.3.4.6: Electronic States localized at the first and the last atom with the same probability, at near bands.

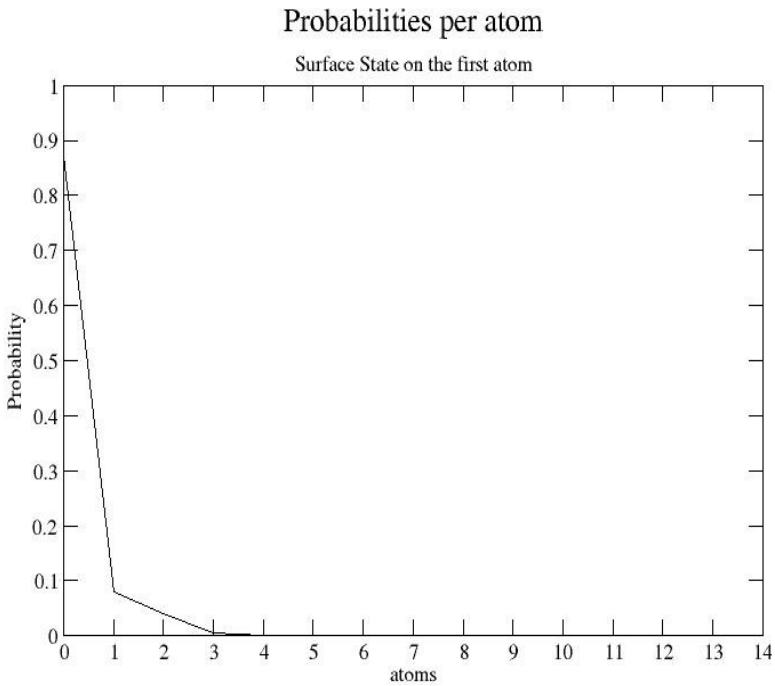

Figure 2.3.4.4: Probability of localization for a Au(111) slab with 15 layers.

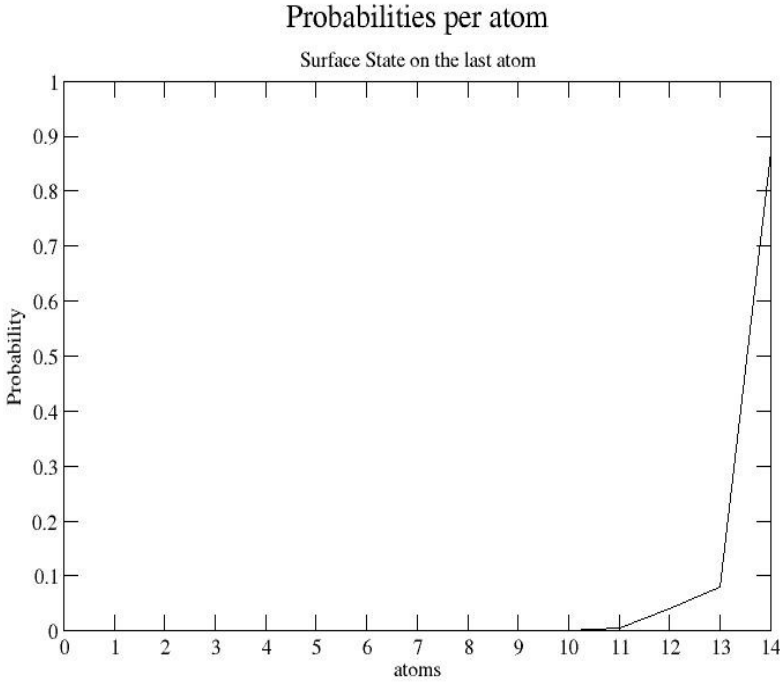

Figure 2.3.4.5: Same as Fig. 2.3.4.4 for the last atom-layer slab.

Figure 2.3.4.6: Contour plot of $|\psi|^2$ for band 52 in Au(111) slab with 15 layers. Compare to Fig. 2.3.4.4 .

Figure 2.3.4.7: Contour plot of $|\psi|^2$ for band 50 in Au(100) slab with 15 layers. Compare to Fig. 2.3.4.5 .

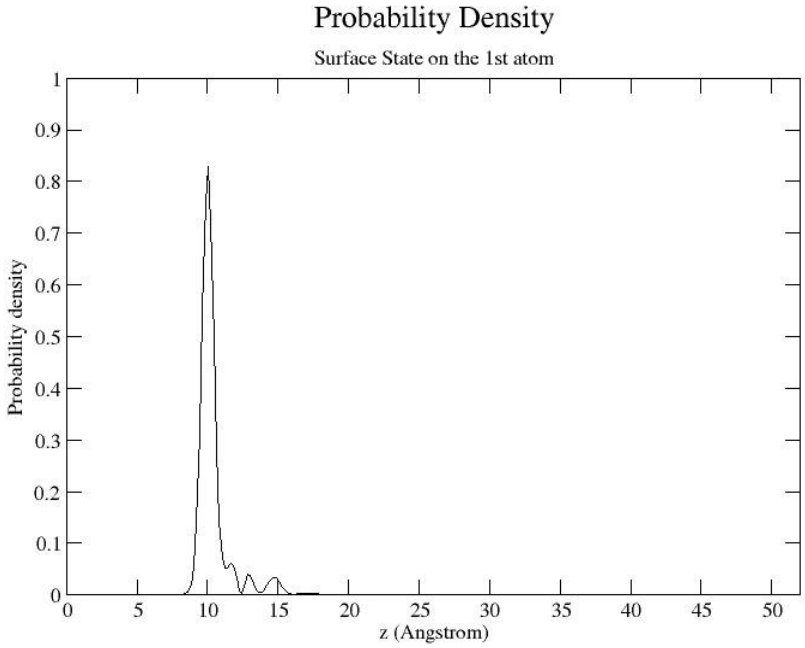

Figure 2.3.4.8: Probability density for Au (111) slab with 15 layers and for band 52. Compare to Fig. 2.3.4.4 and 2.3.4.6 .

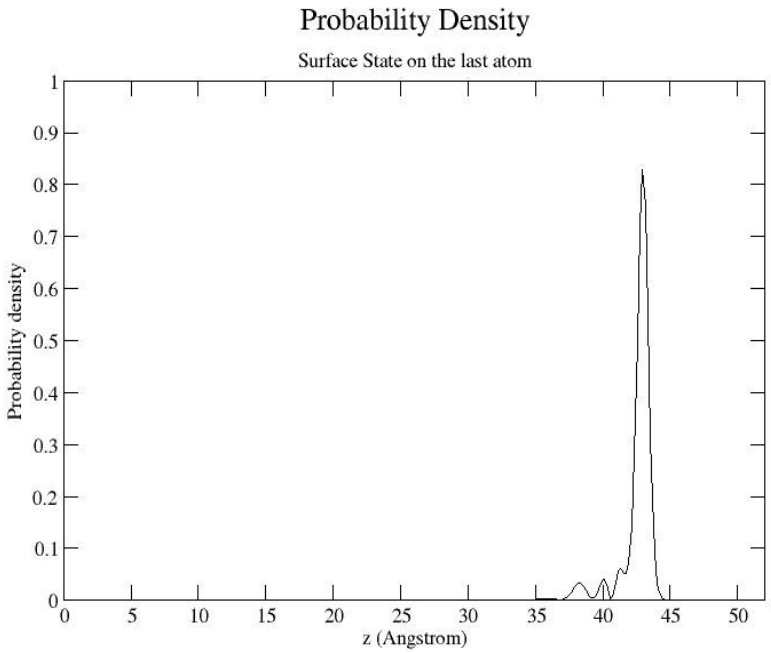

Figure 2.3.4.9: Probability density for Au (111) slab with 15 layers and for band 52. Compare to Fig. 2.3.4.5 and 2.3.4.7 .

Atom	*X – axis*	*Y – axis*	*Z - axis*
0	1.4425	0.8328	10.0000
1	0.0000	1.6657	12.3556
2	0.0000	0.0000	14.7112
3	1.4425	0.8328	17.0668
4	0.0000	1.6657	19.4224
5	0.0000	0.0000	21.7779
6	1.4425	0.8328	24.1335
7	0.0000	1.6657	26.4891
8	0.0000	0.0000	28.8447
9	1.4425	0.8328	31.2003
10	0.0000	1.6657	33.5559
11	0.0000	0.0000	35.9115
12	1.4425	0.8328	38.2671
13	0.0000	1.6657	40.6227
14	0.0000	0.0000	42.9782

Table 2.3.4.7: Cartesian coordinates (in Å) of atoms in a ten-layer Au(111) slab.

Observing the Figures below and the Table 2.3.4.5, there is a clear Surface State on the first and the last atom correspondingly. It is confirmed by the three ways.

The value of the probability is about 88%.

It is remarkable that the same probabilities for a surface state appearance present at neighboring bands for the first and the last atom respectively. As I refered below for the case of the 10 atom-laywer slab, these bands are almost degenerated because differ from the second decimal place and later. Exactly the same occurs here.

		First atom	*Last atom*
Bands	***Energy (eV)***	$E - E_{Surf.\ St.}$ *(eV)*	$E - E_{Surf.\ St.}$ *(eV)*
50	-9.0554	-	0
51	-9.0551	-	0,0003
52	-9.0470	0	-
53	-9.0466	0,0004	-

Table 2.3.4.8: Near Band Energies of the electronic state that localized at the first and the last atom for a Au(111) slab with 10 layers and the Energy difference with the SS.

Table 2.3.4.8 contains values of the Energy bands that observe the surface states and the differentiation between the Energy of the Surface State and the Energy bands of the table. The dashes are because the interest is to compare the Energy of the surface state with the energy of the band that present the same probability. So, it appears the same situation as the case of the 10 atom-laywer slab. In this case, the same probability appears only at one band, which is neighbor. The reason is the that the bands are almost degenerated, as I refered it previously. Although all the bands, that is presented a surface state on the first or the last atom, are neighboring. The explaination of this is the symmetries. There is a symmetry on z-axis and another one on xy-plane, on where there is periodicity. If I fold the chain, the one edge come to the other and the new chain is similar to the previous one. If I rotate the chain relative to z-axis, the chain never changes. These are the two explaination for the symmetries respectively.

2.4 Relaxed Surfaces

In this subchapter we repeat the calculation after relaxation of the atomic coordinates. Atom near the edges of each slab are allowed to move, so that the total energy is minimized. Using this process, surface states could be distinguished even to slabs with a few atoms. Below are data in tables, comparing the results before and after the minimization.

2.4.1 Relaxed Au(100):

Surface State on the 1st atom

Layers	Band no.	Energy (eV)	E_{fermi} (eV)	$E - E_{fermi}$ (eV)	Probability on surface atom
10	52	-6,7475	-4,8850	-1,8625	~ 55 %
	55	-6,7457	-4,9442	-1,8015	~ 85,5 %
11	58	-6,7905	-4,9488	-1,8417	~ 73,5 %
	59	-6,7898	-5,0386	-1,7512	~ 86,6 %
12	63	-6,7776	-4,9137	-1,8639	~ 61 %
	63	-6,7750	-4,9788	-1,7962	~ 85,2 %
13	70	-6,7798	-4,9259	-1,8541	~ 72 %
	69	-6,7808	-5,0054	-1,7754	~ 86,2 %
14	76	-6,7815	-4,9261	-1,8554	~ 74 %
	76	-6,7811	-4,9965	-1,7846	~ 84,1 %
15	80	-6,7800	-4,9084	-1,8716	~ 74 %
	81	-6,7730	-4,9966	-1,7764	~ 86,4 %

Table 2.4.1.1: Surface State for Au (100) slabs. For every atom-laywer slab, the first line gives the surface state before the relaxation and the second after relaxation of atomic coordinates.

atom	*X – axis*	*Y – axis*	*Z - axis*
0	0.0000	0.0000	9,8390
1	1.4425	1.4425	12.0400
2	0.0000	0.0000	14.0800
3	1.4425	1.4425	16.1200
4	0.0000	0.0000	18.1600
5	1.4425	1.4425	20.2000
6	0.0000	0.0000	22.2400
7	1.4425	1.4425	24.2800
8	0.0000	0.0000	26.3200
9	1.4425	1.4425	28.3600
10	0.0000	0.0000	30.4000
11	1.4425	1.4425	32.4400
12	0.0000	0.0000	34.4800
13	1.4425	1.4425	36.5200
14	0.0000	0.0000	38.7210

Table 2.4.1.2: *Atom positions of the 15 atom – layer slabs, builded by the Au (100) after relaxation.*

The Table 2.4.1.2 has positions of 15 atom-layers on the (100) plane after the minimization. Comparing with the Table 2.3.3.2 is clear that the only difference between the two Tables is the z-component of the surface atoms. The minimization is applied on the edge atoms. So, these atoms are moving to minimize the total energy of the system. The distance of the edge atoms to the rest of chain is the same and is 2.20 Å on z-axis. The atoms of the relaxed slab has the same distance between them, 2.04 Å.

Observing the Table 2.4.1.1 it is clear that the probability of a surface state converges from the 10 atom-layer chain. And a matter of fact is that after the relaxation the probability is getting higher than before. Furthermore, surface state is presented at lower bands, so the SS Energy minimizes. A characteristic case is the chain of 12 atoms, where the SS presents on the same band as before the minimization, although the Energy of the band that appear the SS is minimized. Also, the difference between the SS Energy and the Energy Fermi is about 1,78 eV.

The Table 2.4.1.1 refers to the first atom of each slab. Exactly the same are applied to the last atom SS. The corresponding table is in the appendix.

2.4.2 Relaxed Au(111)

Surface State on the 1st atom:

Layers	Band	Energy (eV)	E_{fermi} (eV)	$E - E_{fermi}$ (eV)	Probability on surface atom	Similarly Bands
10	32	-9,0378	-4,9778	-4,0600	~ 44 %	33 , 34 , 35
	32	-8,9046	-5,0505	-3,8541	~ 94,5 %	33
11	38	-9,0385	-5,0091	-4,0294	~ 87 %	39
	36	-8,9280	-5,1017	-3,8262	~ 93,3 %	37
12	39	-9,0620	-4,9881	-4,0739	~ 87 %	40
	40	-8,9498	-5,1027	-3,8471	~ 94,6 %	41
13	45	-9,0731	-5,0381	-4,0350	~ 87 %	46
	43	-8,8886	-5,0691	-3,8195	~ 95 %	44
14	49	-9,0695	-5,0187	-4,0508	~ 87 %	50
	47	-8,9397	-5,1029	-3,8368	~ 94,2 %	-
15	52	-9,0470	-5,0061	-4,0409	~ 88 %	53
	51	-8,9290	-5,1151	-3,8139	~ 95 %	52

Table 2.4.2.1: Surface State for Au (111) slabs. For every atom-laywer slab, the first line gives the surface state before the relaxation and the second after relaxation of atomic coordinates.

atom	X – axis	Y – axis	Z - axis
0	0.0000	0.0000	9,8090
9	0.0000	0.0000	31.3920

Table 2.4.2.2: Cartesian coordinates (in Å) of edge atom for a relaxed 15-layer slab.

In this plane was followed exactly the same process as the (100). The same comments apply as before. The distance of the edge atoms to the rest of chain is the same and is 2.55 Å on z-axis.

The atoms of the rest chain has the same distance between them, 2.356 Å. This is the case, in which the same situation appears at a near band. It was explained before, at 2.3.4 subchapter. The explanation is coming from the two symmetries, the fold and rotate of the chain relative to the z-axis. The rotation gives a symmetry on the xy-plane. So, the two components of the plane gives the degeneracy and this gives the same results. The corresponding table for the last atom is in the appendix.

2.5 Workfunction

The next step of the project is to calculate the workfunction for the two surfaces I considered. The workfunction, can be obtained from the potential energy curve from either sides of the slab.

In the theory, the slabs are semi-infinite, so the potential energy could be measured from the one side. Although, in my case, in which the chain is finite, the potential energy have to be measured in either sides.

The two planes might have different workfunctions. This is caused to the structure and the distance between the atoms respectively.

2.5.1 Potential Energy

In this subchapter we present results for an electron as a function of its z-coordinate. Below are Tables with the results, in which V_{left} is the workfunction from the left side of the slab and V_{right} is the workfunction from the right side.

For the Plane 100:

- *Before minimization*

Layers	V_{left}	V_{right}	E_{Fermi}
10	4,856	4,858	-4,885
11	4,839	4,840	-4,949
12	4,798	4,798	-4,914
13	4,801	4,802	-4,926
14	4,801	4,801	-4,926
15	4,791	4,794	-4,908

Table2.5.1.1: Potential Energy from the two sides of the slabs and the Fermi level before relaxed Au (100) slabs.

- *After minimization:*

Layers	V_{left}	V_{right}	E_{Fermi}
10	4,878	4,826	-4,944
11	5,059	5,086	-5,035
12	5,008	5,007	-4,979
13	4,908	5,056	-5,005
14	4,973	4,958	-4,997
15	4,919	4,966	-4,997

Table2.5.1.2: Same as Table 2.5.1.1 for relaxed Au (100) slabs.

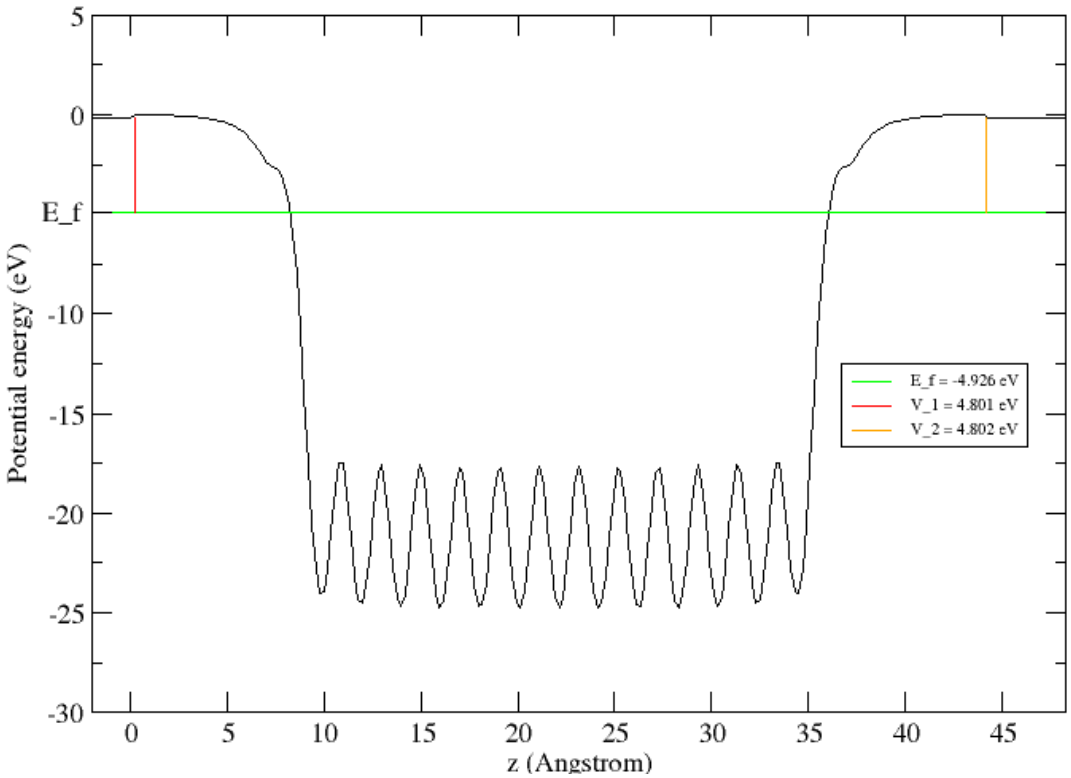

Figure 2.5.1.1: Total electronic potential for 13-layer Au (100) slab before minimization.

In the Figure 2.5.1.1, it is clear that at the positions that the atoms are located, there is a minimum peak. Observing the total Figure, the potential energy looks like a cosine function, similarly to the Schockley model. The constant value of the potential energy from the left side is about 4,801 eV and at the right 4,802 eV. These energies are calculated from the differnce between the Fermi level and the point that begins the potential energy.

In the Figure 2.5.1.2 occurs exactly the same situation as the Figure 2.5.1.1 . The only difference is the number of the atoms. So as the number of the atoms grows, the length of the chain is getting bigger. The potential energy from the left side is about 4,791 eV and at the right 4,794 eV. The number of the peaks corresponds to the number of the atoms.

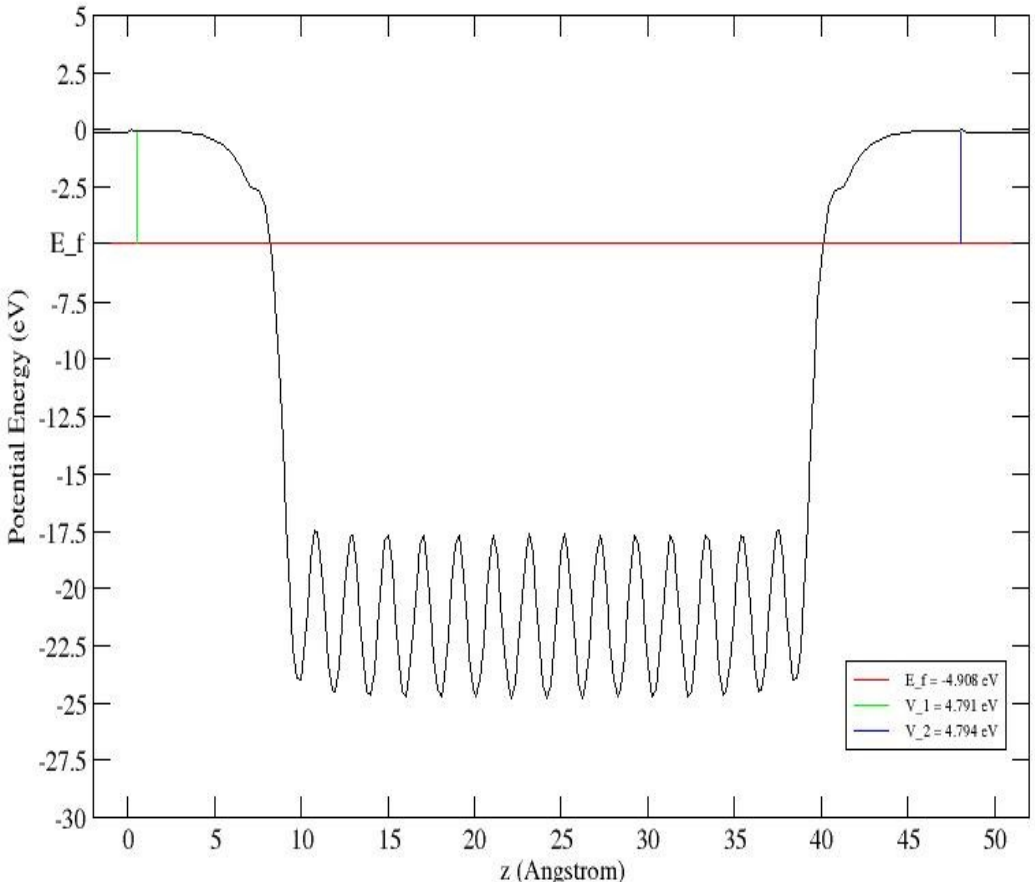

Figure 2.5.1.2: Same as Fig. 2.51.1 for 15-layer Au (100) slab.

For the Plane (111):

- *Before minimization*

Atoms	V_{left}	V_{right}	E_{Fermi}
10	4,894	4,894	-4,978
11	4,889	4,891	-5,009
12	4,949	4,937	-4,988
13	5,048	5,058	-5,038
14	5,003	5,042	-5,019
15	4,945	5,007	-5,006

Table 2.5.1.3: Same as Table 2.5.1.1 before relaxed Au (111) slabs.

- *After minimization:*

Atoms	V_{left}	V_{right}	E_{Fermi}
10	5,032	5,032	-5,050
11	5,109	5,124	-5,102
12	5,118	5,126	-5,103
13	5,049	5,054	-5,069
14	5,187	5,037	-5,103
15	5,092	5,092	-5,115

Table2.5.1.4: Same as Table 2.5.1.1 for relaxed Au (111) slabs..

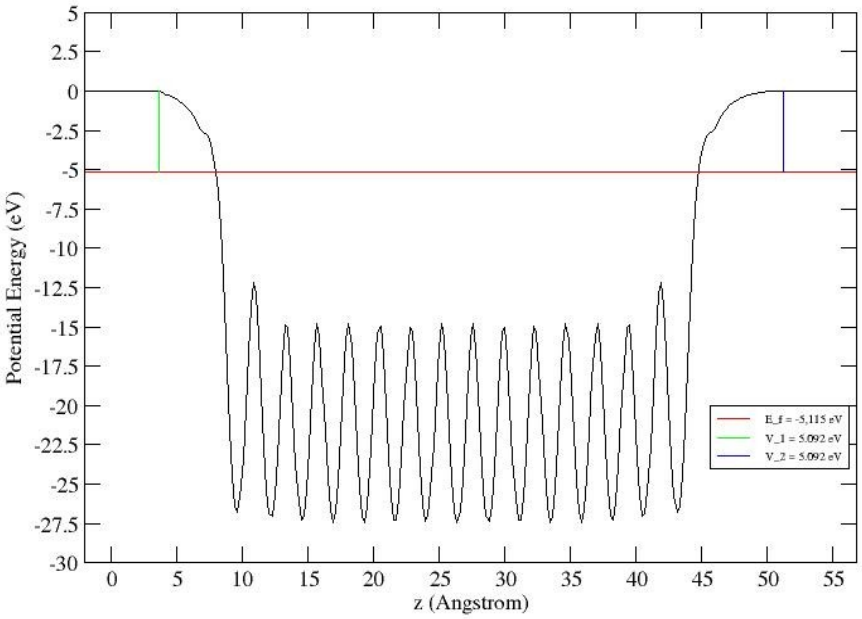

Figure 2.5.1.3: Same as Fig. 2.5.1.2 for 15 layer relaxed Au (111) slab.

The Figure 2.5.1.3 present the workfunction for the (111) plane at the case of 15 atoms chain after the use of the minimization. The location of every peak represents the atoms and the height of the peaks shows the potential energy of the atoms. The first and the last atom feature tall peaks becuase of the minimization. Using the minimization for the first and the last atom, these atoms are moving to minimize the total energy of the system.

So, these atoms are further away than the others and minimizing the potential energy because of the distance. The potential energy from the left side is about 5,092 eV and at the right 5,092 eV.

Comparing the Figures 2.5.1.2 and 2.5.1.3, it is clear that there is a difference for the length of the peaks for the plane (100) and the (111). The reason is the structure of the two planes. The atoms of the (111) plane are closer than the (100) plane, so the potential energy increases.

The next step of the project concerns the compare between the computational measurement of the workfunction and the workfunction which coming from the fitted values of the density probability.

2.5.2 COMPARISON TO THE SCHOCKLEY MODEL

Tables 2.5.1.1 – 2.5.1.4 contains the workfunction at the left and the right side of the chain. The values of the this table are rounded at the third decimal point. At the subchapter 2.3.3 is presented the third way of the proof of the surface states. There are some diagrams of the probability density. Using the fitted values of the diagrams, it will be found the function that describes the graph.

William Schockley developed a theory for semiconductors. However, as we can see at the below subchapters, this theory is allowed to be used aslo at metals and the proof is coming from the density probability. The Schockley Surface States theory predicts for the density probability that:

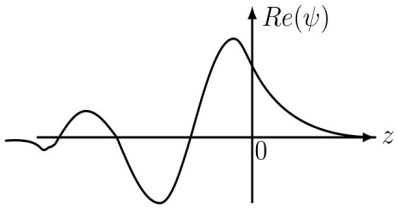

Figure 1.5.5 : Real part of one electron wavefunction for a surface state localized at the surface

$$\begin{cases} |\Psi'_i(z\le 0)|^2 \sim e^{2qz}\cos^2\left(\frac{\pi}{\alpha}z \pm \delta\right) \\ |\Psi'_i(z\le 0)|^2 \sim e^{2qz}\sin^2\left(\frac{\pi}{\alpha}z \pm \delta\right) \end{cases} \quad \text{and} \quad |\Psi'_i(z>0)|^2 \sim e^{-2\sqrt{\frac{2m}{\hbar^2}(V_0-E)}z}$$

$$\text{where} \quad |(V_0 - E_k)| = E \quad , \quad E_k = \frac{\hbar^2 k^2}{2m}$$

and $E = E_q = \frac{\hbar^2 q^2}{2m}$ at the other side of z_0 and it is valid because of the continuity of functions.

$$\text{So,} \quad V_0 = |E_k - E_q| = \frac{\hbar^2}{2m}|(k^2 - q^2)|$$

The Figure 1.5.5 describes the real part of one electron wavefunction for a surface state localized at the surface. Here, we rather use the probability density $|\psi|^2$. The computational method didn' t locate the first atom at the z=10, because the code leaves spacing between the slabs.

So, the first atom is located around the point of z_0=10 (10 Å on z-axis). For example, for Au (100) the first atom is located at z_0 = 9,839. The equation for $|\psi|^2$ will be:

$$\begin{cases} |\Psi'_i(z\le 0)|^2 \sim e^{2q(z-z_0)}\cos^2\left(\frac{\pi}{\alpha}(z-z_0)\pm\delta\right) \\ |\Psi'_i(z\le 0)|^2 \sim e^{2q(z-z_0)}\sin^2\left(\frac{\pi}{\alpha}(z-z_0)\pm\delta\right) \end{cases} \quad \text{and} \quad |\Psi'_i(z>0)|^2 \sim e^{-2k(z-z_0)}$$

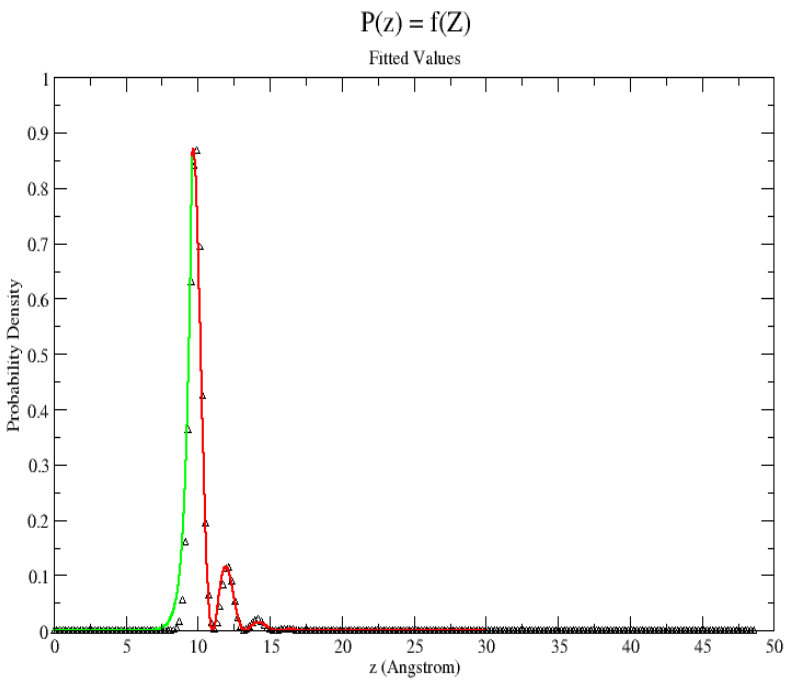

Figure 2.5.2.1: Fitted values on the first atom of the density probability of the Au (100) plane at the case of the 15 layers using minimization.

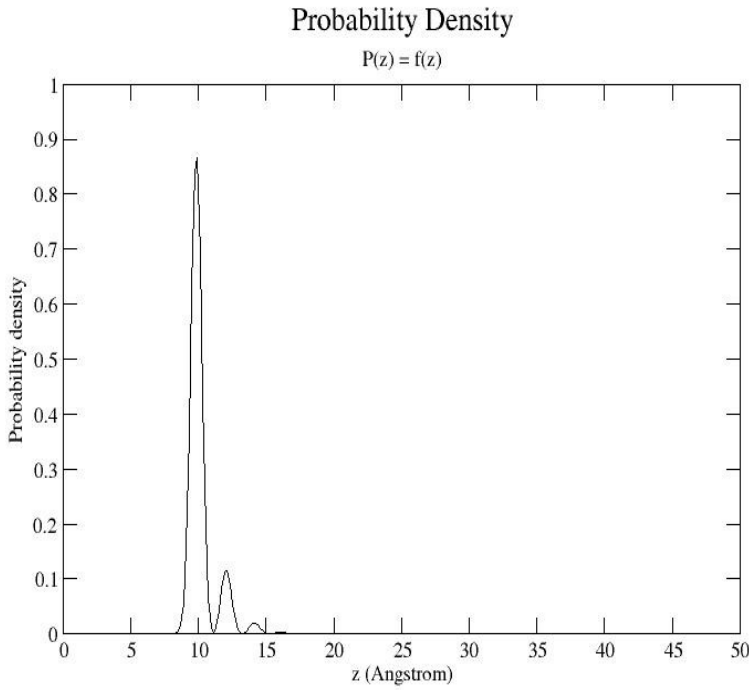

Figure 2.5.2.2: Probability Density of the 15 layers at the Au (100) plane with minimization.

For the fitted values, it was used the below function at the left side of the chain:

$$\begin{cases} y = A_0 \cdot e^{-\frac{(z-z_0)}{A_1}} \cdot \sin^2\left(\frac{\pi}{A_2}(z-z_0)+A_3\right), for\ z \ge z_0 \\ y = A_0 \cdot e^{\frac{(z-z_0)}{A_4}}, for\ z < z_0 \end{cases}$$

At the Figure 2.5.2.1, the triangles up describes the Probability Density, the red dashed line describes the function for $z \ge z_0$ and the green for $z < z_0$.

From the values of A_1 and A_4, it will be determined the values of q and k correspondingly. The parameters A_0, A_1, A_2, A_3, A_4:

A_0 : Amplitude of the descending oscillation

A_1 and A_4 : Decay time

A_2 : Distance between the atoms

A_3 : Phase difference

In the case that describes the Figure 2.5.2.1, it is:

$$\begin{cases} y = 0{,}861 \cdot e^{\frac{(z-9{,}810)}{1{,}110}} \cdot \sin^2\left(\frac{\pi}{2{,}26}(z-9{,}810)+1{,}431\right), for\ z \geq z_0 \\ y = 0{,}861 \cdot e^{\frac{(z-9{,}603)}{0{,}409}}, for\ z < z_0 \end{cases}$$

Consequently, $\begin{cases} 2q = \frac{1}{1{,}11} \\ 2k = \frac{1}{0{,}409} \end{cases} \Rightarrow \begin{cases} q = 0{,}451 \\ k = 1{,}223 \end{cases}$ and $V_0 = |E_k - E_q| = \frac{\hbar^2}{2m}\left|(k^2 - q^2)\right| = 4{,}920918\, eV$

The computational value of the workfunction holding 6 decimal points is 4,919408 eV. The Table 2.5.1.2 contains values of workfunction holding 3 decimal points.

The percentage difference is $\frac{\left|V_0^{comp} - V_0^{fitted\ values}\right|}{V_0^{comp}} \cdot 100\,\% = \frac{|4{,}919408 - 4{,}920918|}{4{,}919408} \cdot 100\,\% \sim 0{,}0003\,\%$

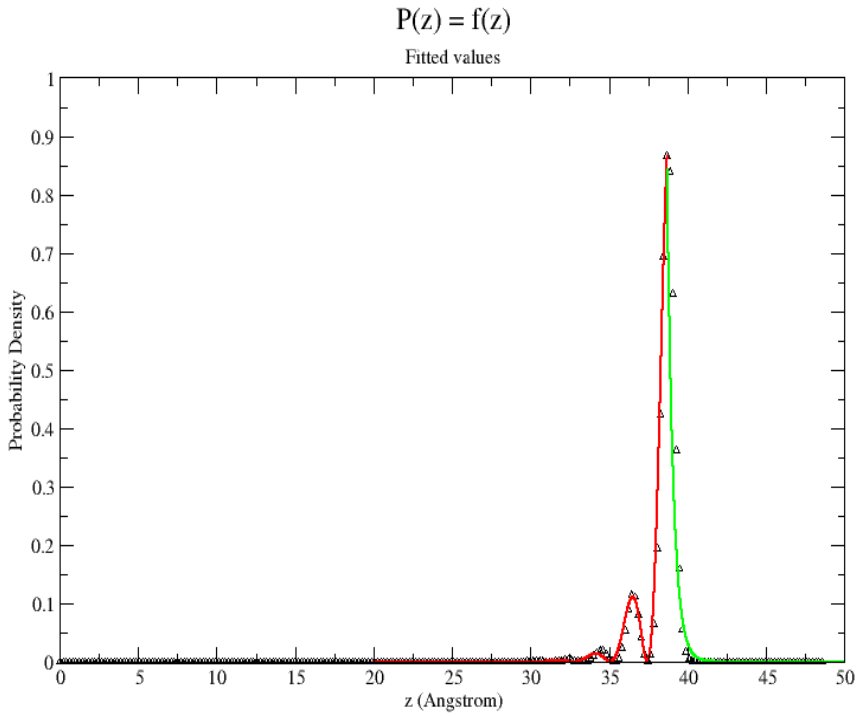

Figure 2.5.2.3: Fitted values on the last atom of the density probability of the Au (100) at the case of the 15 layers using the minimization.

At the other side of the chain, the Figure 2.5.2.3 describes a surface state using the way of the density probability. In this case is used:

$$\begin{cases} y = A_0 \cdot e^{\frac{(z-z_0)}{A_1}} \cdot \sin^2\left(\frac{\pi}{A_2}(z-z_0)+A_3\right), for\ z \leq z_0 \\ y = A_0 \cdot e^{-\frac{(z-z_0)}{A_4}}, for\ z > z_0 \end{cases}$$

The z_0 is about 40 Å. Specifically, the last atom is located at $z_0 = 38{,}721$.

Following the same process, the functions that describe the Figure are:

$$\begin{cases} y = 0{,}8 \cdot e^{\frac{(z-38{,}501)}{1{,}116}} \cdot \sin^2\left(\frac{\pi}{2{,}357}(z-38{,}501)+1{,}541\right), for\ z \le z_0 \\ y = 0{,}520 \cdot e^{-\frac{(z-38{,}202)}{0{,}399}}, for\ z > z_0 \end{cases}$$

Consequently, $\begin{cases} 2q = \frac{1}{1{,}116} \\ 2k = \frac{1}{0{,}399} \end{cases} \Rightarrow \begin{cases} q = 0{,}449 \\ k = 1{,}254 \end{cases}$ and $V_0 = |E_k - E_q| = \frac{\hbar^2}{2m}\left|(k^2 - q^2)\right| = 5{,}225702\, eV$

The computational value of the workfunction holding 6 decimal points is 4,965701 eV.

The percentage difference is $\frac{\left|V_0^{comp} - V_0^{fitted\ values}\right|}{V_0^{comp}} \cdot 100\,\% = \frac{|4{,}965701 - 5{,}225702|}{4{,}965701} \cdot 100\,\% \sim 0{,}052\,\%$

The parameter A_2 is very close to the distance that the code locate the atoms. It is a parameter that corresponds to the distance of the atoms. The distance between the the atoms on the (100) plane is 2,04 Å. The first atom is located at the point z=10, although it is moving at z=9,839 because of the minimization. The next atoms are at the points z=12,04 , z=14,08 . . . The last atom is at z=38,721. Without the minimization, the last atom would be at z=38,56. The last atom is 2,201 Å away to the semifinal. In the two cases, first and last atom gets away from the rest of the chain to minimize the Energy. The first atom is 2,201 Å away from the second, the distance between the rest except the last are 2,04 Å.

The (111) Plane:

The process for the (111) plane is exactly the same as the (100). The difference between the two planes is the structure, in other words the atom-coordinates are changed to create the slab.

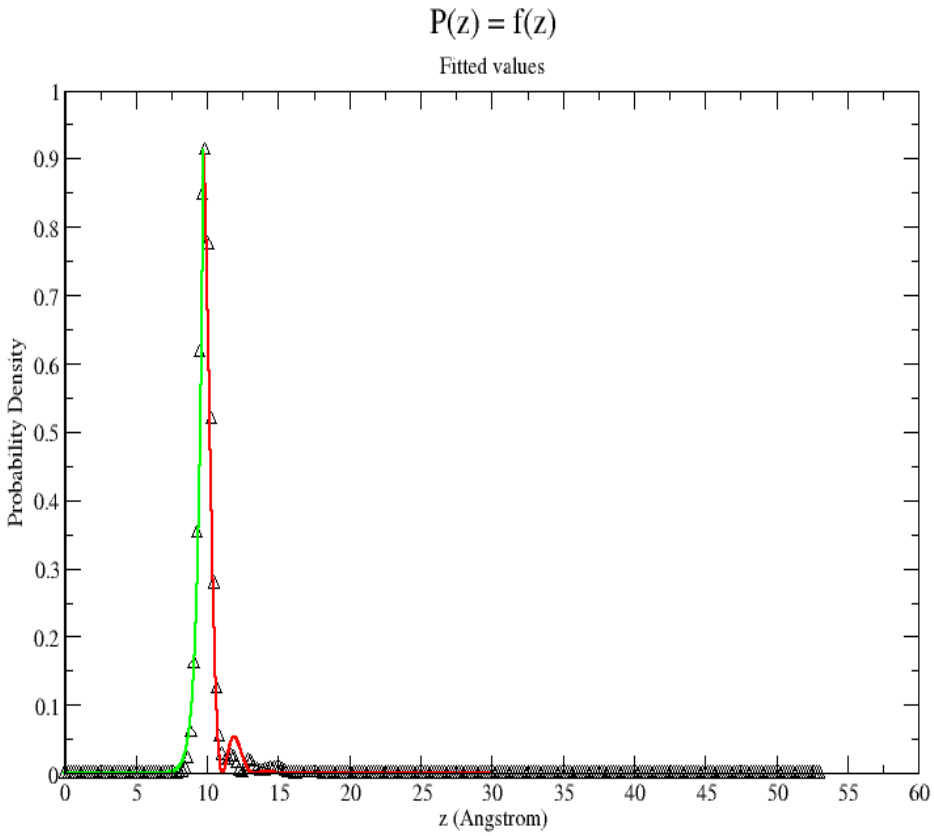

Figure 2.5.2.4: Fitted values on the first atom of the density probability of Au (111) at the case of the 15 layers using minimization. The triangles up describes the Probability Density, the red dashed line describes the function for $z \geq z_0$ *and the green for* $z < z_0$

The distance between the the atoms on the (111) plane is 2,356 Å. The first atom is located at the point z=10, although it is moving at z=9,792 because of the minimization. The next atoms are at the points z=12,356 , z=14,711 . . . The last atom is at z=42,986. Without the minimization, the last atom would be at z=43,186. So, the distance between the edge atoms and the rest atoms of the chain is 2,564 Å, and the distance between the atoms of the rest chain is 2,356 Å.

The functions that describe the Figure are:

$$\begin{cases} y = 0{,}923 \cdot e^{-\frac{(z-9{,}805)}{0{,}786}} \cdot \sin^2\left(\frac{\pi}{2{,}246}(z-9{,}805)+1{,}351\right), \text{for } z \geq z_0 \\ y = 0{,}925 \cdot e^{\frac{(z-9{,}775)}{0{,}381}}, \text{for } z < z_0 \end{cases}$$

Therefore, $\begin{cases} 2q = \frac{1}{0{,}786} \\ 2k = \frac{1}{0{,}381} \end{cases} \Rightarrow \begin{cases} q = 0{,}636 \\ k = 1{,}311 \end{cases}$ and $V_0 = |E_k - E_q| = 5{,}007697\, eV$

The computational value of the workfunction holding 6 decimal points is 5,091697 eV.

The percentage difference is $\frac{\left|V_0^{comp}-V_0^{fitted\ values}\right|}{V_0^{comp}}\cdot 100\,\%=\frac{|5{,}091697-5{,}007697|}{5{,}091697}\cdot 100\,\%\sim 1{,}65\,\%$

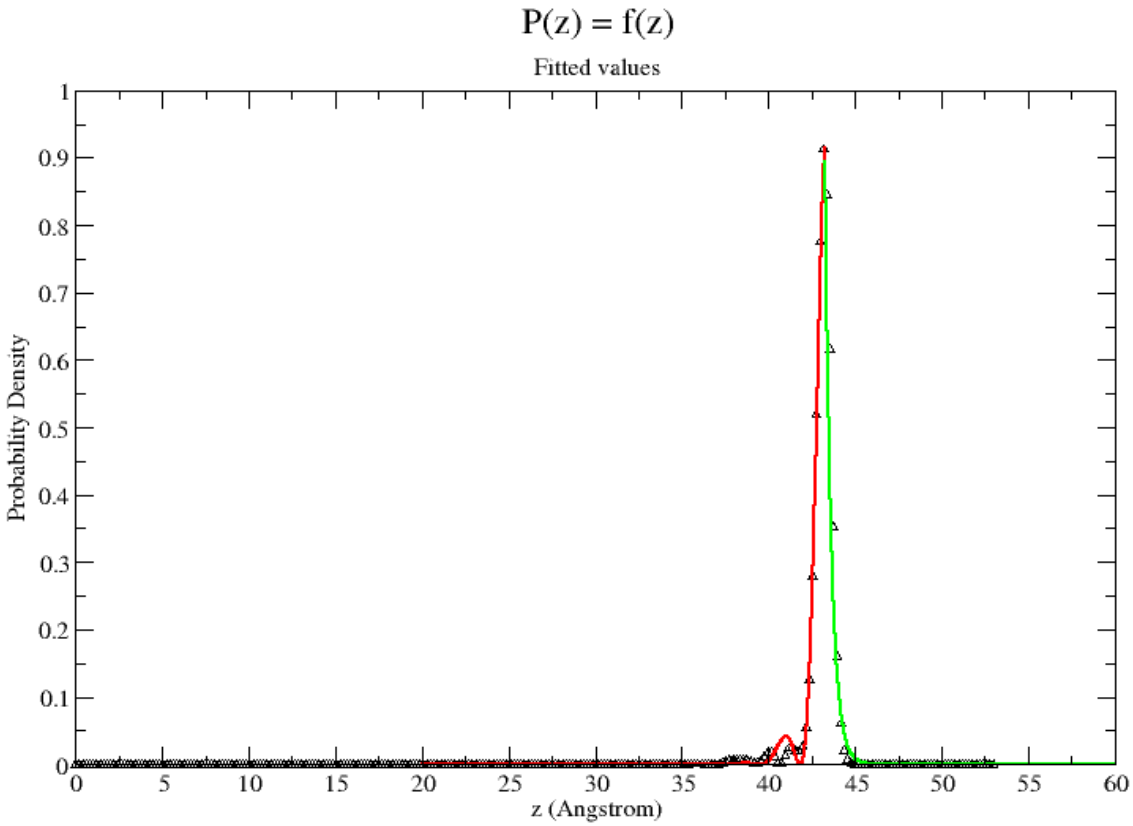

Figure 2.5.2.5: Fitted values on the last atom of the Density Probability of Au (111) at the case of the 15 layers using minimization.

$$\begin{cases} y=0{,}910\cdot e^{\frac{(z-43{,}167)}{0{,}746}}\cdot\sin^2\left(\frac{\pi}{2{,}315}(z-43{,}167)+1{,}794\right), for\ z\le z_0 \\ y=0{,}901\cdot e^{-\frac{(z-43{,}267)}{0{,}378}}, for\ z>z_0 \end{cases}$$

Consequently, $\begin{cases} 2q=\frac{1}{0{,}746} \\ 2k=\frac{1}{0{,}378} \end{cases}\Rightarrow\begin{cases} q=0{,}671 \\ k=1{,}324 \end{cases}$ and $V_0=|E_k-E_q|=\frac{\hbar^2}{2m}\left|(k^2-q^2)\right|=4{,}967895\,eV$

The computational value of the workfunction holding 6 decimal points is 5,091630 eV.

The percentage difference is $\frac{\left|V_0^{comp} - V_0^{fitted\ values}\right|}{V_0^{comp}} \cdot 100\,\% \sim 2{,}43\,\%$.

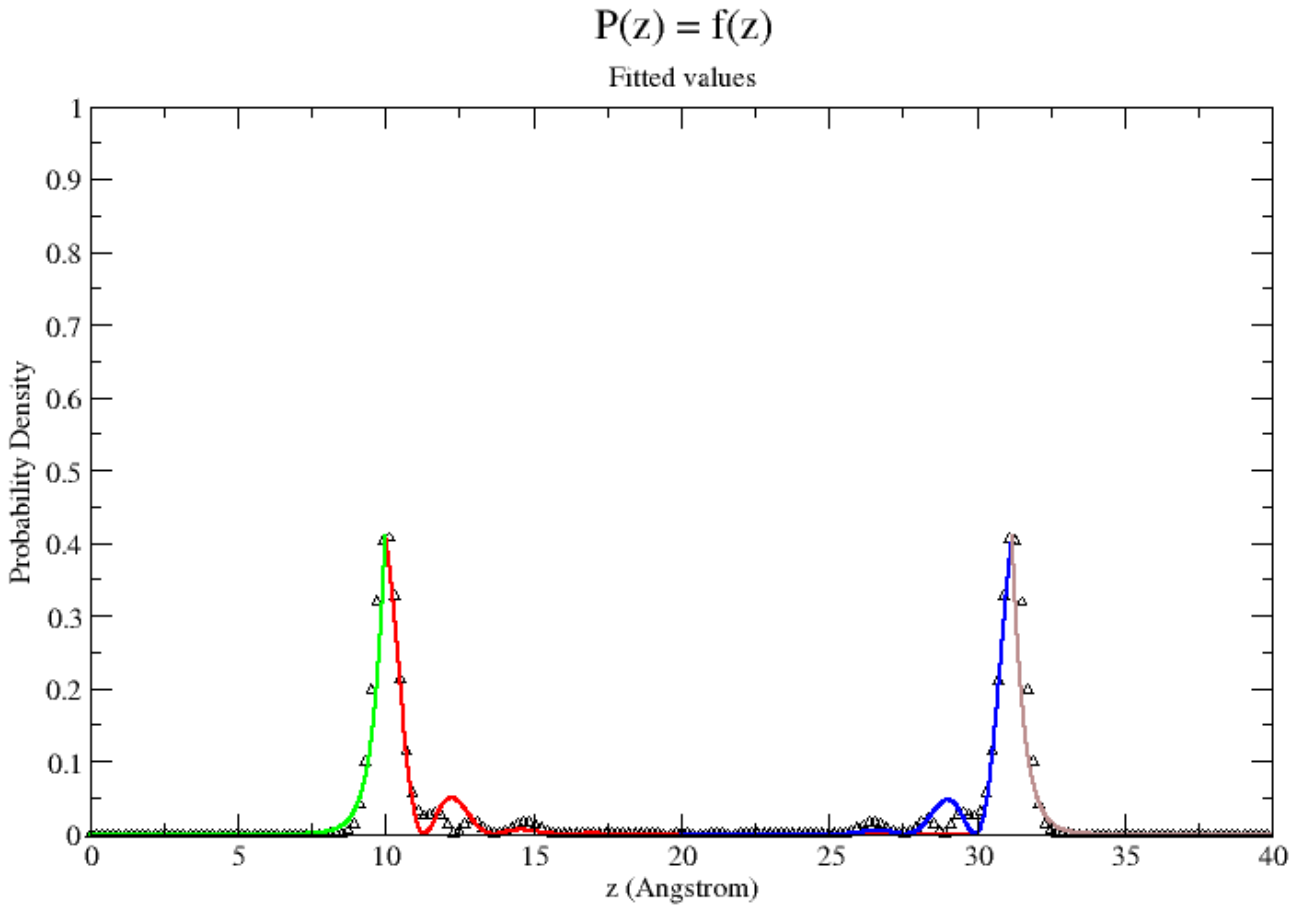

Figure 2.5.2.6: Fitted values on the last atom of the density probability of the Au(111) for a 10- layer before relaxation.

Figure 2.5.2.6 describes the case of the 10 atom-layer slab. The characteristic in this Figure is that there is the same probability density on either the sides of the slab. In this case, wasn' t used the minimization, so the first and the last atom didn' t move away from the rest chain. The first atom is located on z = 10 (at z-axis) and the last on z = 31,2003. So, $z_1 = 10$ and $z_2 = 31{,}2$.

From the left side of the slab:

$$\begin{cases} y = 0{,}421 \cdot e^{-\frac{(z-10)}{1{,}069}} \cdot \sin^2\left(\frac{\pi}{2{,}356}(z-10) + 1{,}388\right), \text{for } z \le z_1 \\ y = 0{,}409 \cdot e^{\frac{(z-10)}{0{,}409}}, \text{for } z > z_1 \end{cases}$$

Consequently, $\begin{cases} 2q = \frac{1}{1{,}069} \\ 2k = \frac{1}{0{,}408} \end{cases} \Rightarrow \begin{cases} q = 0{,}468 \\ k = 1{,}226 \end{cases}$ and $V_0 = |E_k - E_q| = \frac{\hbar^2}{2m}\left|(k^2 - q^2)\right| = 4{,}894802\, eV$

The computational value of the workfunction holding 6 decimal points is 4,893904 eV.

The percentage difference is $\frac{\left|V_0^{comp} - V_0^{fitted\ values}\right|}{V_0^{comp}} \cdot 100\,\% \sim 0{,}02\,\%$.

From the right side of the slab:

$$\begin{cases} y = 0{,}409 \cdot e^{\frac{(z-31{,}2)}{1{,}062}} \cdot \sin^2\left(\frac{\pi}{2{,}356}(z - 31{,}2) + 1{,}671\right), \text{for } z \ge z_2 \\ y = 0{,}409 \cdot e^{-\frac{(z-31{,}2)}{0{,}406}}, \text{for } z < z_2 \end{cases}$$

Consequently, $\begin{cases} 2q = \frac{1}{1{,}062} \\ 2k = \frac{1}{0{,}406} \end{cases} \Rightarrow \begin{cases} q = 0{,}471 \\ k = 1{,}232 \end{cases}$ and $V_0 = |E_k - E_q| = \frac{\hbar^2}{2m}\left|(k^2 - q^2)\right| = 4{,}934549\, eV$

The computational value of the workfunction holding 6 decimal points is 4,893903 eV.

The percentage difference is $\frac{\left|V_0^{comp} - V_0^{fitted\ values}\right|}{V_0^{comp}} \cdot 100\,\% \sim 0{,}83\,\%$.

2.6 Cu slabs

In this chapter of the project, we present the same work on the same planes at the Cooper. The structure of the cooper is also FCC with lattice constant at 3,597 Å. The atomic number is 29, so the electron configuration is [Ar] $3d^{10}$ $4s^{1}$, where Ar is Argon. Copper is at the same column of the Periodic Table, so the number of the valence electrons is the same. The computational solution of the problem, using GPAW, uses 11 valence electrons. Although, there is 1 valence electron. The reason is that the d-level is completed and there is only one electron in 4s. So, this electron is used as valence.

All the calculations have done using the minimization.

2.6.1 Cu(100)

Beginning with Cu(100), the Tables 2.6.1.1 and 2.6.1.2 describes the features of the first and the last atom respectively.

- *First atom*

Layers	***Band no.***	***Energy (eV)***	***E_{fermi} (eV)***	***$E - E_{fermi}$ (eV)***	***Probability on surface atom***
5	27	-5,8189	-4,3430	-1,4753	~ 46,7 %
10	56	-5,7838	-4,3219	-1,4619	~ 90,3 %
11	61	-5,8303	-4,4314	-1,3989	~ 92,7 %
12	68	-5,8064	-4,3604	-1,4460	~ 91,8 %
13	74	-5,7860	-4,3615	-1,4245	~ 91,6 %
14	78	-5,8130	-4,3648	-1,4482	~ 90,2 %
15	84	-5,8109	-4,3832	-1,4282	~ 92,4 %

Table 2.6.1.1: Electronic States localized at the first atom of each Cu(100) slab. For each slab, we present the energy at the localized state, its difference from the Fermi Level and the probability that this electron will be found at the first atom.

- *Last atom*

Layers	***Band no.***	***Energy (eV)***	***E_{fermi} (eV)***	***E - E_{fermi} (eV)***	***Probability on surface atom***
5	27	- 5,8189	- 4,3430	- 1,4753	~ 46,7 %
10	55	- 5,7912	- 4,3219	- 1,4693	~ 90,3 %
11	62	- 5,8292	- 4,4314	- 1,3978	~ 92,7 %
12	67	- 5,8114	- 4,3604	- 1,4510	~ 91,7 %
13	73	- 5,7996	- 4,3615	- 1,4381	~ 91,6 %
14	79	- 5,8079	- 4,3648	- 1,4310	~ 90,2 %
15	85	- 5,8102	- 4,3832	- 1,4270	~ 92,4 %

Table 2.6.1.2: Same as Table 2.6.1.1 for the last atom of Cu(100) slab.

Observing the Tables 2.6.1.1 and 2.6.1.2, it is clear that at the ten atom-layers, the probability of a surface state is starting to converge. The surface state for each case is being observed five to eight bands above (on average six bands). As layers increases, the total number of the bands increases correspondingly. So, the SS is being observed at “similar” number of band as the number of atoms increases.

A proof of this, is that the difference between the enegy of the band that a surface state is being observed and the Fermi level, is approximately constant as the number of atoms increase and the difference starts from the second decimal point.

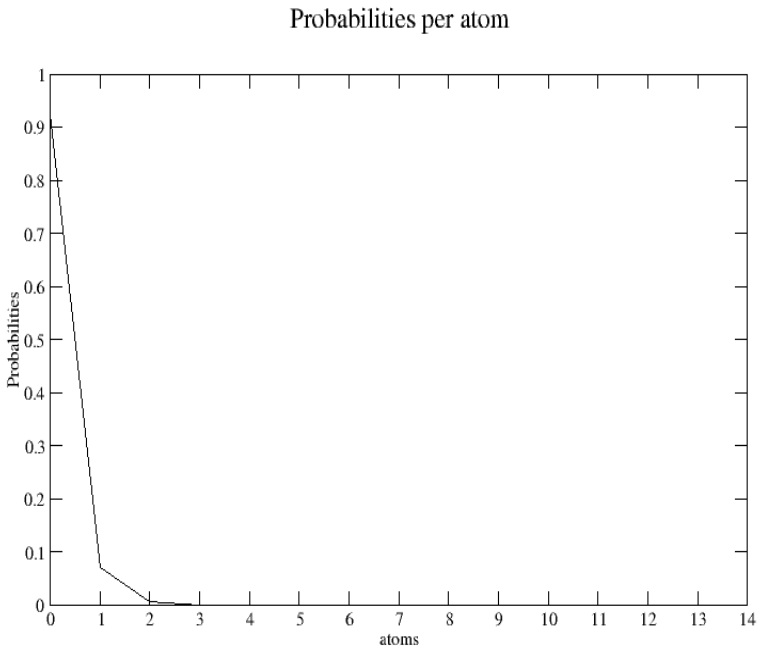

Figure 2.6.1.1: Probability of localization for a Cu(100) slab with 15 layers.

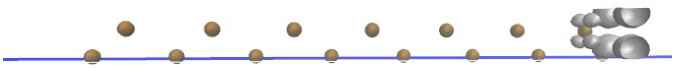

Figure 2.6.1.2: Contour plot of $|\psi|^2$ for band 85 in Cu(100) slab with 15 layers. Compare to Fig. 2.6.1.1 .

Comparing the two tables, someone could observe that the surface states for either the first or the last layer, occur at nearby (or 'neighboring') bands.

It is the same situation as the Au nanostructures.

atom	*X – axis*	*Y – axis*	*Z - axis*
0	0,0000	0,0000	9,9490
1	1,2763	1,2763	11,8050
2	0,0000	0,0000	13,6100
3	1,2763	1,2763	15,4150
4	0,0000	0,0000	17,2200
5	1,2763	1,2763	19,0250
6	0,0000	0,0000	20,8300
7	1,2763	1,2763	22,6350
8	0,0000	0,0000	24,4400
9	1,2763	1,2763	26,2450
10	0,0000	0,0000	28,102

Table 2.6.1.3: Cartesian coordinates (in Å) of atoms in an 11-layer Cu(100) slab.

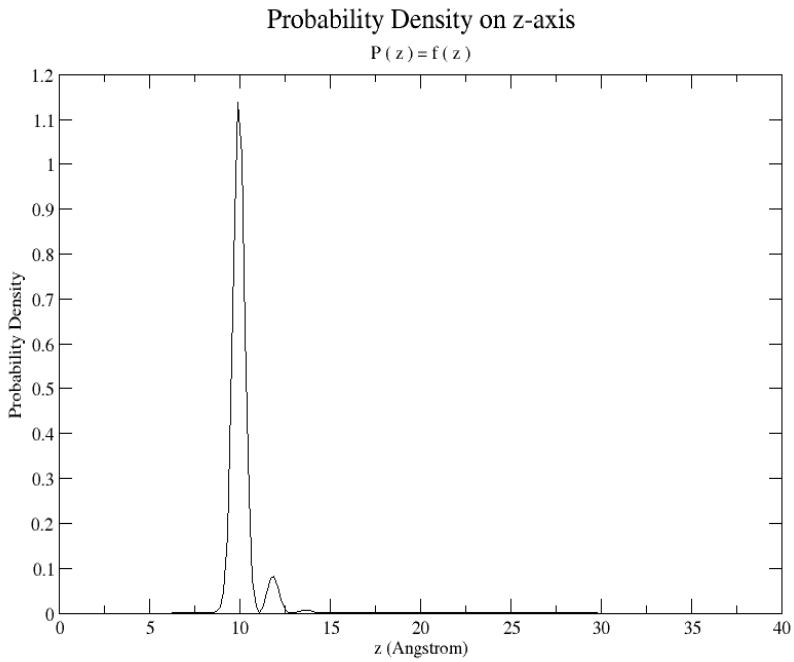

Figure 2.6.1.3: Probability density for Cu(100) slab with 11– layers and for band 62.

Figure 2.6.1.3 presents exactly the same situation as the Figures 2.6.1.1 and 2.6.1.2, but using another way. Observing the Table 2.6.1.3, there is periodicity on the xy plane, in contrast of the z-axis, where the slab is developing.

Firstly, the edge atoms are at the points z=10.00 and z=28.05 respectively. After, five repetition, the system converges and these atoms are situated at positions z=9.9490 and z=28.1020 correspondingly. The relaxationation is applied on the edge atoms. These atoms are moving to minimize the total energy of the system. The distance of the edge atoms to the rest of chain is the same and is 1.856 Å on z-axis. The atoms of the rest chain has the same distance between them, 1.805 Å.

Subsequently, the workfunction is the next step.

Atoms	V_{left} *(eV)*	V_{right} *(eV)*	E_{Fermi} *(eV)*
5	4,324	4,324	- 4,3430
10	4,314	4,312	- 4,3219
11	4,409	4,409	- 4,4314
12	4,348	4,344	- 4,3604
13	4,338	4,338	- 4,3615
14	4,352	4,351	- 4,3648
15	4,360	4,359	- 4,3832

Table 2.6.1.4: Potential Energy from the two sides of the slabs and the Fermi level for relaxed Cu (100) slabs.

The Table 2.6.1.4 contains the workfunction from two sides of slab. Our chain is finite. Schockley's theory study models for semi-infinite chains, consequently there is potential only at the the one side, in contrast with our slabs where there is at either the sides.

In Figure 2.6.1.4, it is clear that at the positions that the atoms are located, there is a minimum peak. The height of the curve of the edge atoms is smaller than the others. It occurs because of the relaxation and the distance of the edge atoms and the rest of the slab. As the distance is getting bigger and biggrer, the potential energy getting smaller. Observing the total Figure, the potential energy looks like a cosine function, similarly to the Schockley model.

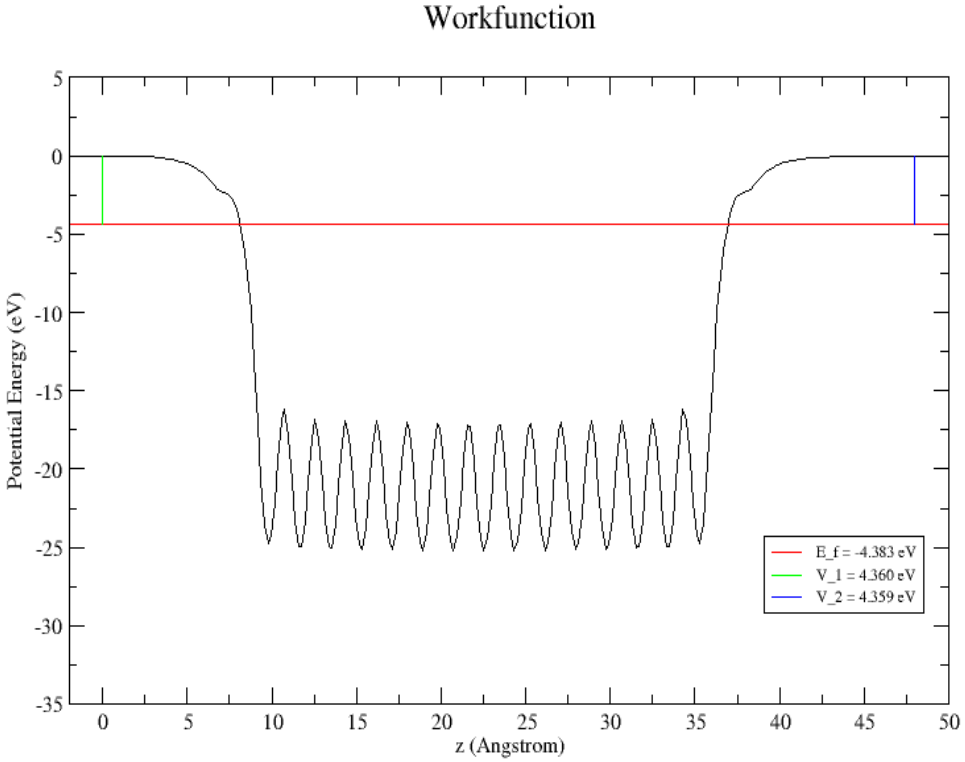

Figure 2.6.1.4: Total electronic potential for relaxed 15-layer Cu (100) slab.

The potential energy from the left side is about 4,360 eV and at the right 4,359 eV. These energies are calculated from the differnce between the Fermi level and the point that begins the potential energy.

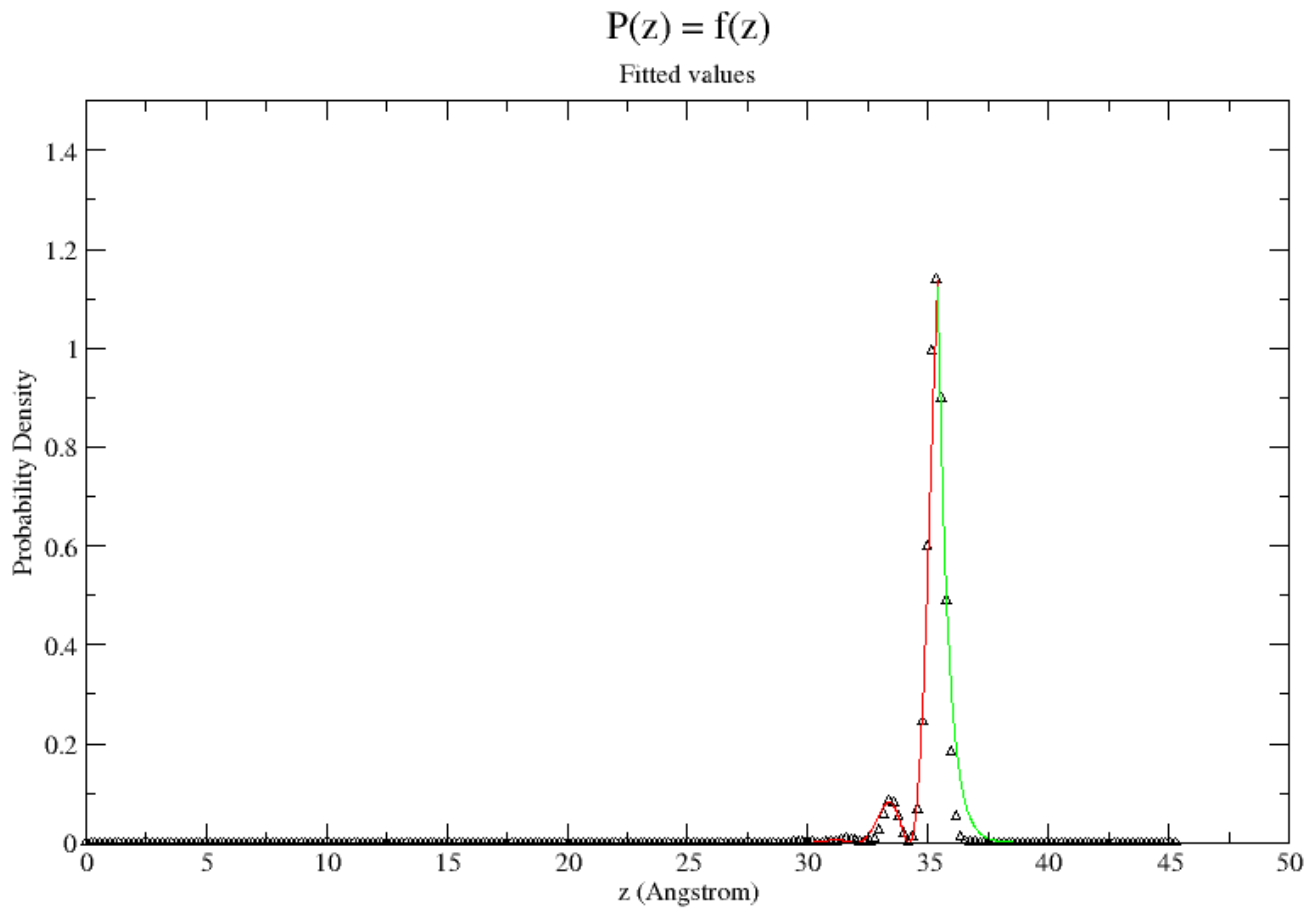

Figure 2.6.1.5: Fitted values on the last atom of the Density Probability of Cu(100) at the case of a 15-layers slab after relaxation.

From the theory is known that:

$$\begin{cases} |\Psi'_i(z\le 0)|^2 \sim e^{2q(z-z_0)}\cos^2\left(\frac{\pi}{\alpha}(z-z_0)\pm\delta\right) \\ |\Psi'_i(z\le 0)|^2 \sim e^{2q(z-z_0)}\sin^2\left(\frac{\pi}{\alpha}(z-z_0)\pm\delta\right) \end{cases} \quad \text{and} \quad |\Psi'_i(z>0)|^2 \sim e^{-2k(z-z_0)}$$

atom	***X – axis***	***Y – axis***	***Z - axis***
0	0.0000	0.0000	9,955
15	0.0000	0.0000	35,314

Table 2.6.1.5: Cartesian coordinates (in Å) of edge atom for a relaxed 15-layer slab.

The same comments apply as before. The distance of the edge atoms to the rest of slab is the same and is 1,85 Å on z-axis. The atoms of the rest slab are 1,81 Å away.

The last is at the position $z_0 = 35{,}314$.

In the case that describes the Figure , it is:

$$\begin{cases} y = 1{,}125 \cdot e^{\frac{(z-35{,}377)}{0{,}815}} \cdot \sin^2\left(\frac{\pi}{2{,}220}(z-35{,}377)+1{,}671\right), for\ z \le z_0 \\ y = 1{,}122 \cdot e^{-\frac{(z-35{,}4)}{0{,}403}}, for\ z > z_0 \end{cases}$$

Consequently, $\begin{cases} 2q = \frac{1}{0{,}815} \\ 2k = \frac{1}{0{,}403} \end{cases} \Rightarrow \begin{cases} q = 0{,}614 \\ k = 1{,}241 \end{cases}$ and $V_0 = |E_k - E_q| = \frac{\hbar^2}{2m}\left|(k^2 - q^2)\right| = 4{,}443618\, eV$

The computational value of the workfunction holding 6 decimal points is 4,359434 eV. The Table 2.6.1.4 contains values of workfunction holding 3 decimal points.

The percentage difference is $\frac{\left|V_0^{comp} - V_0^{fitted\ values}\right|}{V_0^{comp}} \cdot 100\,\% = \frac{|4{,}359434 - 4{,}443618|}{4{,}359434} \cdot 100\,\% \sim 1{,}9\,\%$

For the Figures 2.6.1.1, 2.6.1.2 and 2.6.1.5, the corresponding Figures for the atoms of the opposite edge are at the appendix.

2.6.2 Cu(111)

Continuing with the plane (111), the Tables describes the features of the first and the last atom respectively.

- *First atom*

Layers	***Band no.***	***Energy (eV)***	***E_{fermi} (eV)***	***$E - E_{fermi}$ (eV)***	***Probability on surface atom***	***Similar Bands***
5	14	- 7,2891	- 4,6639	- 2,6252	~ 73,1 %	15
10	35	- 7,1466	- 4,5510	- 2,5956	~ 88,9 %	36
11	37	- 7,1971	- 4,5781	- 2,6190	~ 87,1 %	38
12	41	- 7,1841	- 4,5523	- 2,6318	~ 87,2 %	42
13	45	- 7,2097	- 4,5650	- 2,6447	~ 82,2 %	47

Table 2.6.2.1: Electronic States localized at the first atom of each Cu(111) slab. For each slab, we present the energy at the localized state, its difference from the Fermi Level and the probability that this electron will be found at the first atom.

- *Last atom*

Layers	***Band no.***	***Energy (eV)***	***E_{fermi} (eV)***	***$E - E_{fermi}$ (eV)***	***Probability on surface atom***	***Similar Bands***
5	16	- 7,2824	- 4,6639	- 2,6185	~ 73,1 %	17
10	33	- 7,1576	- 4,5510	- 2,6066	~ 88,8 %	34
11	39	- 7,1895	- 4,5781	- 2,6114	~ 87,1 %	40
12	43	- 7,1820	- 4,5523	- 2,6297	~ 87,1 %	44
13	44	- 7,2099	- 4,5650	- 2,6449	~ 82,3 %	46

Table 2.6.2.2:Same as Table 2.6.2.1 for the last atom of Cu(111) slab.

Observing the Tables 2.6.2.1 and 2.6.2.2 , it is easy to realize that the explanation is exactly the same as before. At the 10-layer slab, the probability of a surface state is starting to converge. The surface state for each case is being observed two to six bands above (on average 5 bands). As the layers increase, the total number of the bands increase correspondingly. So, the SS is being observed at “similar” number of band as the number of atoms increases.

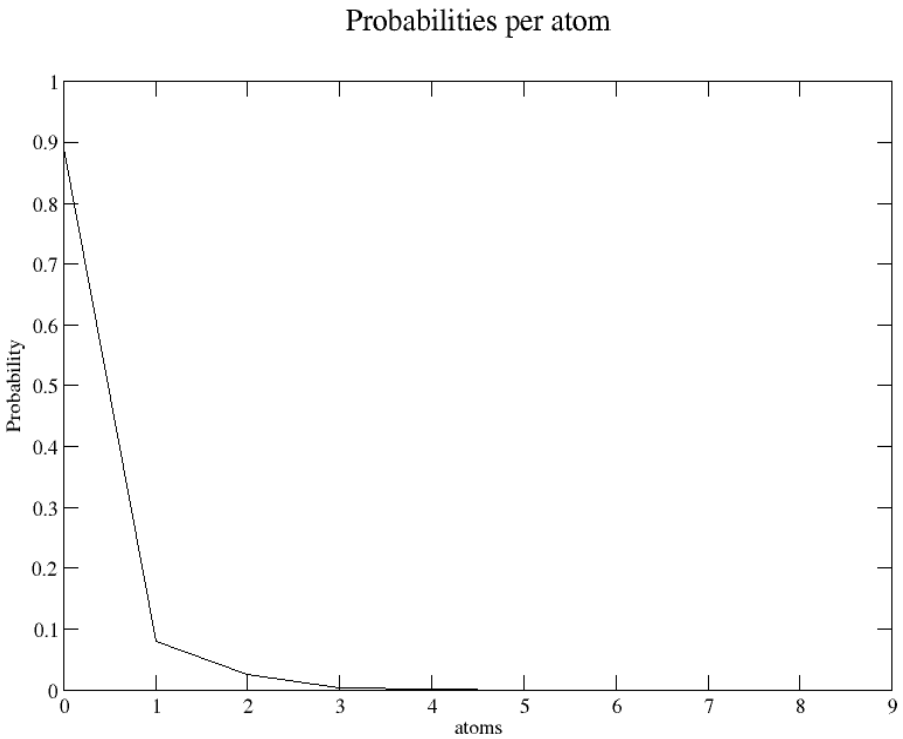

Figure 2.6.2.1: Probability of localization for a Cu(111) slab with 10 layers.

Figure 2.6.2.2: Contour plot of $|\psi|^2$ for band 85 in Cu(111) slab with 11 layers.

A proof of this, is that the difference between the enegy of the band that a SS is being observed and the Fermi level, is approximately constant as the number of layers increases and the difference starts from the second decimal point.

This is the case, in which the same situation appears at near band. Comparing again the two Tables, someone could observe that the surface states for either the first or the last atom, occur at nearby (or 'neighboring') bands. It was explained before, at subchapter 2.3.4 and 2.4.2. The explanation is coming from the two symmetries, the fold and rotate of the chain relative to the z-axis. The rotation gives a symmetry on the xy-plane. So, the two components of the plane gives the degeneracy and this gives the same results.

atom	***X – axis***	***Y – axis***	***Z - axis***
0	1,2763	0,7369	9,9605
1	0,0000	1,4738	12,0842
2	0,0000	0,0000	14,1685
3	1,2763	0,7369	16,2527
4	0,0000	1,4738	18,3369
5	0,0000	0,0000	20,4212
6	1,2763	0,7369	22,5054
7	0,0000	1,4738	24,5896
8	0,0000	0,0000	26,6739
9	1,2763	0,7369	28,7581
10	0,0000	1,4738	30,8423
11	0,0000	0,0000	32,9658

Table 2.6.2.3: Cartesian coordinates (in Å) of atoms in a 12-layer Cu(111) slab.

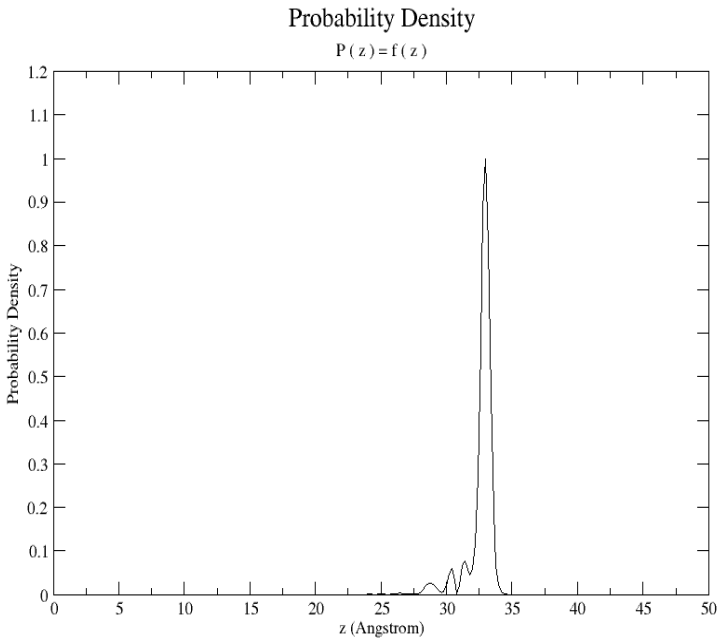

Figure 2.6.2.3: Probability density for Cu(111) slab with 12– layers and for band 42.

Figure 2.6.2.3 presents exactly the same situation as the Figures 2.6.2.1 and 2.6.2.2, but using another way. Observing Table 2.6.2.3, there is periodicity on the xy plane, in contrast of the z-axis, where the slab is developing.

Firstly, the edge atoms are at the points z=10.00 and z=32.93 respectively. After, two repetition of the minimizaion, the system converges and these atoms are situated at positions z=9.96 and z=32.97 correspondingly.

These atoms are moving to minimize the total energy of the system. The distance of the edge atoms to the rest of slab is the same and is 2.1237 Å on z-axis. The atoms of the rest chain has the same distance between them, 2.0842 Å.

The workfunction is the next step.

Layers	V_{left} ***(eV)***	V_{right} ***(eV)***	E_{Fermi} ***(eV)***
5	4,641	4,641	- 4,6639
10	4,529	4,529	- 4,5510
11	4,556	4,556	- 4,5781
12	4,535	4,529	- 4,5523
13	4,520	4,503	- 4,5650

Table 2.6.2.4: Potential Energy from the two sides of the slabs and the Fermi level for relaxed Cu (111) slabs.

Table 2.6.2.4 contains the workfunction from two sides the slab.

In Figure 2.6.2.4, it is clear that at positions that atoms are located, there is a minimum peak. The explanation of the height of the curve of the edge atoms is the same as previously at (100) plane. Observing the total Figure 2.6.2.4, the potential energy looks like a cosine function, as previously.

The potential energy from the left side is about 4,520 eV and at the right 4,503 eV. These energies are calculated from the differnce between the Fermi Level and the point that begins the potential energy.

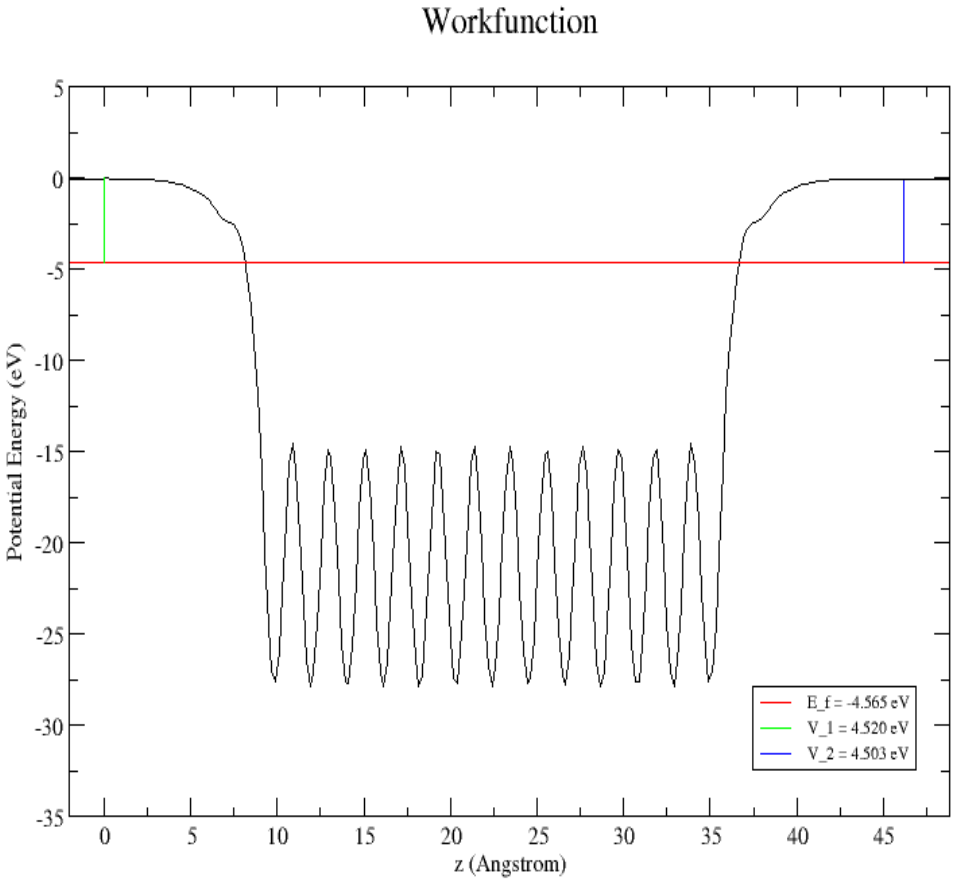

Figure 2.6.2.4: Total electronic potential for relaxed 13-layer Cu(111) slab.

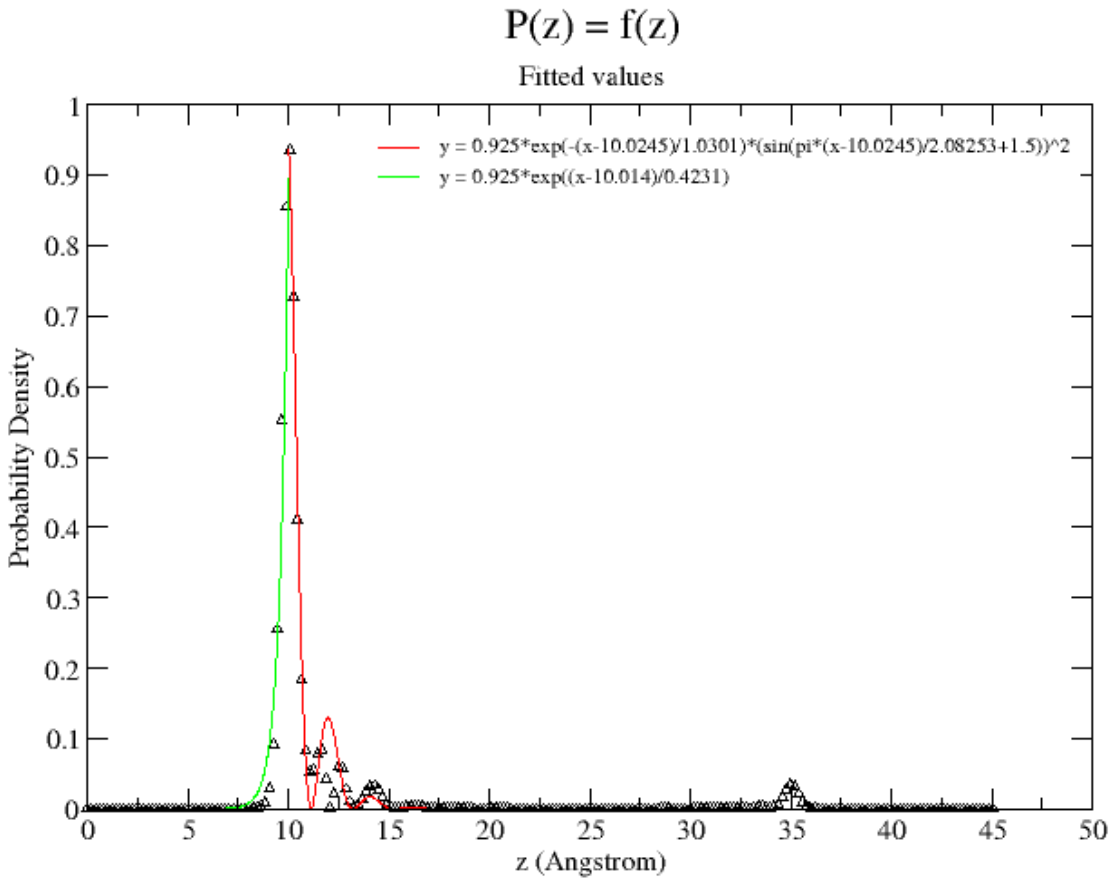

Figure 2.6.2.5: Fitted values on the last atom of the Density Probability of Cu(111) at the case of a 13-layers slab after relaxation.

atom	***X – axis***	***Y – axis***	***Z - axis***
0	0.0000	0.0000	9,994
12	0.0000	0.0000	35,017

Table 2.6.2.5: Cartesian coordinates (in Å) of edge atom for a relaxed 13-layer slab.

The same comments apply as before. The distance of the edge atoms to the rest of slab is the same and is 2,09 Å on z-axis. The atoms of the rest slab are 2,08 Å away.

The last is at the position $z_0 = 35{,}017$.

In the case that describes the Figure 2.6.2.5, it is:

$$\begin{cases} y=0{,}925\cdot e^{-\frac{(z-10{,}0245)}{1{,}030}}\cdot\sin^2\left(\frac{\pi}{2{,}083}(z-10{,}025)+1{,}5\right), for\ z\geq z_0 \\ y=0{,}925\cdot e^{\frac{(z-10{,}014)}{0{,}423}}, for\ z<z_0 \end{cases}$$

Consequently, $\begin{cases} 2q=\frac{1}{1{,}030} \\ 2k=\frac{1}{0{,}423} \end{cases} \Rightarrow \begin{cases} q=0{,}485 \\ k=1{,}182 \end{cases}$ and $V_0=\left|E_k-E_q\right|=\frac{\hbar^2}{2m}\left|(k^2-q^2)\right|=4{,}423138\,eV$

The computational value of the workfunction holding 6 decimal points is 4,519910 eV. The Table 2.6.2.4 contains values of workfunction holding 3 decimal points.

The percentage difference is $\frac{\left|V_0^{comp}-V_0^{fitted\ values}\right|}{V_0^{comp}}\cdot 100\,\%=\frac{|4{,}519910-4{,}423138|}{4{,}519910}\cdot 100\,\%\sim 2{,}14\,\%$

For the Figures 2.6.2.1,2.6.2.2 and 2.6.2.5, the corresponding Figures for the atoms of the opposite edge are at the appendix.

Conclusions

In this thesis we perform a comprehensive study of electronic structure of surfaces of fcc metals Au and Cu within the framework of density functional theory.

We calculate characteristic electronic and structural properties of these surfaces like the electron density and workfunction. Surface States are being observed at “similar” band number, n, of Bloch States $\psi_{n\vec{k}}$ as the slab thickness increases at constant difference between the enegy of that band and the Fermi level. The degeneracy of the bands that surfaces states are being observed on the Au(111) are due to the symmetries of the system.

Atomic relaxation enhances the probability's of localization. Furthermore, surface state is presented at lower bands, so the SS Energy is lowered.

We calculate the workfunction directly and by fitting our surface states to the theory Schockley. The percentage difference between these methods was too small, giving a direct verification of the validity of this theory to metals. It is the first time that Schockley's theory is verified for non-semiconductors.

Repeating the process for Cu(100) and Cu(111), we observed similar results.

So far, Schockley's theory was applied and explained results in semiconductors. We confirmed that this theory could be applied also to metalic surfaces.

Future work could include comparison of the observed surface states to Tamm theory.

References – Bibliography

[1] https://socratic.org/questions/how-many-atoms-are-there-in-a-face-centered-cubic-unit-cell-of-an-atomic-crystal

[2] http://www.slideshare.net/umairbukhari3/crystal-systems

[3] https://en.wikipedia.org/wiki/Atomic_packing_factor

[4] http://www.iue.tuwien.ac.at/phd/ungersboeck/node24.html

[5] E. N. Economou, Solid State Physics, vol. 1, Crete University Press, 2nd Edition, Heraklion Crete 2012

[6] E. N. Economou, Solid State Physics, vol. 2, Crete University Press, 2nd Edition, Heraklion Crete 2003

[7] N. W. Arschoft and N. D. Mermin, Solid State Physics, Saunders College Publishing, Cornell 1976

[8] https://www2.le.ac.uk/departments/physics/people/mervynroy/lectures/pa4311/quantum-chemistry-summary.pdf

[9] W. Kohn and L. J. Sham, Self – consistent equations including exchange and correlation effects, Phys. Rev. 140, 1133, (1965)

[10] P. Hohenberg and W. Kohn , Inhomogeneous electron gas, Phys. Rev. 136, 864, (1964)

[11] H. Luth, Surfaces and Interfaces of Solid Materials, Springer , 3rd Edition, Aachen 1996

[12] Bernd Kollmann, Shockley Surface States calculated within Density Functional Theory, Master Thesis,Universität Graz, 2014

[13] William Shockley, On the surface states associated with a periodic potential, Phys. Rev. ,

56:317–323, Aug 1939

[14] Dario Wolf Knebl, Shockley Surface States from First Principles, Matser Thesis, Universität Graz, 2013

[15] F. Forstmann, The concepts of surface states, Progress in Surface Science, Vol. 42, pp 21-31, 1993

[16] Andrew Zangwill, Physics at Surfaces, Cambridge University Press

[17] J. Enkovaara et al., Electronic structure calculations with GPAW: a real-space implementation of the projector augmented-wave method, J. Phys. Condens. Matter 22, 253202, (2010)

[18] https://wiki.fysik.dtu.dk/gpaw/introduction_to_paw.html (retrieved Oct. 22, 2015)

[19] The free software “Atomic Simulation Environment” can be found at : https://wiki.fysik.dtu.dk/ase/

APPENDIX

Surface State on the last atom Plane (100)

Layers	***Band no.***	***Energy (eV)***	***E_{fermi} (eV)***	***E - E_{fermi} (eV)***	***Probability on surface atom***
10	53	-6,7467	-4,8850	-1,8617	~ 55 %
	54	-6,7484	-4,9442	-1,8042	~ 85,5 %
11	57	-6,7994	-4,9488	-1,8506	~ 73,5 %
	60	-6,7870	-5,0386	-1,7484	~ 86,5 %
12	64	-6,7774	-4,9137	-1,8637	~ 61 %
	64	-6,7680	-4,9788	-1,7892	~ 85,2 %
13	69	-6,7800	-4,9259	-1,8538	~ 72 %
	70	-6,7796	-5,0054	-1,7742	~ 86,2 %
14	75	-6,7822	-4,9261	-1,8561	~ 74 %
	75	-6,7861	-4,9965	-1,7896	~ 84,2 %
15	81	-6,7795	-4,9084	-1,8711	~ 74 %
	80	-6,7827	-4,9966	-1,7861	~ 86,4 %

Table A.1: Surface State for the last layer of Au (100) slabs. For every atom-laywer slab, the first line gives the surface state before the relaxation and the second after relaxation of atomic coordinates.

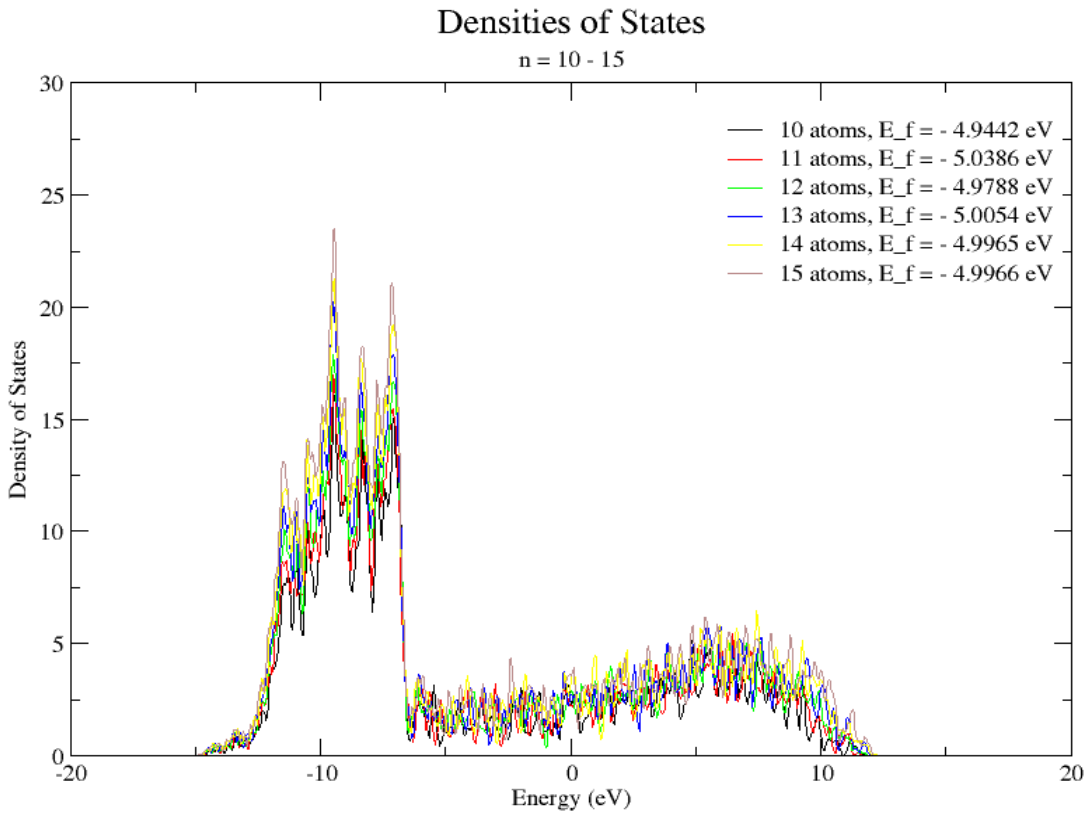

Figure A2: The diagramm of the DOS for the Au(100) after relaxation. There are all slabs and its Fermi Level.

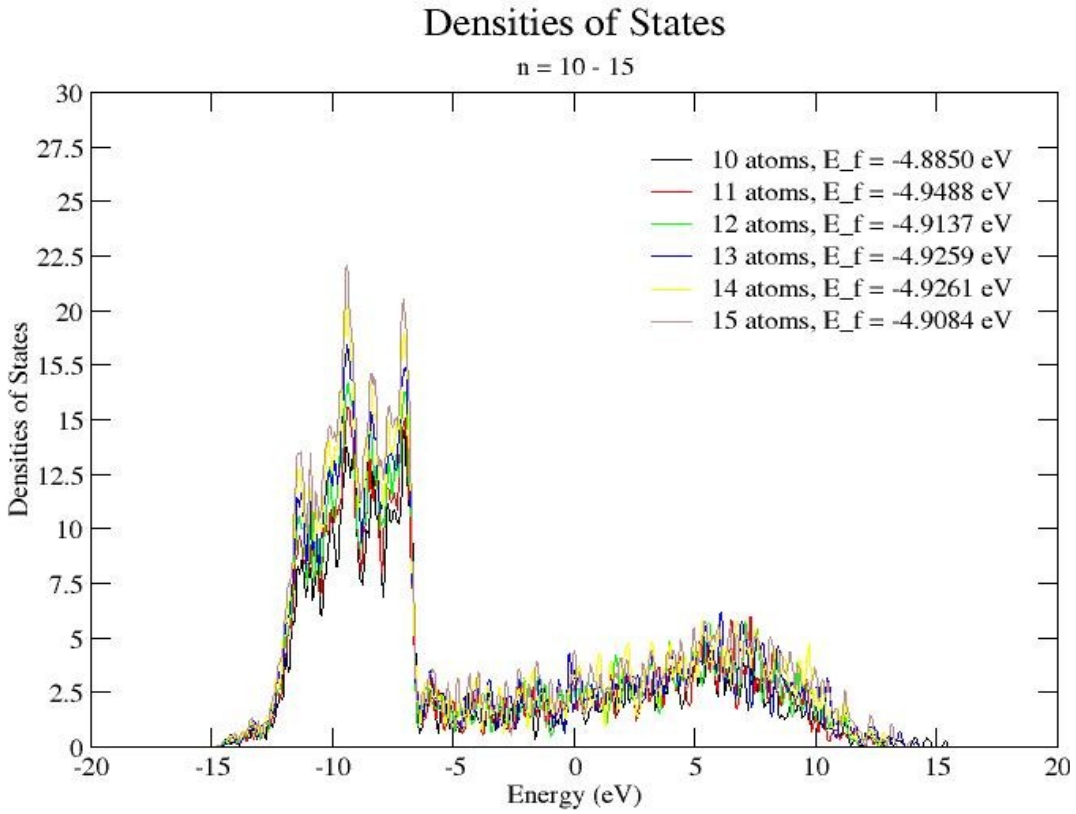

Figure A1: The diagramm of the DOS for the Au(100) before relaxation, using only the xc. There are all slabs and its Fermi Level.

Surface State on the last atom Plane (111):

Atoms	***Band***	***Energy (eV)***	***E_{fermi} (eV)***	***$E - E_{fermi}$ (eV)***	***Probability on surface atom***	***Similarly Bands***
10	32	-9,0378	-4,9778	-4,0600	~ 44 %	33 , 34 , 35
	34	-8,8995	-5,0505	-3,8490	~ 94,6 %	35
11	38	-9,0481	-5,0091	-4,0390	~ 87 %	37
	38	-8,9272	-5,1017	-3,8255	~ 93,3 %	39
12	41	-9,0566	-4,9881	-4,0685	~ 87 %	42
	42	-8,9375	-5,1027	-3,8348	~ 94,6 %	43
13	43	-9,0745	-5,0381	-4,0364	~ 87 %	44
	45	-8,8856	-5,0691	-3,8165	~ 95 %	46
14	47	-9,0797	-5,0187	-4,0610	~ 87 %	48
	48	-8,9395	-5,1029	-3,8366	~ 94,2 %	-
15	50	-9,0554	-5,0061	-4,0493	~ 88 %	51
	53	-8,9286	-5,1151	-3,8135	~ 95 %	54

Table A2: Surface State for the last layer of Au (100) slabs. For every atom-laywer slab, the first line gives the surface state before the relaxation and the second after relaxation of atomic coordinates.

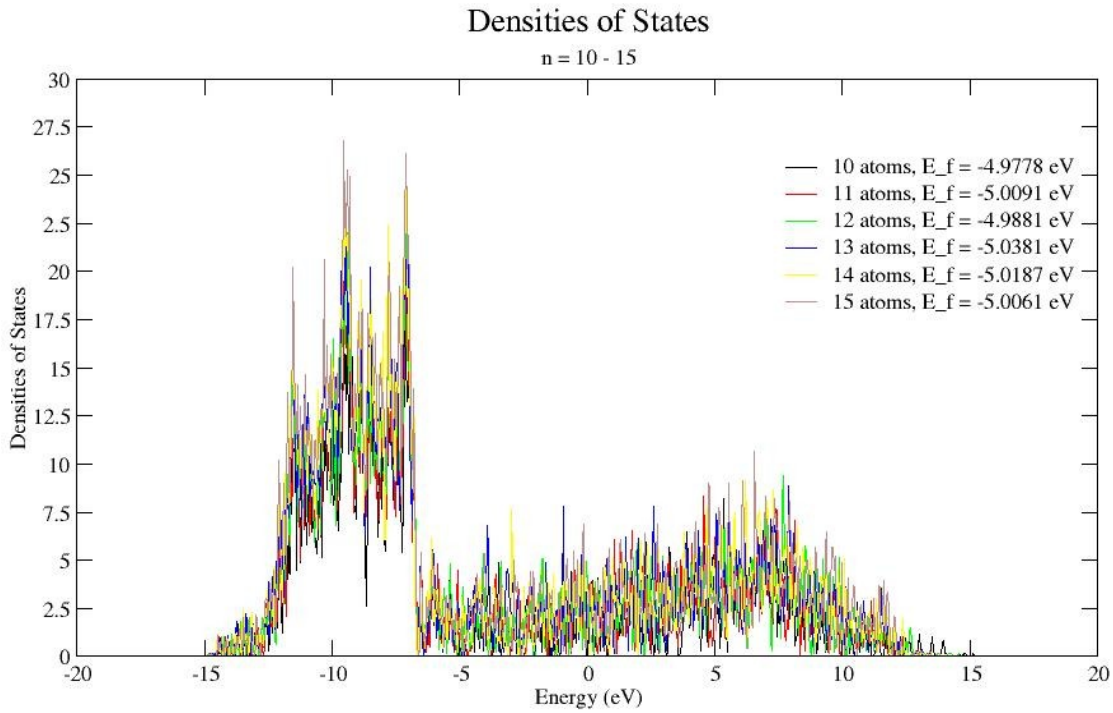

Figure A3: The diagramm of the DOS for the Au(111) before relaxation, using only the xc. There are all slabs and its Fermi Level.

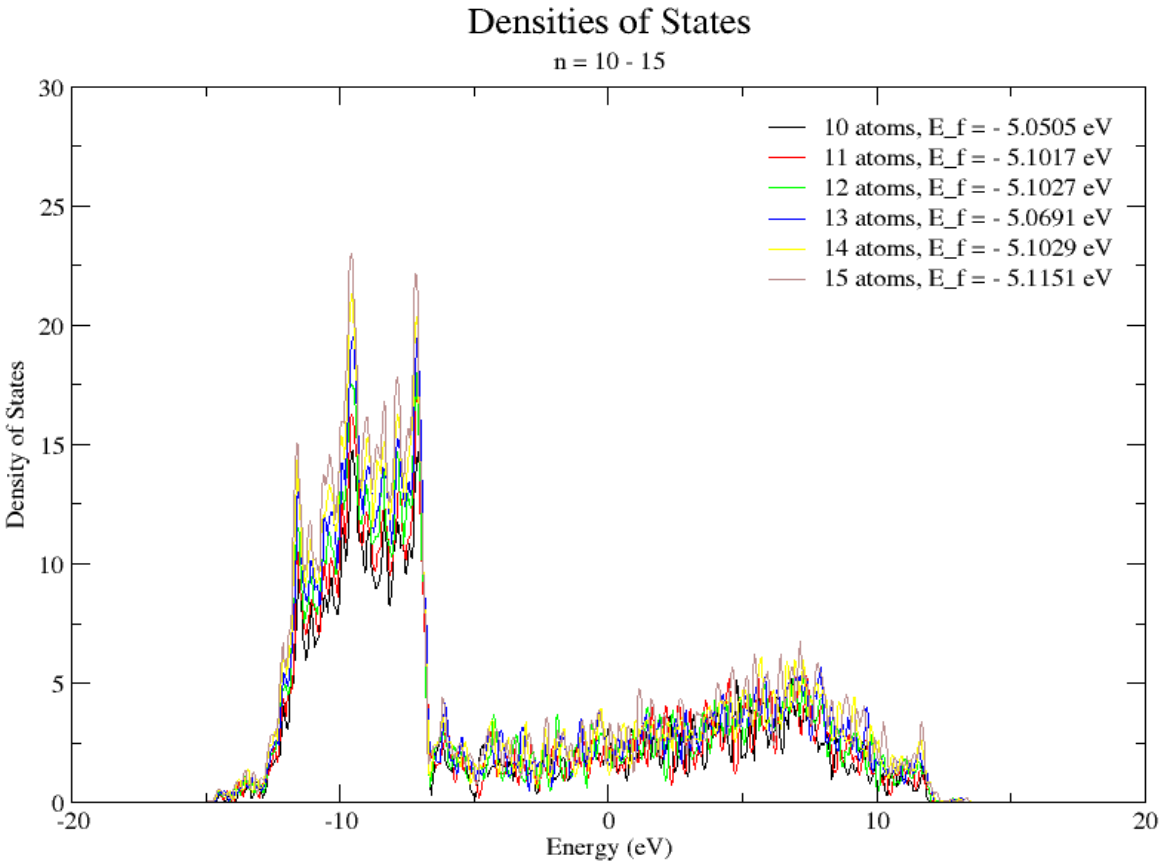

Figure A4: The diagramm of the DOS for the Au(100) after relaxation. There are all slabs and its Fermi Level.

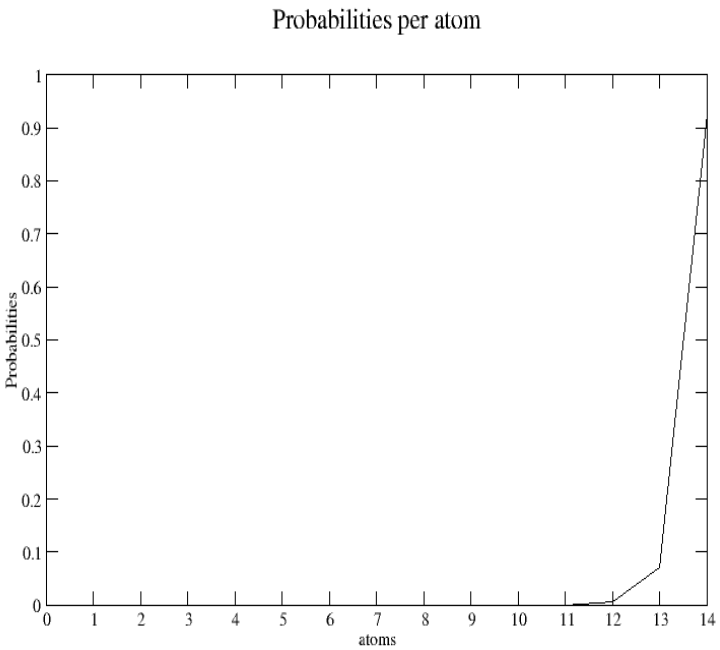

Figure A5: Probability of localization for the last layer of a Cu(100) slab with 15 layers.

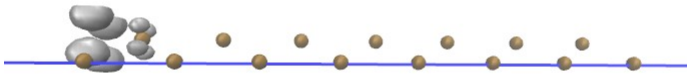

Figure A6:Contour plot of $|\psi|^2$ for band 84 in Cu(100) slab with 15 layers. Compare to Fig. A5 .

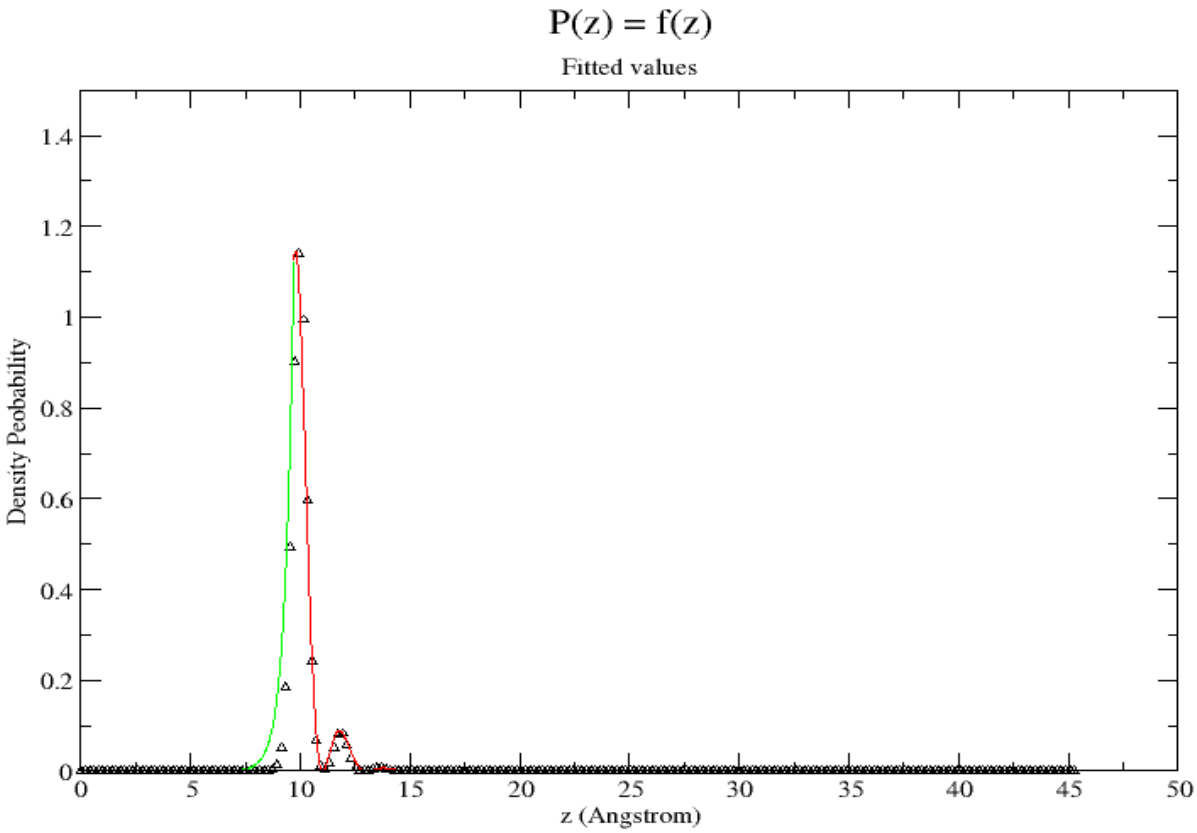

Figure A6: Probability Density for Cu(100) slab with 15-layers. Fitted values on the firs atom after relaxation.The computational workfunction is 4,313575 eV and from the fitted values is 4,417400 eV. The percentage difference is about 2,4 %.

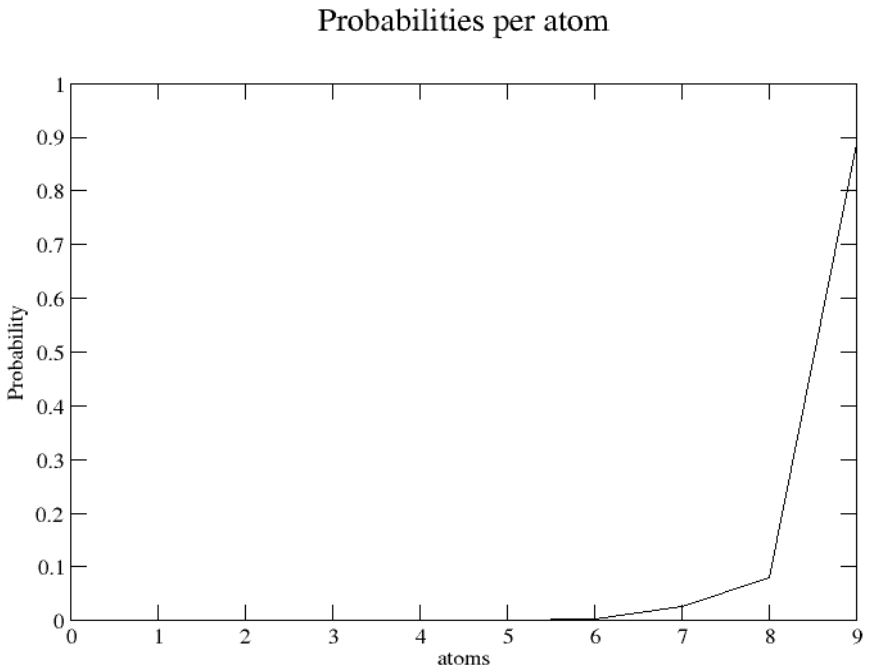

Figure A7: Probability of localization for for the last atom of a Cu(111) slab with 10 layers.

Figure A8: Plane (111) of the Cu-11 atom layer slab (yz plane). the first atom has ~ 87,1% probability. It is a clear surface state.

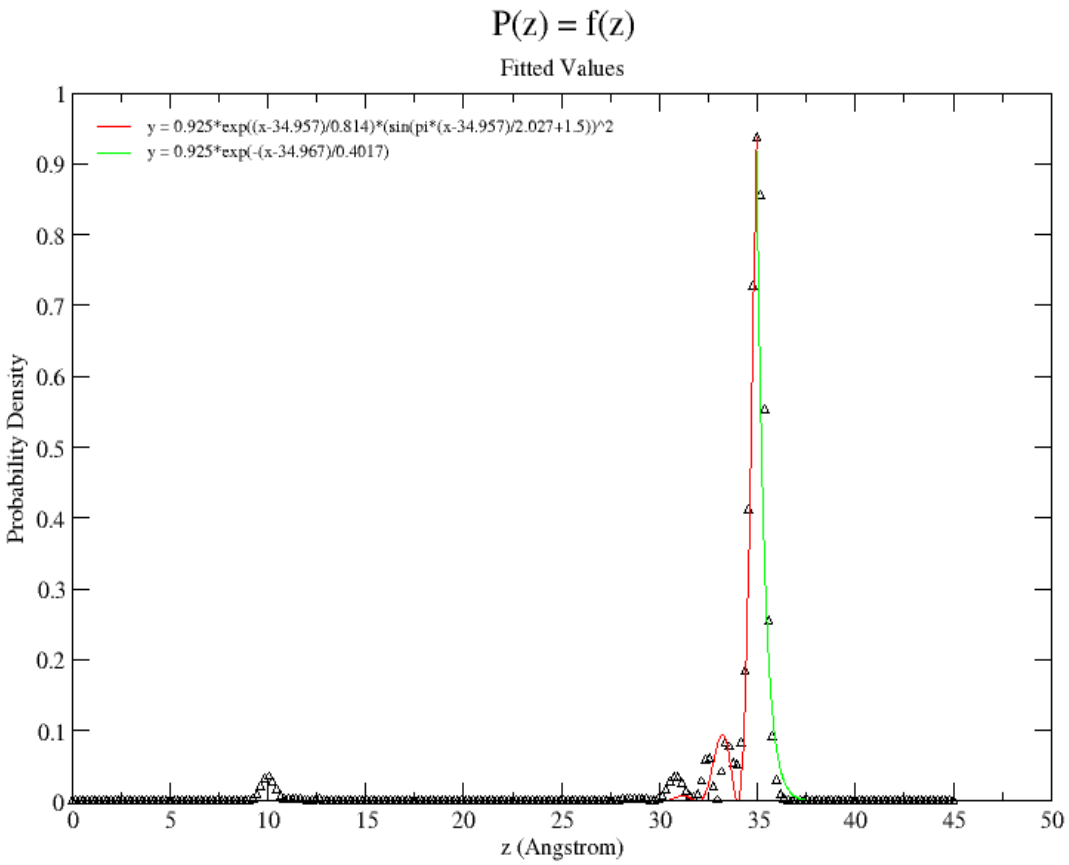

Figure A9: Probability Density for Cu(111) slab with 13-layers. Fitted values on the last atom after relaxation. The computational workfunction is 4,503352 eV and from the fitted values is 4,465295 eV. The percentage difference is about 1,2%.

Plane 211

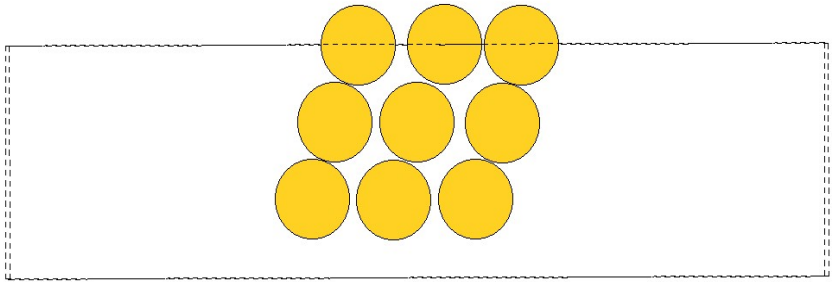

Figure A10: Simulation cell picturing a (211) slab with 3 atomic-layers (3 atoms per layer)

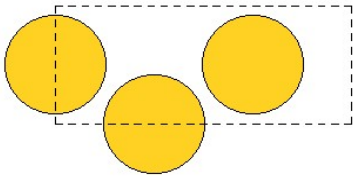

Figure A11: Unit cell of (211) plane of FCC structure ((110) plane)

- ***For the first 3 atom of the layer***

Layers	***no. of Atoms***	***Band no.***	***Energy (eV)***	***E_{fermi} (eV)***	***Probability on surface atom***
3	9	66	6,7423	-0,8786	~ 46 %
4	12	32	-3,6802	0,0049	~ 41 %
5	15	42	-2,9012	0,9211	~ 41 %
6	18	98	0,2350	1,5458	~ 44 %
7	21	113	0,8117	2,1513	~ 64 %
8	24	74	-1,1057	2,6835	~ 66 %
9	27	148	1,7596	3,0827	~ 66 %
10	30	165	2,1567	3,5066	~ 68 %
11	33	180	2,5107	3,8520	~ 67 %
12	36	196	2,8342	4,1734	~ 68 %

Table A3: *Electronic States localized at the first layer of each Cu(211) slab. For each slab, we present the energy at the localized state, the Fermi Level and the probability that this electron will be found at the first layer (both three atoms).*

- **For the last 3 atom of the layer**

Layers	***no. of Atoms***	***Band no.***	***Energy (eV)***	***E_{fermi} (eV)***	***Probability on surface atom***
3	9	66	6,7423	-0,8786	~ 46 %
4	12	32	-3,6802	0,0049	~ 41 %
5	15	43	-2,9008	0,9211	~ 42 %
6	18	97	0,2313	1,5458	~ 43 %
7	21	114	0,8153	2,1513	~ 64 %
8	24	76	-1,0896	2,6835	~ 66 %
9	27	147	1,7573	3,0827	~ 66 %
10	30	164	2,1527	3,5066	~ 68 %
11	33	181	2,5152	3,8520	~ 67 %
12	36	197	2,8385	4,1734	~ 68 %

Table A4: *Electronic States localized at the last layer of each Cu(211) slab. For each slab, we present the energy at the localized state, the Fermi Level and the probability that this electron will be found at the last layer (both three atoms).*

Figure A12: The diagramm of the DOS for the Au(100) after relaxation. There are all slabs and its Fermi Level.